University of Zurich[UZH]

Department of Geography

Lipid biomarkers for the source apportionment of organic matter in a multi-layered plaggen soil profile

GEO 511 Master`s Thesis

Author

Rahel Widmer

09-196-882

Supervision by:

PD Dr. Guido Wiesenberg

guido.wiesenberg@geo.uzh.ch

Dr. Martina Gocke

mgocke@uni-bonn.de

Faculty representative

Prof. Dr Micheael W. I. Schmidt

michael.schmidt@geo.uzh.ch

Date of Submission: 29.09.2016

Department of Geography, University of Zurich

Summary

Organic matter (OM) from aboveground and belowground sources has rarely been differentiated. Soil studies commonly compromise only the uppermost meter. The aim of this masterthesis was to distinguish aboveground and belowground biomass sources of soil and sedimentary OM in a sandy multi-layer profile in the Netherlands. Extractable lipids have been used to investigate the contribution of root-, fresh aboveground biomass (that included plant tissues like leafs, bark and branches) and microbial-derived compounds to the OM. It was found that, the upper layers, the Epialbic Podzol and the Plaggen Anthrosol were derived from fresh biomass sources and the sub soil layers relict Entic Podzol and the driftsand were derived from post-sedimentary incorporation of root- or rhizomicrobial- derived inputs. It was found, that the Plaggic Anthrosol had another plant source of OM than the relict Entic Podzol. The source for plaggen soil reached back to the plaggen cultivation in the Middle Ages. In the Epialbic Podzol, where beneficial conditions in terms of e.g. nutrient contents were found, deep roots were enriched and had a higher influence to its rhizosphere than roots located in the plaggen soil. In the coversand, root- and rhizomicrobial- inputs were an important source of fresh OC. Further was shown, that deep roots in the coversand had an influence up to 11 cm distance to the central root where in other root-transects the effect was much lower (2-8 cm). Potential overprint of the results for OM, especially for post-sedimentary incorporated root- or rhizomicrobial inputs is supposed. Therefore, more research with ^{14}C analysis is required.

CONTENT

LIST OF FIGURES

LIST OF TABLES

Abbreviations

cs	coversand
CO_2	Carbon dioxide
Ca	Calcium
C_{org}	organic carbon
DCM	dichloromethane
ds	driftsand
EP	Epialbic Podzol
FA	fatty acid
Fe	iron
FID	flame ionization detector
GC	gas chromatography
K	potassium
KOH	potassium hydroxide
MeOH	methanol
Mn	manganese
MS	mass spectrometry
MUFA	mono-unsaturated fatty acid
Na_2SO_4	natriumsulfate
OC	organic carbon
PA	Plaggic Anthrosol
Phy	phytane
Pr	pristane
rEP	relict Entic Podzol
SOC	soil organic carbon
TOC	total organic carbon

1. Introduction

1.1 Background

Soil organic carbon (SOC) from aboveground and belowground sources had rarely been differentiated even if it is crucial to better identify the location of SOC from different sources for parameterization of SOC models (Angst, John, et al. 2016). Especially subsoil were less investigated but has increasingly been recognized because of there importance for SOC storage and the terrestrial carbon cycle (Rumpel & Kögel-Knabner 2011). The main source of SOC is plant derived organic matter (OM). The OM stemming from either aboveground or belowground plant tissues. Belowground and aboveground organic matter sources may substantially different in its turnover and stabilization (Crow et al. 2009; Chabbi et al. 2009). Crow et al. (2009) showed that root derived compounds be a source of SOC with greater relative stability, whereas aboveground leaf litter was found to be a source of most actively cycling organic carbon (OC). This points to the importance to have a look to the origin and spatial distribution of SOC. There is still considerable debate on the origin of OM in subsoil – if it is supplied either from roots or transported down the profile from the aboveground litter and humus layer (Rasse et al. 2005; Kalbitz et al. 2000; Ohta et al. 1986). In forest soils there is also an influence of OM input with distance to the trees (Jandl et al. 2007). Aboveground even then belowground inputs may be strongly dependent on the spatial dimension that was mostly been overtaken in several studies. In a few studies, "distance" is becoming an interesting factor. One study found a significant small- scale variability of SOC stocks (Schöning et al. 2006). Another study investigated in chemical composition of soil organic matter fractions and SOC contents. Along these parameters no influence of the distance to individual tree could be found (Angst, Kögel-Knabner, et al. 2016). Both studies did not differentiate aboveground and belowground sources of OM. Other studies investigate in influence of rhizosphere and its effects to deep rooting plants (Gocke, Peth, et al. 2014). In this study, root- derived OM with distance from rhizolith center in loess sediment, was analyzed. Lipid molecular proxies deriving from *n*-alkanes and fatty acids (FA) were used to assess former rhizosphere processes (Gocke, Peth, et al. 2014). Angst et al. (2016) used a multi-biomarker approach to differentiate the source of SOC in subsoil. The study found no effect with the distance to trees, but a vertical zonation with high root derived inputs to the SOC in deeper subsoil.

Different sources of OM in soils still remain largely unknown and require further investigations.

1.2 Recent insights

When plant litter is incorporated into soil, it is loosing its morphology during degradation and is no longer of any value for inferring the origin. “Biomarker analyses may help to reconstruct plant type and even the type of plant tissue it originated from and whether or not the organic material was derived from above- or below- ground plant material” (Amelung et al. 2009). An approach to distinguish aboveground and belowground sources involves the analysis of solvent extractable lipids (Angst, John, et al. 2016; Wiesenberg & Gocke 2016). Lipids and hydrocarbons were performed in plant tissues, soils, sediments, peat deposits and other materials. The analysis of lipids contribute to different biological and anthropogenic sources of organic matter as well as environmental changes and the fate of organic matter like degradation (Wiesenberg & Gocke 2016). The plant derived aliphatic compounds included lipids, biopolyesters cutin and suberin and nonhydrolyzable biopolymers (Tegelaar et al. 1989). This masterthesis is using solvent extractable lipid biomarkers. Lipids are relatively stable in soils and could be detected after a certain period of time (Amelung et al. 2009).

Gocke et al. (2014) analyzed several horizontal transects compromising rhizolith and surrounding loess and analyzed for their carbon (C), alkane and fatty acid composition. This analysis obtains information on the source vegetation, of rhizolith and surrounding soil. The study relates to the assumption, that deep- rooting plants are a potential source for OM in subsoil (Gocke et al. 2010; Wiesenberg et al. 2010; Gocke, Peth, et al. 2014). An differentiation of the aboveground source vegetation for the upper soil is also possible with the lipid- analysis even than the stability of OM and microbial activity (Gocke et al. 2010).

The previous study at the study site at Bedafse Bergen described by a multi- proxy approach the multilayered plaggen soil (see 2.1). High root frequencies were not typically located in the topsoil. They were maximized in deep subsoil and therefore required further investigations even than the sources of the different soil layers that seemed to be derived from different aboveground biomass vegetation.

1.3 Research Questions and Aims

This thesis continues from the research of Kessler (2015) and will analyse the given profile with the help of lipid biomarkers. The aims of this study were to reveal the contributions to soil OC from aboveground and belowground plant sources in different soil layers and distance to collected roots using solvent extractable lipid biomarker. The plant aboveground biomass and also below ground roots were included to the lipid analysis. The aboveground- derived source of OC is representative in the plant aboveground biomass and could be compared to the soil.

It is hypothesized that the SOC in the recent Podzol should derive from the recent vegetation. Second, the lipid biomarkers from the recent Podzol and the buried relict Podzol will be compared. Based on a study by Van Mourik et al. (2012) we assume comparable vegetation conditions and similar plant types in the natural forest, which was located at the study site before the cut of the vegetation in the early Middle Ages.

It is known that roots alter the chemical composition in their direct vicinity (D. Sauer et al. 2006). However, the lateral extension of this influence is still discussed (e.g. Gocke et al., 2014). Therefore we assume deep-rooting plants as source for OC that were confirmed by *n*-alkane and FA proxies like average chain length and carbon preference index.

Thus this thesis has two key research questions or objectives:

- From which vegetation does the soil and sedimentary organic matter in the individual layers originate?
- Does soil and sedimentary organic matter at the study site origin mainly from plant aboveground biomass, as usually assumed, or do roots contribute considerable portions?

2 Methods and Materials

2.1 Study site

The study site for this field study is located near Bedaf in the vicinity of Uden. It is located in the Maashorst area in south east of the Netherlands (51°40.1891` N, 5°34.660`E). The soil- sediment sequence investigated in the current study was prepared in an oak stand (east) of the natural reserve of "Bedafse Bergen", a sand dune of > 10 m height which was formed during the early Middle Ages (Van Mourik et al. 2012). The land use history (*figure 1*) reached back to a deciduous forest growing on Late Glacial to Preboreal eolian coversand. After the clear of natural forest caused the transition into heath land (Van Mourik et al. 2012). During the Middle Ages (ca. 1500 AD) introduction of industrial fertilizer started (Blume & Leinweber 2004). Straw, fermented forest litter, grass and heath sods from the nearby landscape (van Mourik et al. 2016) were brought into stables and enriched with animal excrements. The plaggic manurs brought back to the field and allowed so agriculture on poor sandy soils (Giani et al. 2014). Intensification of land use after 1600 AD caused the degradation of the heath land (Driessen & Dudal 1991). Driftsand delivered from adjacent exposed landscape covered the Plaggic deposits. The sand was stabilized in the course of the 19th century under naturally regenerated and planted forest, which is still characteristic for the area in the natural reserve of "Bedafse Bergen". The recent vegetation comprises oak (*Quercus ruber*) with ages of up to 200 years, birch (*Betula alba*) and mountain ash (*Sorbus aucuparia*) as well as fern (*Dryopteris carthusiana*) and blackberry (*Rubus fruticosus*) (Gocke et al. 2015).

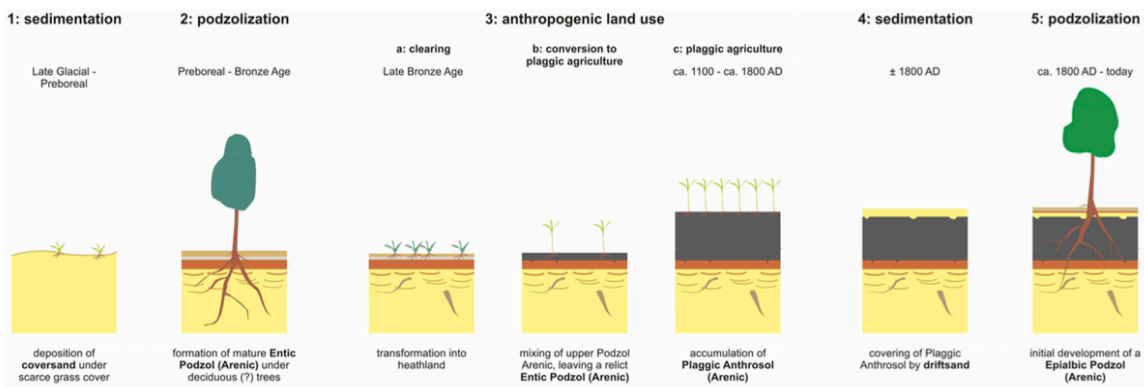

Figure 1: Development of the profile in Bedaf Bergen from Gocke et al., (2016).

2.2 Multi-layer profile

The investigated soil-sediment sequence comprised five layers. The deepest layer is a light yellowish cover sand (cs), which reaches from at least 1.8 m to 3.5 m. The transition between the coversand to the dark reddish-brown horizon of a relict Entic Podzol (1.5–1.8 m; rEP) is formed by sporadic, orange-reddish mottles that are found between 1.8 m and 2.25 m. In the depth from 0.4 to 1.5 m the grey colour Plaggen Anthrosol (PA) is found. This layer is characterized by the darkest colour and most dense, clayey material at the bottom, whereas the material was lighter and sandier towards the top. The top of the PA has an irregular boundary that was formed by plowing during the last phase of ancient agricultural use at this site. A yellow driftsand (ds) is overlaying the plaggen anthrosol (0.25–0.4 m) and filled up the plow furrows. Terminated is the profile by an Epialbic Podzol (0–0.25 m, EP) (Gocke et al. 2016). The complete Profile is shown in *figure 2*.

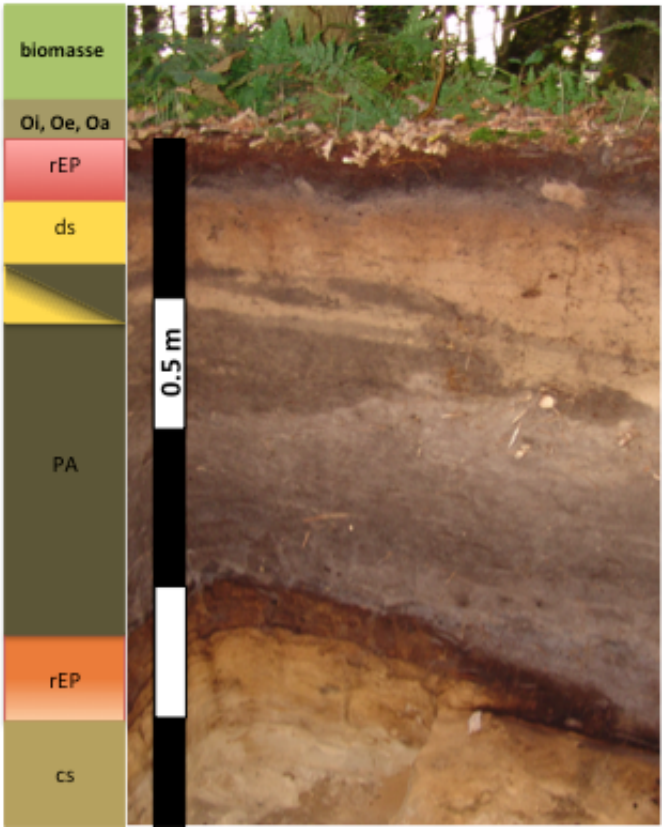

Figure 2: Multilayer profile in Bedaf Bergen modified from Gocke et al. (2016).

2.3 Profile preparation and field methods

The soil pit in "Bedafse Bergen" was prepared at ca. 1 m distance of a dead (< 10 years) standing oak tree at the left (N) side and a living oak tree at the right (S) side. The soil profile has a thickness of ca. 2.4 m. In the pit, the material was removed layer by layer in 10 cm depth increments down to 0.6 m. The increments from 0.6 m to 2.25 m have a depth of 15 cm. This sampling resolution was chosen to obtain samples from two different depths of each unit instead of pooled samples as described by Gocke et al. (2015). Because of the low thickness of the driftsand, one planar horizontal level was created at 0.25 m instead of 0.3 m to include its top and base. By analysing the soil-sediment sequence, it was investigated profile wall and each of the 18 horizontal areas

(lateral accounting for 0.8 m x 1.4 m). In both levels, roots were counted (see Gocke et al., (2015); chapter 2.4). During the time of sampling, the base of the coversand was not reached, similarly like the groundwater level which should be in a depth > 3.5 m (Gocke et al. 2016).

To assess of the influence of the roots on the surrounding soil or sediment, root- transect samples and root-core-transects samples were collected. From interesting levels (appearance of roots in soil) from horizontal profile, cylinders were punched out (*figure 3, A*). Horizontal growing roots in profile wall were sampled directly. Root and rhizosphere were separated in different plastic bags.

Root-core-transect samples were further processed in the lab and cut into concentric slices of 2 cm thickness around the central root (*figure 3, B-D*). Rhizosphere and root samples were further processed (see 2.4.2).

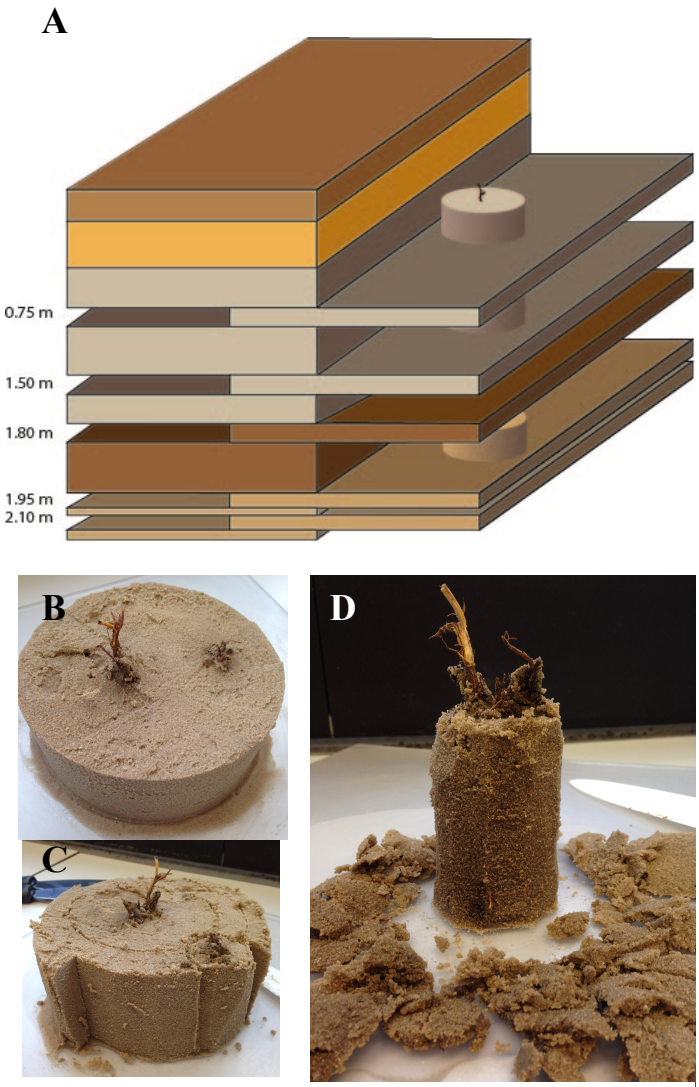

Figure 3: Sampling and preparation of root- transect. From different soil depth cores were punched into the soil (A) and further processed in the lab. Therefore in 2 cm distance, slices were cut (B-D).

Fresh soil were all oven-dried at 40 °C and were sieved using 2 mm sieves. The mineral soil fraction < 2 mm has to be further proceeded to remove organic particles with the tweezers as good as possible.

2.4 Sampling of plant material and sample preparation

2.4.1 Aboveground vegetation

The recent vegetation in Bedaf Bergen compromise different plants. There are 200 years old oak trees (*Quercus ruber*), some birch (*Betula alba*) and mountain ash (*Sorbus aucuparia*), as well as fern (*Dryopteris carthusiana*) and blackberry (*Rubus fruticosus*) (Gocke et al. 2016). The plants were collected and pre-processed in the lab. After oven dried (40 °C) the different plant parts were separated. The *Rubus fructiosus* was separated in leave and branches. From *Quercus ruber* bark, branches and leaves were collected. The bark was covered with lichen and moss, which had to be removed with the help of a toothbrush. From fern the leaves were separated from its stipe. Because Dryopteris carthusiana roots were very thin, they were collected with some soil and had to be further proceeded. By the help of a tweezers, roots were pitched on the soil and washed. In this sample set additional thin feathers were found. It could not be ruled out that these feathers contaminated the root sample from *Dryopteris carthusiana*. After the separation in different plant part, each part was milled in a horizontal ball mill (Retsch MM400; Retsch, Germany) after being oven-dried. All root samples were pre-treated. They were washed in deionised water before drying. This procedure guarantees the measurement of only plant sample itself without any adhering soil or sediment.

2.4.2 Root distribution

To determine quantities of roots along the profile, a grid with a side length of 0.5 m x 0.5 m subdivided into 9 squares was applied (see *figure 4*). Every horizontal level was careful brush cleaned and then the roots were counted in the different subdivided squares, which were then extrapolated to 1 m^2. A root classification along their different sizes (different classes include: fine (≤ 2 mm), medium (2-5 mm) and coarse roots (> 5 mm)) was used to account for the various source plants and the appearance of root processes in the rhizosphere. The root distribution, using the same grid for the counting, was quantified also at the profile wall, left and right side walls as well as the back of the profile wall. Dead and decaying roots were quantified separately from the living roots found in the profile. The method was used and described by Gocke et al. (2016) and Kessler (2015). After root counting, at each horizontal level four replicates of soil or sediment were collected (Gocke et al. 2015).

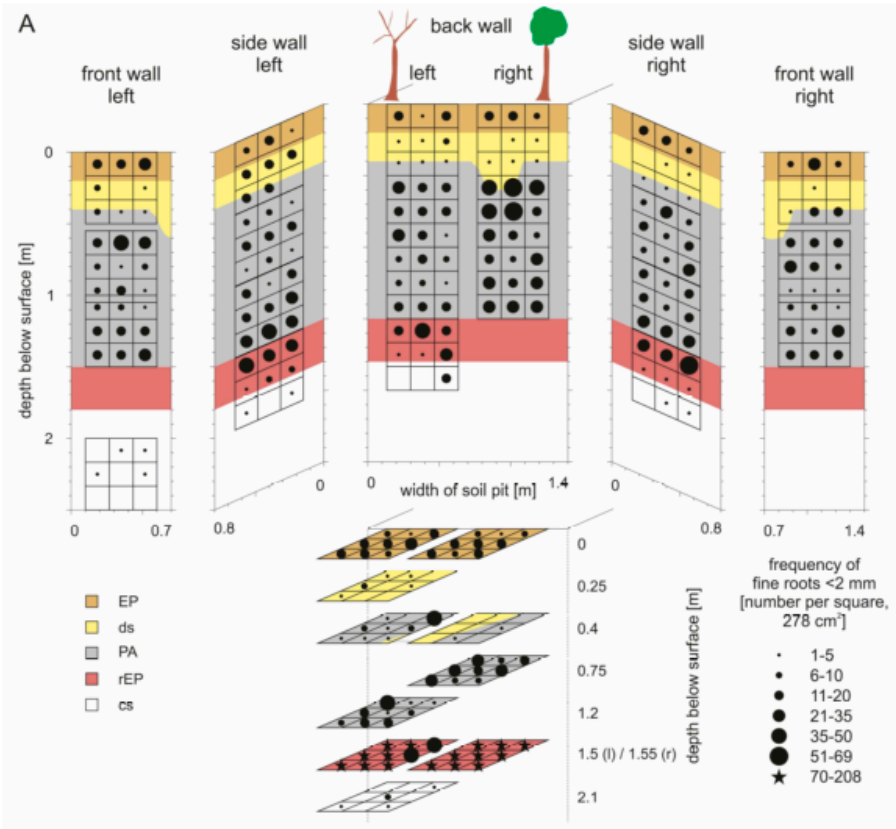

Figure 4: Root distribution with increasing depth in Bedafse Bergen. Shown is here the sampling method that include horizontal and vertical numbers of root. From Gocke et al., (2016).

2.5 Physical and geochemical analyses

For the measurement of to total carbon content the samples were sieved (< 2 mm) and milled in a horizontal mill (Retsch MM400; Retsch, Germany). The profile samples were previously measured using the Picarro instrument (Picarro SRDS G2131-i; Costech Analytical Technologies Inc., U.S.) and included in a previous master thesis (Kessler, 2015). The vegetation samples and some additional soil samples were measured at the elemental analyser-isotope ratio mass spectrometry (EA-IRMS) (Flash 2000 delta V plus isotope ratio MS). For measurement on Picarro but also for the measurement with EA-IRMS, 10-20 mg soil samples were filled in tin capsules (5x9 mm). For plant only 0.1–1.0 mg was used.

2.6 Biomarker analysis

2.6.1 Lipid Extraction

All soil and plant samples were extracted for free-extractable lipids via Soxhlet extraction, using solvent mixture of dichloromethane/methanol (93:7, v:v). The stainless glass thimbles were filled with 20-50 g of dried soil. For plant samples less plant material was needed, 0.5-3.5 g. The latter ones were run for at least 24 h, soil samples 48 to 96 h. The extraction resulting in the total lipid extract (TLE), that is transferred to a pre- weighted small (8 ml) glass. After the solvent mixture was completed dissolved, the vials were weighted again to be able to determine the TLE. The lipid extraction procedure was adopted from (Wiesenberg & Gocke 2016).

2.6.2 Separation of Lipid extracts into fatty acid and low polarity fractions

Lipid extracts were sequentially separated into 3 fractions of different polarity by solid phase extraction (SPE) using silica gel columns. 3 ml glass columns were half filled with potassium hydroxide (KOH)-coated silica gel. The silica gel was conditioned with DCM and air bubbles were removed using a Pasteur pipette. The TLE was dissolved in DCM and transferred to the column. From plant samples less than 30 mg of the total lipid extract were used for separation, whereas from soil samples max. 50 mg were used. Using ca. 50 ml of DCM, the first fraction (N), containing the low polarity compounds, was eluted from the column and collected. Afterwards, the fatty acid fraction (H) was eluted from the column using ca. 30 ml of a solvent mixture of higher polarity, DCM:formic Acid (99:1, v:v). After elution of the fatty acid fraction, the third fraction, containing high polarity and high molecular weight compounds (P) was eluted with methanol (MeOH) into a 4 ml glass vial. This fraction was not used for further analysis. Solvents of fractions N and H were reduced, then transferred to pre-weighted 4 ml vials (Wiesenberg & Gocke 2016).

Fraction H is now ready for the next step the methylation before it can be measured on the GC/MS.

2.6.3 Separation of low polarity fractions into aliphatic and aromatic hydrocarbons and heterofunctionalized organic compounds

As described in Wiesenberg and Gocke (2016) the low polarity fraction (N) was further separated into three fractions. To avoid an overload of columns, for plant samples <10 mg and for soil samples <20 mg of the low polar fraction was used. A glass pipette was filled up to a height of about 5 cm with silica gel (100 Å). The silica gel was activated in the oven (120 °C) over night. After pre-conditioning the column with *n*-hexane and removing air bubbles from silica gel, by pipette ball pressure, the respective N fraction, dissolved in a small amount of *n*-hexane, is transferred to the column. The column is flushed with ca. 20 ml of *n*-hexane to elute the aromatic hydrocarbons (A).

Afterwards, the heterocompounds (B) were eluted by a solvent mixture of *n*-hexane:dichloromethane (1:1; v:v). The fractions of the aliphatic and aromatic hydrocarbons (A) and the fraction of heterofunctionalized organic compounds (B) were each transferred into a 1.5 ml GC vial.

The last fraction that contains the long chain compounds (C) is eluted from the column with the solvent mixture dichloromethane:methanol (93:7; v:v). Fraction A and B could be measured directly via GC/MS. 50 µg of a deuterated (D) standard D_{50}-*n*-C_{24} alkane (tetracosane, Cambridge Isotope Laboratories Inc. DLM–2209– 0.5) is added in the A-fraction.

Fraction A includes the *n*-alkanes. Fraction B includes the mainly polycyclic aromatic hydrocarbons which derive from fires (Amelung et al. 2009). Because of limited time, the B- and C- fraction could not be evaluated and included in this masterthesis.

2.6.4 Methylation of the fatty acids

The fatty acid fraction (H) was methylated prior to GC/MS and (GC- flame ionization detector (FID); Agilent 6890) to make compounds amenable for measurement. Therefore, < 2 mg of the fatty acid fraction were dissolved in dichloromethane, 50 µg of the internal standard D_{39}-*n*-C_{20} acid and 500 µl boron trifluorid/methanol were added. Samples were shaken on a vortex than placed in a heating block at 60 °C for 15 minutes. After cooling down to room temperature, 500 µl water (Millipore quality) was added to the vial, and the sample was mixed on the vortex mixer again. The sample was

centrifuged for 1 min at 300 g. A glass Pasteur pipette was filled up to a height of about 1-2 cm with sodium sulphate (Na_2SO_4). The lower (organic) phase of the derivatized sample was transferred to the autosampler vial through the Pasteur pipette. DCM is added to the sample vial and the sample was mixed again on the vortex mixer, centrifuged, and the organic phase was transferred over the column to an autosampler vial. This process is repeated for about 5 to 7 times or until the organically phase looked colourless (Wiesenberg & Gocke 2016).

In some samples, the wrong standard (D_{50}-*n*-C_{24} alkane) was added. For those samples, the internal standard D_{39}-*n*-C_{20} acid was methylated as described above and was then added to these samples.

2.6.5 Measurement on GC/MS

The GC/MS measurement could identify and quantify defined amounts of various samples (G. L. B. Wiesenberg et al. 2004). The measurement of the different compound assignment and quantification of different samples was performed on GC instrument (Agilent 128-5552; Column 50 m x 200 µm x 0.33 µm; Flow: 1.07 ml/min) with split less injector and flame ionisation detection. For *n*-alkanes the measurement was programmed for 70°C; fatty acids at 50°C. The outputs from GC-MS were used for identification of the different accounts. After peaks were apportioned to a specific molecule, the GC-FID data were used for quantification. Therefore integrals were calculated.

2.6.6 Calculations of biomarker proxies

2.6.6.1 Alkanes

The carbon preference index (CPI_{ALK}) was calculated for long chain alkanes C_{25} – C_{33} Alkanes. The CPI_{ALK} is applied as a proxy for (bio-) degradation and microbial reworking (Freeman, K.H., Colarusso 2001; Zhaohui Zhang et al. 2006). Fresh plant biomass is typically enriched in odd n-alkanes (Eglinton et al. 1962). This circumstance is shown by high CPI_{ALK} values (>10). Strong degradation of OM is characterised by CPI_{ALK} values close to 1 (Cranwell 1981).

$$CPI_{ALK} = ½* \Sigma (X_i + X_{i+2} + .. + X_n)/ \Sigma(X_{i-1} + X_{i+1} + .. + X_{n-1}) + 1/2* \Sigma(X_i + X_{i+2} + .. + X_n)/ \Sigma (X_{i+1} + X_{i+3} + .. + X_{n+1}),$$ with i = 25 and n=33; X= abundance.

The average chain length (ACL_{ALK}) is an indicator to evaluate changes in paleo environmental conditions and vegetation composition (Zhaohui Zhang et al. 2006). The ACL_{ALK} of alkanes is known to could differentiate between higher plant derived organic matter with values higher than 25 (Eglinton et al. 1962) and degraded organic matter, which is microorganism derived (< 25) (Bray & Evans 1961).

$$ACL_{ALK}= \Sigma(i* X_i)/ \Sigma X_i,$$ where X is abundance and i ranges from 16 to 33

The ratios of the acyclic isoprenoids pristane (Pr) to *n*-C_{17} and phytane (Phy) to *n*-C_{18} are frequently used in environmental geochemistry for estimating and monitoring biodegradation patterns (Cameron et al. 2007). It is known, that acyclic isoprenoids are commonly derived from chlorophyll during diagenesis (Rontani & Volkman 2003). Regarding this fact one could suggest that higher values in pristine/C_{17} and phytane/C_{18} indicate a higher biodegradation.

The long-chain n-alkane ratios (LARs) could be indicators to differentiate different plant groups (Borges del Castillo, J., Brooks, C.J.W., Cambie, R.C., Eglinton, G., Hamilton, R.J., Pellitt 1967; Schwark, L., Zink, K. and Lechterbeck 2002). Long chain n-alkanes distribution patterns dominated by *n*-C_{27} or *n*-C_{29} in woody vegetation. Grassland plants often dominated by *n*-C_{31} and *n*-C_{33} alkanes (Borges del Castillo, J., Brooks, C.J.W., Cambie, R.C., Eglinton, G., Hamilton, R.J., Pellitt 1967; Schwark, L., Zink, K. and Lechterbeck 2002). Hence these compounds are useful tools for the source determination of fossil organic material (Schwark, L., Zink, K. and Lechterbeck 2002; Zhaohui Zhang et al. 2006).

$$C_{27}/C_{31}, C_{29}/C_{31}, C_{31}/C_{29}$$

The ratio $C_{31}/(C_{27}+C_{29}+C_{31})$ is an indicator that represents relative molecular fossil abundance of grass and plants in samples (Zhang et al. 2008).

$$C_{31}/(C_{27}+C_{29}+C_{31})$$

2.6.6.2 Fatty acids

Carbon preference index (CPI_{FA}) was calculated for $C_{20} - C_{32}$ fatty acids. Similar to the calculations of the alkanes, the CPI_{FA} was calculated for FAs with even-over-odd predominance. Low CPI_{FA} values (< 4) are characteristic for strongly degraded OM (Cranwell 1981; Cranwell et al. 1987)

$$CPI_{FA} = ½* \Sigma (X_i + X_{i+2} + .. + X_n)/ \Sigma(X_{i-1} + X_{i+1} + .. + X_{n-1}) + 1/2* \Sigma(X_i + X_{i+2} + .. + X_n)/ \Sigma (X_{i+1} + X_{i+3} + .. + X_{n+1}),$$ with i = 20 and n= 32.

The average chain length (ACL_{FA}) is also calculated for fatty acids. The parameter has been used in soils for the differentiation of microorganism and plant derived OM. Higher values (> 20) contribute input from plant biomass (Kolattukudy, Croteau & Buckner 1976a).

$$ACL_{FA}= \Sigma(i* X_i)/ \Sigma X_i,$$ where X is abundance and i ranges from 9 to 33

Ratio of saturated vs. unsaturated (RSU) C_{16} and C_{18} acids were calculated (Schwark, L., Zink, K. and Lechterbeck 2002). It is known, that plants and microbial biomass are rich in unsaturated fatty acids (Harwood & Russell 1984). Regarding the fact, that the latter are susceptible to fast degradation one could suggest that high RSU values indicate a low degree of preservation of organic matter.

$$RSU = (C_{16:0} + C_{18:0})/ (C_{16:1} + C_{18:2})$$

Fatty acids mainly derived from microorganisms were $< C_{20:0}$ and $C_{16:1}$, $C_{18:1}$ (Jobbágy & Jackson 2000). Therefore the sum of mono-unsaturated FAs (MUFA) are calculated.

$$MUFA = \sum(C_{16:1}; C_{18:1})$$

2.6.7 Statistical analyses

Data sets of alkanes (CPI_{ALK}, ACL_{ALK}, LAR_{1-4}, pristane/C_{17} and phytan/C_{18}) and fatty acids (CPI_{FA}, ACL_{FA}, unsaturated/saturated fatty acids) were tested for significance of differences between sample groups (leaves, branches, roots, bark, organic layer, EP, ds, PA, rEP, cs) using one-way ANOVA with a significance level of $p = 0.05$, followed by post- hoc (LSD and Bonferroni) test. Homogeneity of variances was only achieved for LAR_4, ACL_{ALK} and pristan/C_{17} in alkanes and CPI_{FA} in fatty acid data set. For all samples were homogeneity of variances was not achieved the Welch and Brown-Forsythe test was additionally launched. Because of missing values, some groups where excluded for post-hoc test. For pristane/C_{17} group roots, EP and cs where excluded. In LAR_2 and LAR_3 group "bark" and in phytane/C_{18} all plant groups were omitted. The statistical evaluations were performed using IBM©SPSS© Statistics, version 21 software.

3 Results

3.1 Profile and Plants

3.1.1 Organic carbon and lipid content of the profile

The profile and its physical parameters of the profile were analysed by Kessler (2015). The profile is dominated by a sandy texture with sand content between 91 and 99 %. Highest clay values were found in the Plaggic Anthrosol.

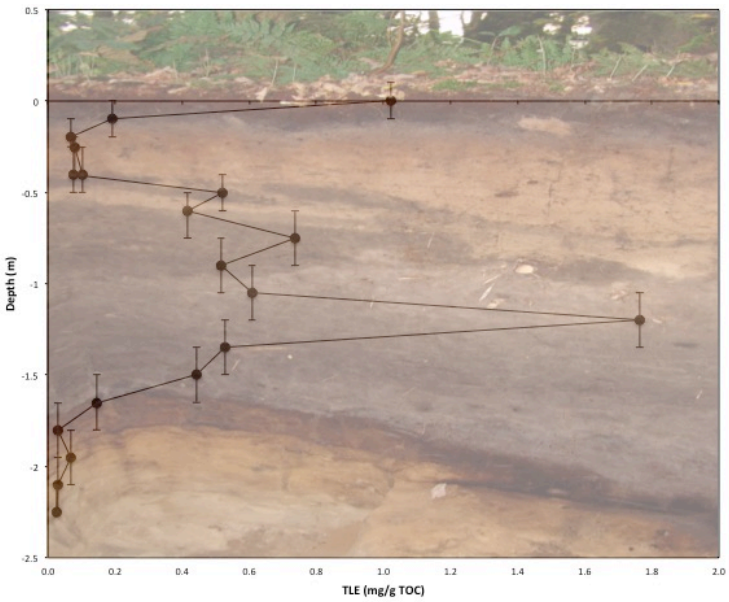

Figure 5: Total lipid extract (mg/g TOC) along the profile. From Kessler (2015).

The whole profile shows acidic pH values that were fluctuating along the profile between 3.1 and 4.7. Highest organic carbon (C_{org}) contents were found in the organic layers and the plaggen soil. They correlate with enriched total lipid extract (TLE) values (*figure 6*). *Figure 5* shows the distribution of the TLE along the profile excluding the organic layers. Variations within a soil layer could result from the heterogeneity of the soil. The organic carbon content varies in the profile and correlates with the TLE yields.

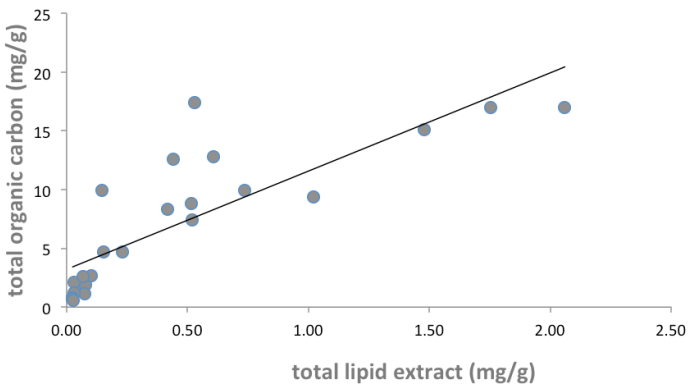

Figure 6: Total organic carbon and total lipid extract show a correlation in there values.

3.1.2 *n*-Alkane composition

The aliphatic hydrocarbons fraction consists of *n*-alkanes and lower amounts of isoprenoid alkanes (pristine and phytane) and very low amounts of pentacyclic triterpenoids (G.L.B. Wiesenberg et al. 2004). Pentacyclic triterpenoids are not discussed further in this master thesis.

In the profile, the distribution pattern of *n*- alkanes ranging from C_{16} to C_{33}. Between the layers, differences in the range of the *n*-alkanes distribution are visible *figure 7.*

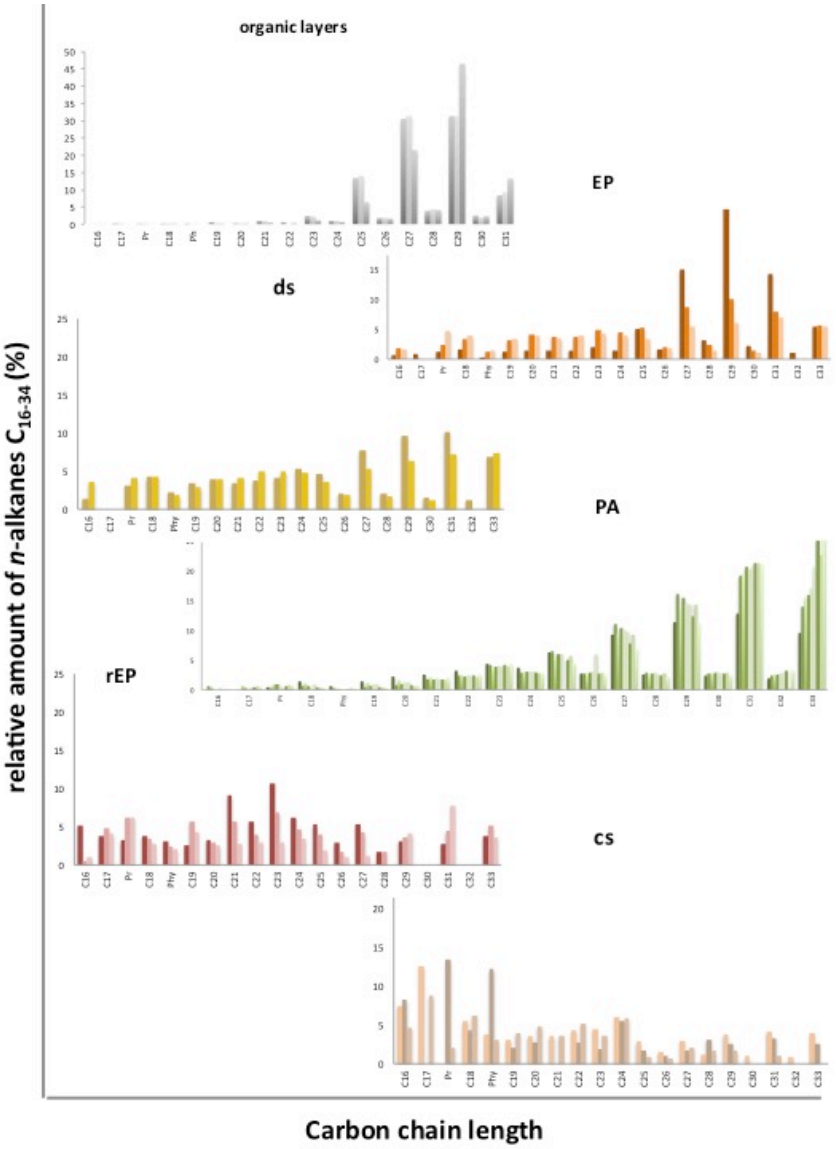

Figure 7: Relative distribution of n-alkanes in different profile layers normalized to alkanes C_{16-33}. The different color variations stands for different samples from a specific layer.

For EP and ds layer C_{27}, C_{29} and C_{31} are the *n*-alkanes identified as the most abundant components. In the plaggen horizon, C_{27}, C_{29}, C_{31} and C_{33} showed high amounts. For deeper parts in the profile (rEP and cs) a shift of the most abundant components to lower chain length was visible. In relict Podzol (rEP) C_{21} an C_{23} are dominant. In coversand layer (cs) C_{16}, C_{17} and C_{24} have the highest concentration. The different samples from a specific layer showed small variability in the amounts of different *n*-alkanes. In general, the sample within a layer followed the same trend in their chain length distribution of the different *n*-alkanes (*figure 7*).

Odd *n*-alkanes are dominant for all leave and branches samples shown in *figure 9*. Plant samples obtained from the aboveground biomass yield results of n-alkane from C_{17} to C_{31} with the most abundant component C_{29}. Depicted in *figure 8* is the most represented range from C_{23} to C_{31}. The bars represent single values. Only in *Dryopteris carthusiana* leave sample, C_{30} to C_{31} could not be found in the GC output. In *Quercus ruber* leaves, C_{27} and C_{29} *n*-alkanes are almost similarly abundant. In *Sorbus aucuparia* C_{29} dominated the alkane distribution pattern with 75%. The other leave samples showed percentages from 25 to 50% for their maxima at C_{29}. In branch samples, C_{29} exhibit the maximum for *Quercus robur* (50%) and *Rubus fructiosus* (27%). *Sorbus aucuparia* leaves were dominated by C_{27} (28%). In root saples, the dominance of odd *n*-alkanes is only visible for *Rubus fructiosis* and *Sorbus aucuparia*. In *Quercus robur* root, a dominance of odd-chain homologues was detected in the range C_{26} to C_{31}. The *n*-alkanes abundance in *Dryopteris carthusian* roots increased from C_{23} to C_{29} maximizing at C_{29}.

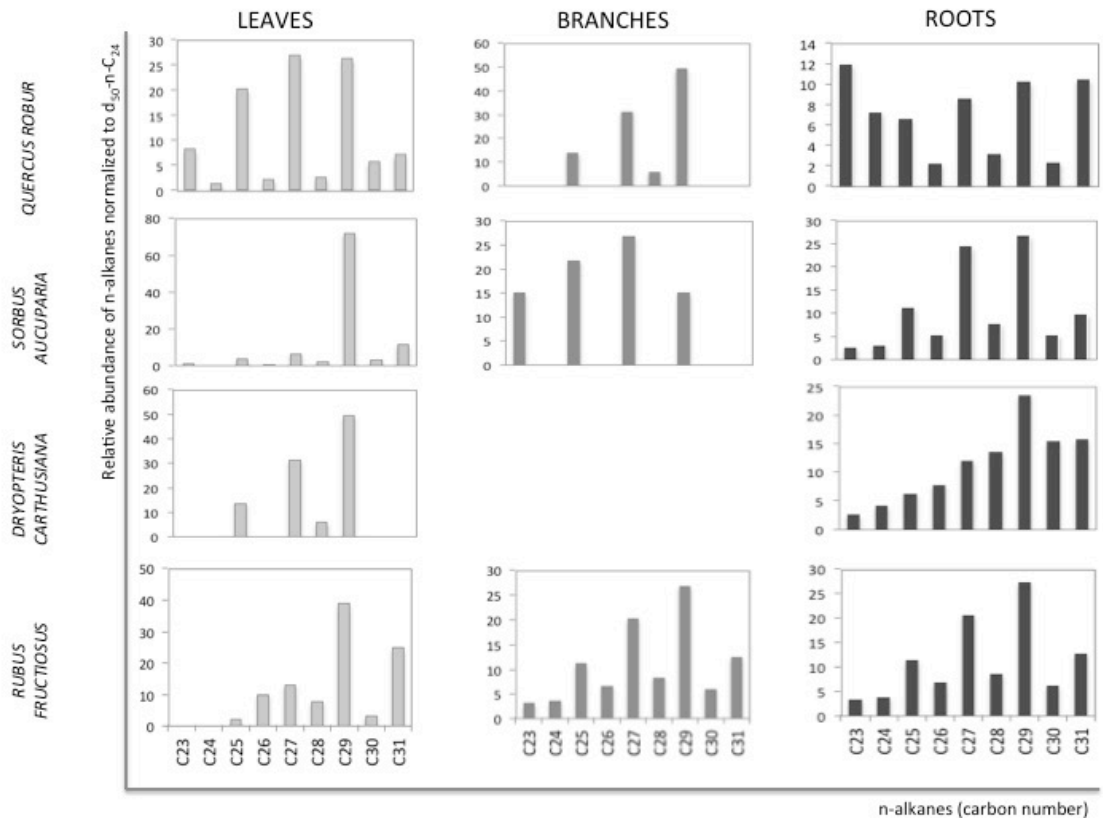

Figure 8: Quantitative n-alkane patterns of different plant parts normalized to D_{50}*–n-*C_{24}*.*

The ternary diagram (*figure 9*) shows the relative composition of the most abundant *n*-alkanes in the profile and the aboveground biomass C_{25}, C_{27}, C_{29} C_{31} and C_{33}. The data points are matter of single values of the different classes EP, ds, PA, rEP, cs and organic layers (Oi, Oe, Oa). Plant aboveground biomass (leaves, branches, roots, bark) was also included. Discrimination between soil samples and aboveground biomass could be achieved by plotting long-chain *n*-alkanes as molecular indicators for plant biomass. Plant samples were plotted in the right corner with higher C_{29} *n*-alkanes and lower $C_{31,33}$ $_n$-alkanes than the soil layers. The organic layers were plotted in the same corner than the plant samples. The soil samples contained higher relative very long chain *n*-alkanes ($C_{31,33}$). Plaggen soil contained the highest relative $C_{31,33}$ and C_{29} contetns and low C_{27} *n*-alkanes compared to the other soil layers. Driftsand and coversand have a relative distribution of C_{29} (40-50%), $C_{25,27}$ (35-45%) and $C_{31,33}$ (60-70%) $_n$-alkanes. The coversand shows one single value that is closely blotted to the roots. This sample was found at the bottom of the profile in the coversand layer. Another sample from the recent Podzol is also blotted next to the root samples. The grey boundary in *figure 9* shows the distribution of the different soil samples within the ternary diagram. With also high values than the Plaggic Anthrosol, the relict Podzol had lower relative C_{29} contents and

higher relative $C_{25,27}$ contents than Plaggen soil, dirftsand and coversand. The recent Podzol is blotted closer root samples from aboveground plants.

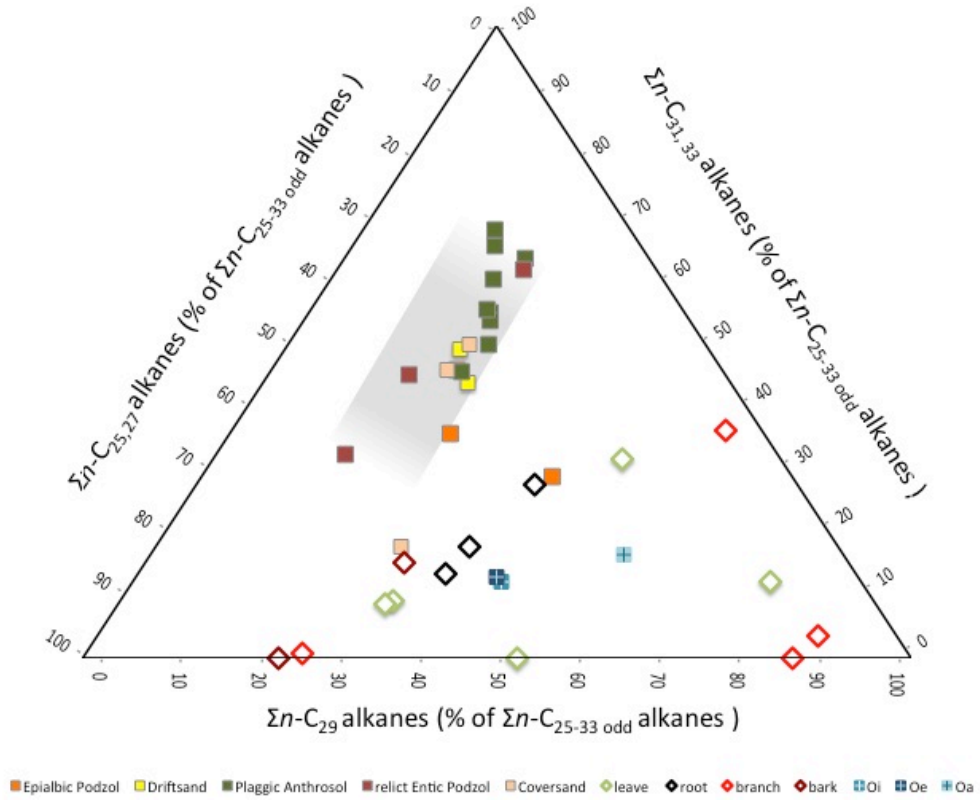

Figure 9: Relative portions of odd long chain n-alkanes (C_{25-33}) for single soil and plant samples.

As shown in *figure 9* there were differences in the distribution patterns between plant and soil, between different plant organs, and between the different soil layers. Different parameters (ACL, CPI, different *n*-alkane ratios) were calculated along the profile and within plant tissues (leave, bark, branch, root). The results of these calculations are shown in *table 1*. Fresh plants had its maximum of relative portions of *n*-alkane normalized to total *n*-alkanes (C_{16-33}) by the majority at C_{27} or C_{29}. Maximum portions of n-alkanes were different between plaggen soil and the remaining layers. In Plaggen Anthrosol maxima were recorded at C_{31} or C_{33}. The recent Podzol had its maximum portion of *n*-alkanes normalized to total *n*-alkanes (C_{16-33}) at C_{27}, C_{29} and C_{31}. The rEP is different from the Podzol with maximum portions at C_{31}. Cover sand had most abundant *n*-alkanes in shorter chain length with maximum in portions at C_{16} or C_{24}.

The hydrocarbons pristane and phytane could not be detected in plant samples with only two exceptions. Pristane is found in aboveground biomass and roots of *Dryopteris carthusiana.* In soil and organic layers pristane and phytane are found in most of the

samples. The statistical analysis with one-way ANOVA and post-hoc test shows nonsignificant differences between groups (= bark, branches, leaves, organic layer, EP, ds, PA, rEP and ds) for pristine/C_{17} ratio (F (6,9)= 2.119, p= 0.168). In phytane/ C_{18} ratio there are differences between groups (F (5,17)= 1.963, p= 0.136. Significantly different are organic layer to cs group (p= 0.023) and plaggen anthrosol to coversand (p= 0.017). Plant groups were not included in the analysis because of missing values in these groups.

LAR_1 showed the ratio [$C_{31}/(C_{27}+C_{29}+C_{31})$] from Zhang et al. (2008). These ratios reflect the relative proportion of waxy hydrocarbons that derived from plants (Duan & He 2011). In branch samples the values ranged from 0.01 to 0.37. Leaves had values at 0.11-0.32 for LAR_1 and root sample at 0.16-0.31. In the profile, the values were much higher. The organic layer showed similar values to vegetation samples from 0.12 to 0.16. They increased with increasing depth in the profile. Values in the EP layer reached from 0.24 at the top to 0.37, increased with depth. The driftsand layer was similar with value 0.38 ± 0.01. The PA layer reached from upper part with value 0.41 and gained to 0.54 at the base of the layer. The value in the rEP was lower with values at 0.25 to 0.6. The coversand layer at the base had values at 0.32 ± 0.12.

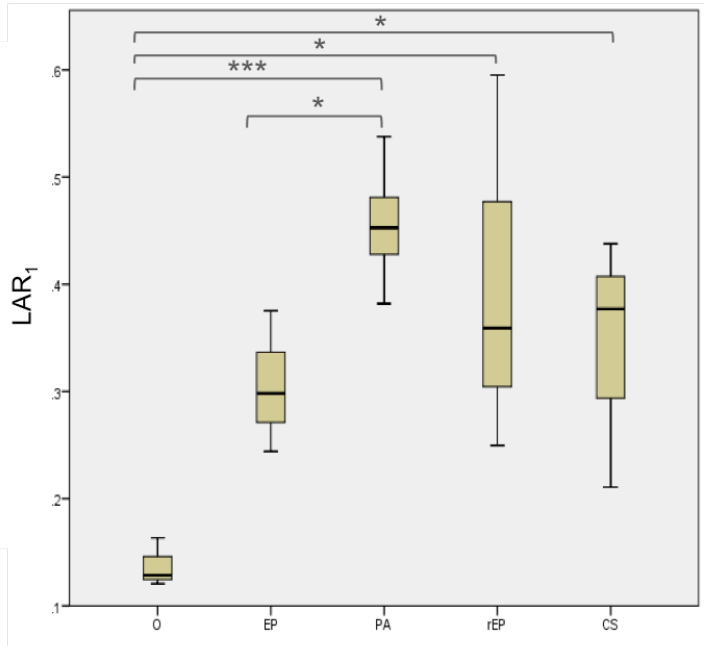

Figure 10: LAR_1 shows $C_{31}/\sum(C27, C29, C31)$ and stands for relative proportions of waxy hydrocarbons that derived from plants. One asterisk stands for significantly differences between different groups, 3 asteriks stands for very high significant differences.

Different plant groups (including leaves, roots, branches, bark and organic layer) do not showed significantly differences (p> 0.05). The boxplot (*figure 10*) showed the difference soil layers. Between the different profile layers, there were significant differences (F(9,25)= 6.185, p=0.000). The organic layers were significantly different to the other soil layers excepting EP (p= 0.063). The Epialbic Podzol was significantly different to bark (p= 0.40), leaves (p=0.37) and the plaggen soil (p= 0.47) (not shown in *figure 10*). The rEP group was also significant different to bark (p= 0.004), leaves (p= 0.002) and

additionally to branches (p= 0.005). Plaggen Anthrosol was significantly different to all plant groups including also the organic layer. Driftsand differed from branches (p= 0.021), bark (p= 0.014), leaves (p= 0.012) and the organic layer (p= 0.021). The coversand was significantly different to the organic layers (p= 0.026).

LAR_2 and LAR_3 represent ratios between predominant *n*-alkanes. LAR_2, that represents C_{27}/C_{31} alkane ratio, showed lower values (0.4 ± 0.2) for PA layer than for the other profile layers (see *table 1*). Leave samples *Quercus robur* had a high ratio of C_{27}/C_{31} at 3.8 (± 0.2). *Rubus fructiosus* (0.5) and *Sorbus aucuparia* (0.6) had lower values. Highest value was found in the organic layers (Oi, Oe, Oa) at values 2.6 ± 1.0 and the recent and relict forest soil (1.0 ± 0.9). The LAR_2 value in rEP decreased strongly top-down (*table 1*). The LAR_2 showed significant differences (F(8,23)=1.287,p=0.031). Between the different layers wasn`t found a significant difference (p> 0.05) of LAR_2 values (post-hoc test). Bark differed (p< 0.05) from soils and different plant tissues (leaves, roots, branch).

LAR_3 depicted the ratio between C_{29} to C_{31} *n*-alkanes. The trends looked similar to those built up by LAR_2 and significant differences were not plotted between different soil layers (*table 1*).

LAR_4 describes the ratio between C_{31}/C_{29}. The levenes test confirmed the varianzhomogenity and one way ANOVA indicated highly significant differences between the different groups (F(9, 26)= 13.393, p= 0.000). The post- hoc test showed that all plant tissues (leave, branch, root, bark, organic layer) had non significantly differendes in there C_{31}/C_{29} values (p> 0.05). All plant tissues (leave, branch, root, bark) were significantly different to the soil groups except for roots which were not significantly different to EP. Between the different soil groups there were a highliy significant difference between PA and EP (p= 0.003). rEP and EP (p= 0.027), cs and PA (p= 0.029)

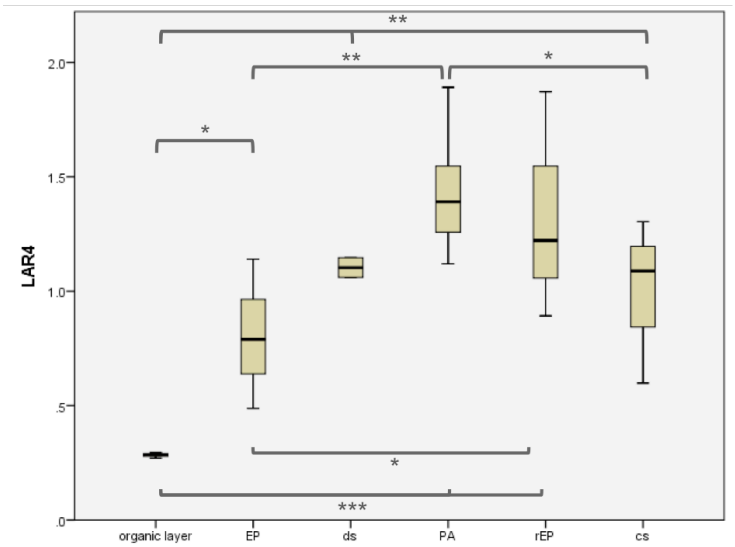

Figure 11: Boxplot of LAR_4 (= C31/C29). One asterisk shows significantly differences between the groups, two asterisk stands for high significant differences.

were significantly different (*figure 11*).

CPI values of C_{25-33} *n*-alkanes (CPI_{ALK}) ranged from 3 to 34 in branch , 7 to 16 in leave , 1 to 4 in root- and 2 to 11 in soil samples. The average CPI_{ALK} for branch samples was 17.5 ± 13.3, for leaves 10.8 ± 5.0, roots had a value of 2.7 ± 1.2. Between soil layers and plant tissues were significant differences ($F(8,25)= 3.167$, $p= 0.001$). In plant samples, leaves and branches were not significantly different ($p> 0.05$). But both differed from root samples ($p_{branche,\ root} = 0.001$, $p_{leaves,\ root}= 0.041$). The organic layer was not significantly different to all plant tissues (leave, branche, root, bark) and soil groups (EP, ds, PA, rEP, cs).

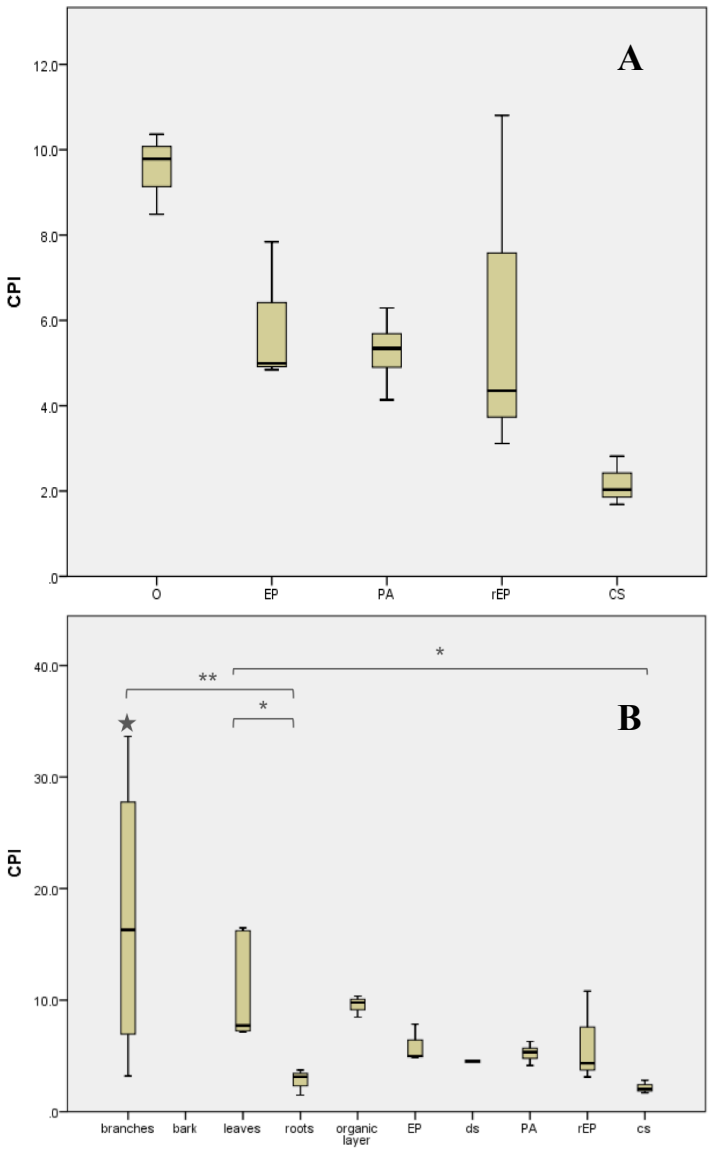

Figure 12: Boxplot of carbon preference index of n-alkanes C_{25-33}. An asterisk marked significant differences between groups. Two asterisk stands for high significant differences. A shows the boxplot from soil layers. In B are different plant groups and soil layers analyzed. The big star for "branches" is B marked the group, that is significant different to every other group.

Part	Species	Range	C_{max}	Pr	Phy	Pr/C_{17}	Phy/C_{18}	Distibution	ACL_{ALK}	CPI_{ALK}	LAR_1	LAR_2	LAR_3	LAR_4
branches	*Quercus robur*	C17; C19 - C31	C27	x	x			multimodal	26.8	11	0.01	-	-	0.0
branches	*Rubus fruticosus*	C23 - C31	C29	x	x			unimodal	29.3	3	0.37	0.1	1.7	0.6
branches	*Sorbus aucuparia*	C21 - C31	C29	x	x			unimodal	28.7	34	0.04	2.1	24.2	0.0
stem	*Rubus fruticosus*	C17; C23 - C29	C29	x	x			-	27.4	22	-	60.9	33.1	0.0
bark	*Quercus robur*	C17; C21-C31	C27	x	x			-	24.9	-	0.00	2.1	2.1	0.2
bark	*Quercus robur*	C19-C29	C27	x	x			-	25.7		0.19	-	-	0.0
leaves	*Sorbus aucuparia*	C23 - C31	C29	x	x			unimodal	28.9	16	0.13	0.6	6.4	0.5
aboveground biomass	*Dryopteris carthusiana*	C25 - C29	C29	✓	x	0.38		unimodal	16.9	16	0.00	-	-	0.0
leaves	*Rubus fruticosus*	C25 - C31	C29	x	x			multimodal	29.1	7	0.32	0.5	1.6	0.6
leaves	*Quercus robur*	*C23 - C31*	C27	x	x			multimodal	27.2	7	0.12	3.7	3.7	0.3
leaves	*Quercus robur*	*C23 - C31*	C27	x	x			multimodal	27.2	8	0.11	4.0	3.8	0.3
roots	*Sorbus aucuparia*	C17; C22 - C31	C29	✓	x	0.41		multimodal	27.2	4	0.16	2.5	2.8	0.4
roots	*Rubus fruticosus*	C23 - C31	C29	x	x			multimodal	27.8	3	0.21	1.6	2.1	0.5
roots	*Dryopteris carthusiana*	C23 -C31	C29	✓	x	34.47		unimodal	27.0	1	0.31	0.8	1.5	0.7
organic layer: Oi	0.75	C17 - C31	C29	✓	✓	0.74	0.52	multimodal	27.5	8	0.12	3.6	3.7	0.3
organic layer: Oe	0.5	C17 - C31	C29	✓	x	0.47		multimodal	27.6	10	0.13	3.4	3.4	0.3
organic layer: Oa	0.25	C18 - C31	C29	x	x			multimodal	28.3	10	0.16	1.6	3.5	0.3
EP	0	C16 - C33	C29	✓	✓	1.63	0.21	unimodal	27.8	8	0.24	1.0	2.0	0.5
EP	-0.1	C16 - C33	C27	✓	✓		0.39	multimodal	25.7	5	0.3	1.1	1.3	0.8
EP	-0.2	C16 - C33	C31	✓	✓		0.38	multimodal	25.2	5	0.38	0.8	0.9	1.1
ds	-0.25	C16 - C33	C31	✓	✓		0.53	multimodal	26.0	4	0.37	0.8	0.9	1.1
ds	-0.4	C16 - C33	C31	✓	✓		0.43	multimodal	25.1	5	0.38	0.7	0.9	1.1
PA	-0.4	C18 - C33	C31	✓	✓		0.38	increasing ltr	27.4	4	0.38	0.7	0.9	1.1
PA	-0.5	C16 - C33	C31	✓	✓		0.51	increasing ltr	28.4	5	0.41	0.6	0.8	1.2
PA	-0.6	C16 - C33	C31	✓	✓	1.26	0.25	increasing ltr	28.2	5	0.45	0.5	0.7	1.4
PA	-0.75	C17 - C33	C31	✓	✓	2.68	0.26	increasing ltr	28.6	5	0.44	0.5	0.8	1.3
PA	-0.9	C17 - C33	C31	✓	X	4.05		increasing ltr	28.7	5	0.45	0.5	0.7	1.4
PA	-1.05	C16 - C33	C31, C33	✓	✓	0.83	0.20	increasing ltr	28.8	4	0.46	0.5	0.7	1.4
PA	-1.2	C17 - C33	C33	✓	✓	1.32	0.49	increasing ltr	29.1	6	0.5	0.4	0.6	1.6
PA	-1.35	C17 - C33	C33	✓	✓	1.64	0.48	increasing ltr	29.2	6	0.54	0.3	0.5	1.9
rEP	-1.5	C16 - C33	C23	✓	✓	0.86	0.81	multimodal	23.2	3	0.25	1.9	1.1	0.9
rEP	-1.65	C16 - C33	C23	✓	✓	1.27	0.73	multimodal	23.9	4	0.36	1.0	0.8	1.2
rEP	-1.8	C16 - C33	C31	✓	✓	1.53	0.74	multimodal	24.3	11	0.60	0.1	0.5	1.9
cs	-1.95	C16 - C33	C16; C17; C24	X	✓		0.70	multimodal	22.4	3	0.38	0.7	0.9	1.1
cs	-2.1	C16 - C33	C16; C24	✓	✓		2.79	multimodal	23.1	2	0.44	0.5	0.8	1.3
cs	-2.25	C16 - C31	C17; C24	X	✓		0.55	multimodal	21.6	2	0.21	2.1	1.7	0.6

Table 1: This table shows the sample set from profile and plant biomass and results from different parameters like ACL_{ALK}, CPI_{ALK}, LAR_{1-4} and other ratios with pristane and phytane. Also shown are distribution and maximum levels of n-alkanes.

EP had a man value of 6 ± 1.7, ds had a CPI_{ALK} mean value of 4 ± 0.4, plaggic anthrosol at 5.1 ± 0.7, rEP around 6 ± 4.1 and cs a value at 2.3 ± 0.6. Highest CPI mean values were recorded in the PA, lowest values in the coversand at the base of the profile. *Figure 12A* shows the single CPI_{ALK} values along the proflie. In a depth of -1.80 m at the base of the relict forest soil (rEP) there was a maximum of CPI_{ALK} found. Similar high values could only be observed in the organic layers. The other CPI_{ALK} values showed a decreasing trend from topsoil downward the profile wall (exept for the outliner at 1.80 m). Between the soil groups, there were no significant differences (P> 0.05). All soil groups had no significant difference between the layers and group leave, organic layer and roots (p>0.05) excepting layer cs. In this layer also the roots were significanty different (p= 0.029). The branches differed from each layer with p> 0.05 (marked in *figure 12B* with a star).

The average chain legth of *n*-alkanes (ACL_{AKL}) showed the highest value in the PA. The statistical analysis showed significantly differences between the plant tissues and the soil layers (F(9,27)= 4.189, p= 0.000). The box plot diagramm (*figure 13*) show the different groups. Significantly differences were indicated by an asterisk. Between the soil layers significantly differences had been detected between EP and cs (p= 0.010), PA and rEP (p=0.003), and cs (p=0.000), rEP and organic layer (p=0.28). The coversand layer was significantly different to every group expecting ds and bark.

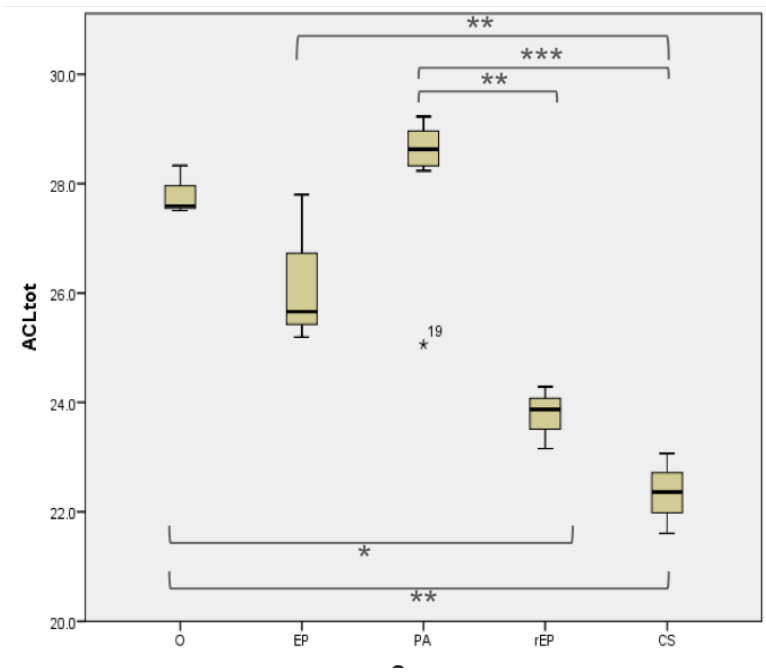

Figure 13: Boxplot of average chain length of different soil layers. An asterisk marked significant differences. Highly significant differences is shown by 2 asterisks, very high significant differences with 3 asterisks.

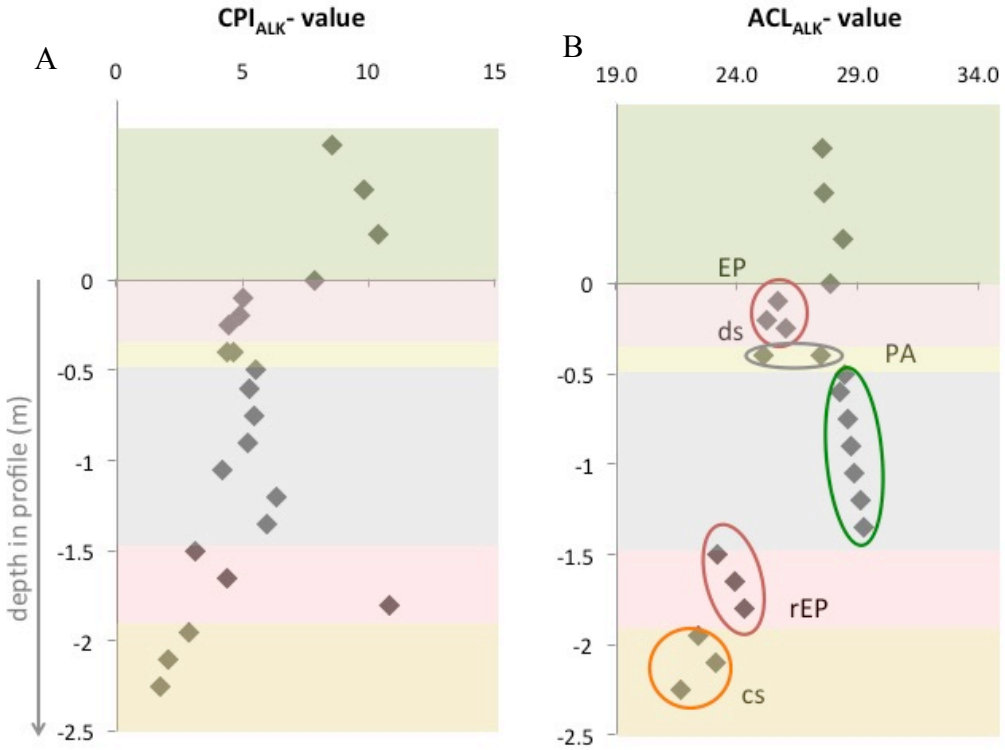

Figure 14: Shown are carbon preference index (A) and average chain length (B) for n-alkanes in the profile. Each data point represents a single soil sample. Cluster were marked by a circle (B). Values for organic layer were schematic shown above the profile with the order top down: OI, Oe, Oa.

Depicted in *figure 14,B* are the distibution clusters within a soil layer of the ACL_{ALK} value. For CPI_{ALK} such a separation was not possible (*figure 14,A*). Noticabel was the high value at the base of the relict Podzol. By having a look at the other values in the relict forest soil there could notice an increas within the rEP layer of CPI values. This high value is all likelihood a spike.

3.1.3 Carboxylic acids

This fraction consists mainly of saturated and mono- as well as di-unsaturated straight chain n-carboxylic acids (G.L.B. Wiesenberg et al. 2004). Polyunsaturated and branched acids occurred in very low amounts and are not further discussed.

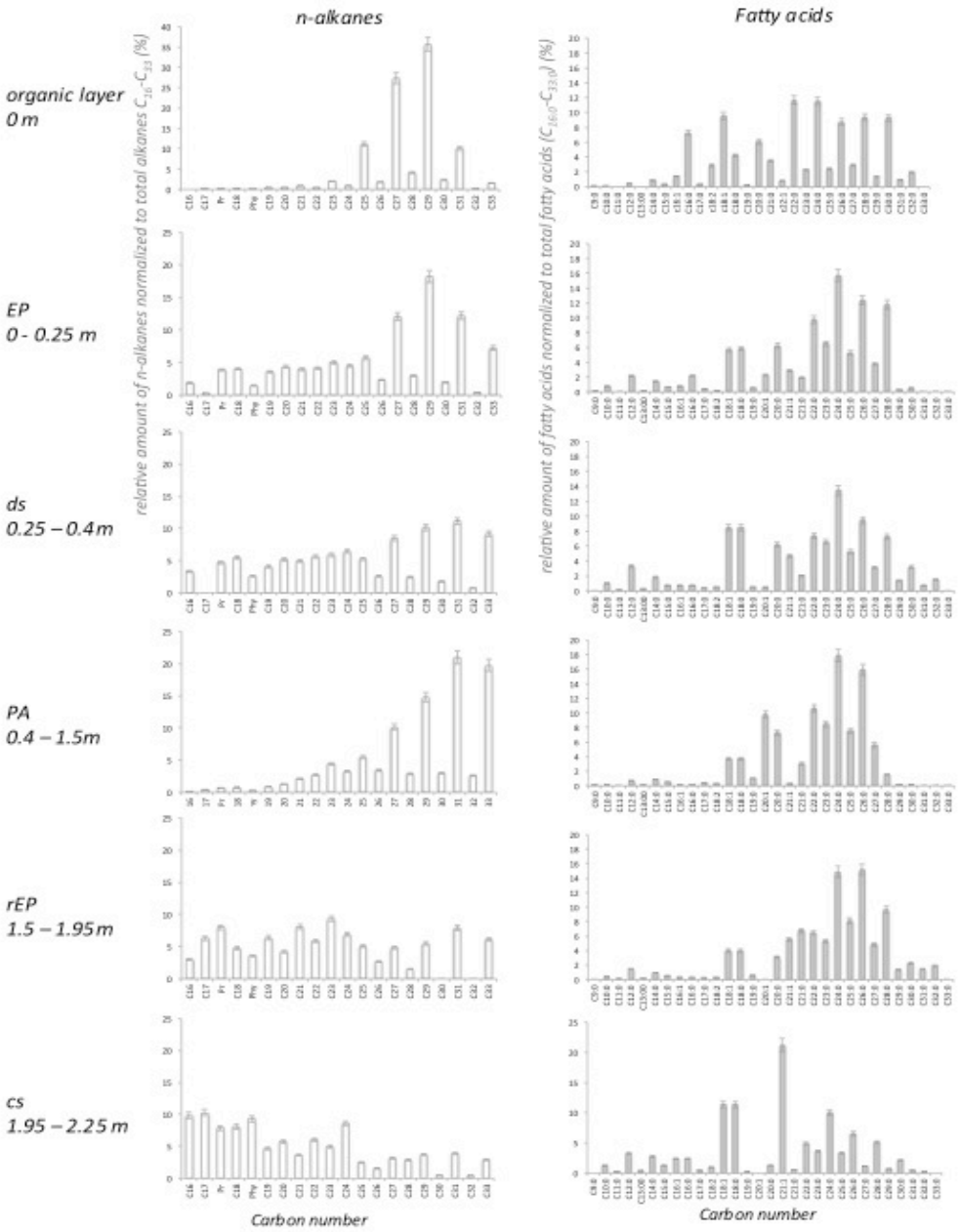

Figure 15: Relative abundance of n-alkanes and fatty acids in different profile layers. The data represent mean value of each layer. Standard deviation is shown by an error bar.

Depicted in *figure 15* is the relative amount of FAs normalized to total FAs ($C_{9:0}$- $C_{33:0}$) and *n*-alkanes normalized to total *n*-alkanes (C_{16-33}) in the profile. Also in fatty acids the different soil layers showed another distribution in their relative amount of different fatty acids. EP, ds and especially cs showed higher amounts of low chain FAs. $C_{24:0}$ and $C_{26:0}$ had high amounts in all layers. All profile samples had high abundance of C_{24}:0 fatty acid and unsaturated C_{18} values. Highest unsaturated C_{16} values could be found in the cover soil at the bottom of the profile. The cs layer differs from the other soil layers because of very low amounts in long chain part and highly unsaturated C_{18} and saturated C_{18} values.

The ternary diagram (*figure 16*) showed the relative portions of short chain (C_{12-19}), long chain (C_{20-26}) and very long chain (C_{27-34}) fatty acids as described by Gocke et al. (2014). Highest portions of long chain FA (70-90%) and very long chain (10-30%) occurred in PA and rEP. The coversand plotted the highest value for short chain FAs (40-80%) with high chain FAs of 20-60%. Root samples were plotted with the highest value for short chain FA (70-90%) and lowest portions of long chain (10-30%) and very long chain (10-15%) fatty acids.

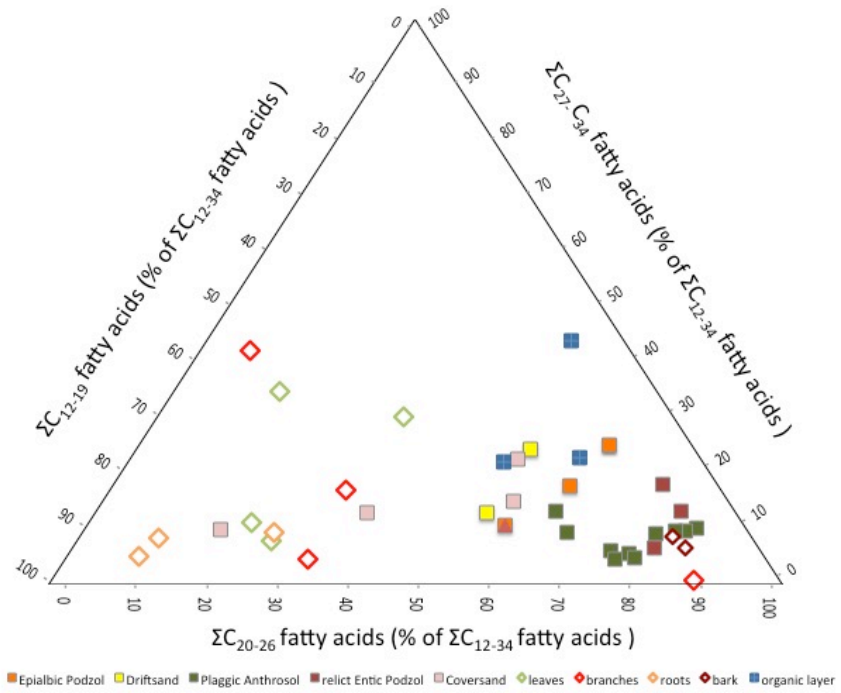

Figure 16: Relative portions of short chain (C_{12-26}), long chain (C_{20-26}) and very long chain (C_{27-34}) fatty acids for plant tissues and soil layers. Modified from Gocke et al. (2014).

The ratio of unsaturated vs. saturated C_{16} and C_{18} was highest in roots and leaves, bark and branches had lower values compared to the other ratio value. There is no significant difference between all groups (= leave, bark, branches, roots, EP, ds, PA, rEP, cs) for the ratio of unsaturated to saturated C_{16} ($F(9, 26)= 0.528$, $p= 0.059$). Even the ratio of unsaturated to saturated C_{18} showed no significant difference between the different plant tissues and soil layers ($F(9,26)= 0.798$, $p= 0.605$).

The carbon preference index for fatty acids (CPI_{FA}) for C_{20}-C_{31} fatty acids revealed high values for bark (mean value = 11 ± 1.4). Roots had the lowest mean value (2.3 ± 0.8). Branches (6.4 ± 2.5) and leaves (7.6 ± 2.9) situated in between. Based on CPI_{FA} it was not possible to separate ds and cs layer from PA or forest soils (EP and rEP). The statistical analysis with one- way ANOVA confirmed this ($p> 0.05$). The highest values were present in the organic layer (mean value 4.8). The values from Oi to Oa decreased from 4.9 to 2.7. In the relict Podzol the amount was decreasing too (4.4 – 2.3). The driftsand layer was similar with CPI_{FA} = 2.5 ± 0.0. In plaggen horizon the values reached from 2.4, increased to the maximum at 3.1 and was then moving to 1.9 from top to down. Between -1.05 m and -1.35 m the CPI_{FA} value increased transiently. In the relict Podzol there was a trend change from lower CPI_{FA} values at the top to higher values at the base of this layer. In cs horizon the values showed any small fluctuations (2.9 ± 0.5). Between all sample groups (plant tissues and soil layers), there were very highly significant differences ($F(9,26)= 10.131$, $p= 0.000$). The post- hoc test showed that those differences reached from differences between soil and plant groups. Only the PA soil was significantly different to the organic layer ($p= 0.028$). Soil layers were highly or high significantly different to plant tissues excepting roots which could not been separated (by its CPI_{FA} value) from soil samples.

The average chain length of fatty acids (ACL_{FA}) along the profile was contrary to the depth trend of CPI_{FA}. In plant tissues (leaves, branches, bark, roots) the same trend was shown than even the CPI_{FA} still had shown. Bark was again the plant tissue with the highest value: ACL_{FA} = 23.6 ± 0.1. Similarly, the lowest mean value was found in the root samples (18.3 ± 0.5) similar to the lowest value for CPI_{FA}. Branches (ACL_{FA} mean value 21.2 ± 1.9) and leaves (ACL_{FA} mean value 20.9 ± 1.7) samples situated in between. The statistical one- way ANOVA test showed very highly significant differences between plant tissues and soil layers (F(9,26)= 5.898, p= 0.000). Most of the plant samples were very significantly different to the values of the other groups. Branches and leaves were not significantly different (p> 0.05). In the soil PA was highly significantly different from cs (p= 0.006), similarly to the pair of rEp and cs (p= 0.004). Depicted in *figure 18* are mean values for different plant tissues compared to different parameters for *n*-alkanes and fatty acids.

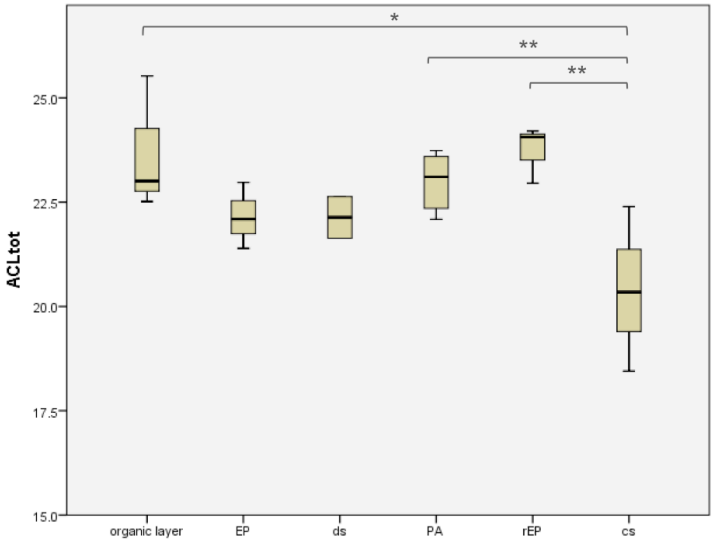

Figure 17: Average chain length of fatty acids shown in a boxplot of the different soil layers. Significant differences were marked by an asteriks, highly significant differences with two asteriks.

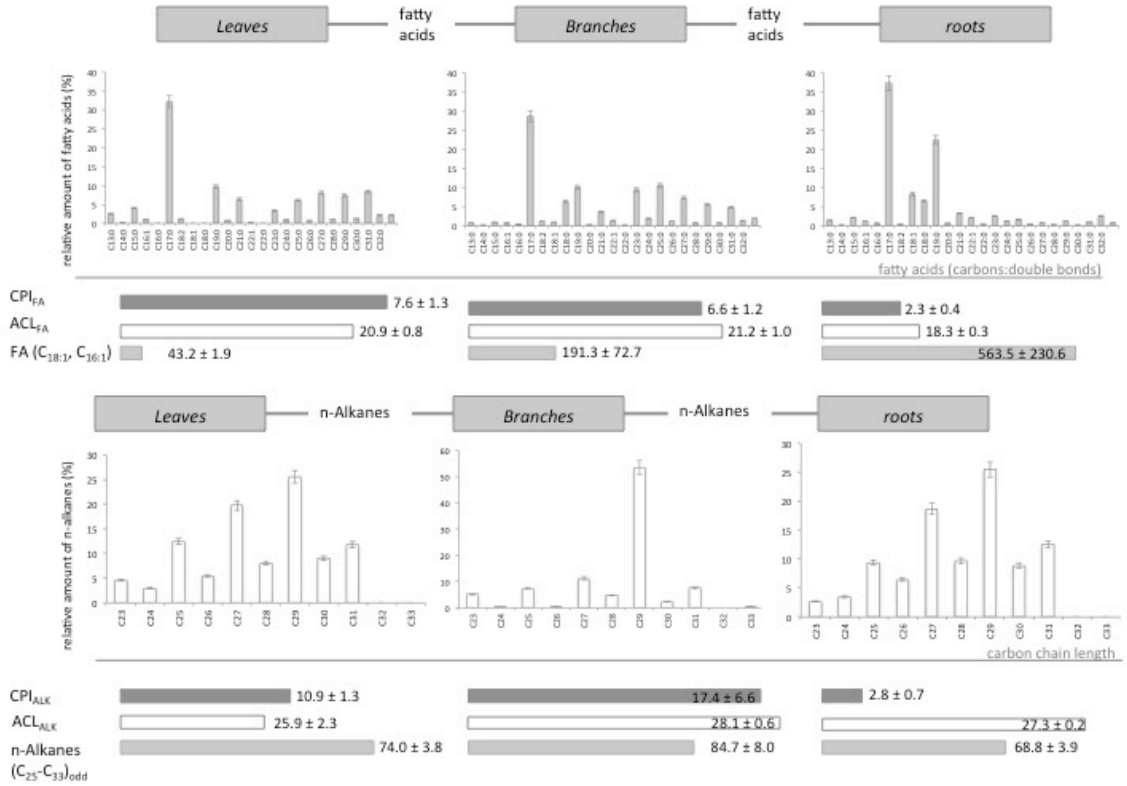

Figure 18: Fatty acid and n-alkane distribution of mean value of different plant tissues. Shown was also different calculated parameters like $CPI_{ALK,FA}$; $ACL_{ALK,FA}$. The relative amount of fatty acids is normalized to the total fatty acid C_{9-33}. N-alkanes were normalized to C_{23-33}.

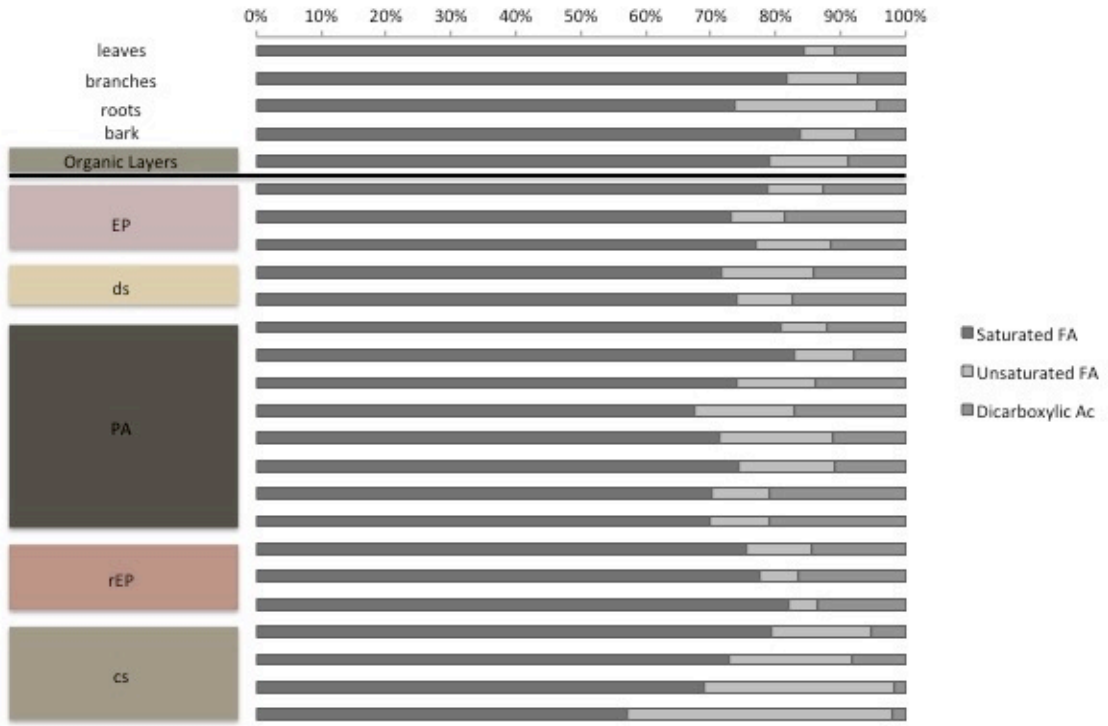

Figure 19: Relative amount of saturated fatty acids, unsaturated fatty acids and dicarboxylic acids. Shown are amounts of single samples from the profile and also mean values of different plant tissues.

Depicted in *figure 19* were the relative amount (%) of saturated-, unsaturated- FAs and dicarboxylic acids. The coversand layer unsaturated FAs were very high (20-40%). In rEP unsaturated FAs had its lowest relative amounts (5-10%). In leave, branch and bark samples, unsaturated FAs were also very low (5-13%). Root had higher relative amount of 23%. Dicarboxylic acids were higher in rEP, PA and EP and very low in root and coversand. Saturated fatty acid amounts were highest in rEP and PA.

Table 2: Sample set of plant tissues and soil layers are shown. Distribution of fatty acids even as different calculated parameters like ACL_{FA}, CPI_{FA}, MUFA, RSU and ratios with saturated and unsaturated FAs were shown in this table.

Part	Species	Range	C_{max}	ACL_{FA}	CPI_{FA}	(C16:1)/C16	(C18:1+2)/C18	MUFA	RSU
branches	*Quercus robur*	C12-C31	C16	20.8	5.1	0.03	0.41	99	8
branches	*Rubus fruticosus*	C12-C32	C16	22.4	4.4	0.03	0.79	12	75
branches	*Sorbus aucuparia*	C12-C22	C16	18.8	9.9	0.01	0.04	941	2
stem	*Rubus fruticosus*	C14-C28	C24	23.0	7.3	0.05	1.01	155	0
bark	*Quercus robur*	C12-34	C24	23.7	12.0	0.11	0.39	402	1
bark	*Quercus robur*	C12-C33	C24	23.6	10.0	0.03	2.61	39	2
leaves	*Sorbus aucuparia*	C9-C32	C16	19.3	6.4	0.00	0.04	10	70
aboveground biomas	*Dryopteris carthusiana*	C10-C32	C16	19.0	7.8	0.01	0.84	6	99
leaves	*Rubus fruticosus*	C12-C32	C16	21.8	4.3	1.65	2.21	114	5
leaves	*Quercus robur*	C12-C32	C16	21.5	7.3	0.04	5.46	72	8
leaves	*Quercus robur*	C12-C32	C28	23.0	12.3	0.02	0.57	90	5
roots	*Sorbus aucuparia*	C12-C31	C16	18.9	1.4	0.11	0.40	1491	1
roots	*Rubus fruticosus*	C12-C31	C16	18.2	2.4	0.07	3.85	87	5
roots	*Dryopteris carthusiana*	C12-C34	C18	18.0	3.0	0.07	1.19	153	4
organic layer: Oi		C12-C32	C16	22.5	4.9	0.19	5.04	797	1
organic layer: Oe		C12-C32	C28	25.5	6.7	0.09	0.90	99	2
organic layer: Oa	0	C9-C32	C22	23.0	2.7	0.14	1.02	171	2
EP	-0.1	C9-C28	C28	21.4	4.4	0.00	0.99	107	2
EP	-0.2	C9-28	C24	22.1	3.0	0.21	1.03	469	2
EP	-0.25	C10-C30	C24	23.0	2.3	0.04	0.71	141	3
ds	-0.4	C10-C30	C16	21.6	2.5	0.05	1.08	239	2
ds	-0.5	C10-C32	C24	22.6	2.5	0.09	0.94	478	2
PA	-0.4	C10-C30	C24	22.3	2.4	0.08	0.49	419	4
PA	-0.6	C12-C28	C20	22.1	3.1	0.00	1.32	105	2
PA	-0.75	C9-C28	C24	22.4	2.1	0.00	0.91	536	2
PA	-0.9	C12-C28	C24	23.7	1.8	0.00	0.66	114	3
PA	-1.05	C12-C28	C24	23.6	2.1	0.00	0.99	124	2
PA	-1.2	C12-C28	C24	23.6	2.2	0.00	0.51	167	4
PA	-1.35	C12-C28	C26	23.6	2.0	0.00	0.33	166	6
PA	-1.5	C9-C28	C24	22.6	1.9	0.02	0.48	48	4
rEP	-1.65	C12-C31	C26	24.2	1.0	0.00	1.35	98	2
rEP	-1.8	C10-C32	C24	24.1	2.6	0.09	1.07	61	2
rEP	-1.95	C10-C32	C24	23.0	3.0	0.08	0.78	112	2
cs	-2.1	C10-C32	C24	22.4	3.6	0.09	0.87	191	2
cs	-2.25	C10-C31	C16, unsaturated C	20.3	2.7	0.16	0.88	103	1
cs	-2.25	C10-c30	C16, unsaturated C	18.5	2.7	0.18	0.86	261	2

3.2 Root-transects

3.2.1 Total lipid content in root-transects

In root-transect at 0.75 m depth (*figure 20,A*) TLE value from root surrounding soil was lower than the soil in more distance to the central root. The reference sample had much lower TLE than the rhizosphere samples. *Figure 20,B* shows TLE of the root- transect situated in the plaggen soil in 1.05 m depth. Highest TLE values occurred in direct vicinity of the root. In 8 cm distance to the central root, the values decreased to lower TLE values. At 12 cm distance the TLE value rose up again to similar values than the ones in direct root vicinity. The reference sample from root- transect shown in *figure 20,B* is lower than that of rhizosphere soil. *Figure 20,C* showed TLE of the rEP. Values decreased from root sample to the wider environment (2-14 cm distance to central root). Sample from root-transect shown in *figure 20,D* showed an exponential decrease of TLE from direct vicinity of the root environment towards more distant rhizosphere. The reference sample TLE exceeded rhizosphere TLE at 10 cm distance to the root.

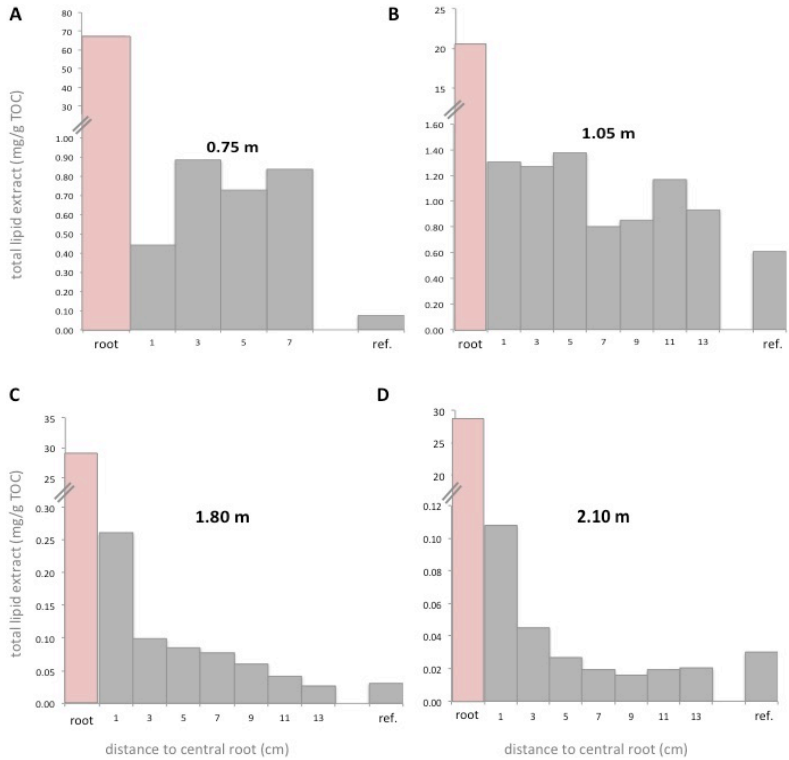

Figure 20: Total lipid content of root transects with increasing distance. The last sample (ref.) is a reference sample from the given soil layer. The central root is shown by the red color bar.

3.2.2 *n*-Alkane composition in root-transects

Table 3 showed different n-alkane parameters (CPI_{ALK}, ACL_{ALK}, LAR_{1-4}) and additional information (distribution *n*-alkanes, *n*-C_{max}) from root-transects. The results where only analysed in a qualitative way.

ACL_{ALK} values in roots compared with soil samples showed lower values. Depicted in *figure 21* is the distribution of ACL_{ALK} with increasing distance to the central root. In root transect in 0.75 m depth (*figure 21,A*) and root transect from 1.05 m depth (*figure 21,B*) a strong change of ACL_{ALK} value from root to its direct root vicinity was showed. Samples from surrounding soil with > 2 cm distance to central root didn`t showed big differences in ACL_{ALK} values and stands in a line with the reference sample from the plaggic layer. In 1.80 m depth, the root transect from the rEP was analysed. Likewise the other root transects, ACL_{ALK} values decreased strongly in root vicinity. The values of ACL_{ALK} increased with increasing distance within 0 to 6 cm distance from central root. Values (ACL_{ALK}) decreased in distances > 6 cm from 24.5 to 22.9. The reference sample from the rEP layer that was not from rhizosphere had values similar to those in rhizosphere (root transect in 1.80 m depth) in 4 to 6 cm distance to the central root. In the coversand in 2.10 m depth, the root transect showed fluctuating ACL_{ALK} values. In general, the values followed the trend of increasing ACL_{ALK} values in direct root vicinity. In distances > 6 cm the values decreased until distance of 6-8 cm was reached, then the ACL_{ALK} value increased again.

The ratio C_{27}/C_{31} (LAR_2) showed higher values compared to to rhizosphere for root samples. Where LAR_2 was higher for roots than the environment, there was also enrichment for C_{29}/C_{31} (LAR_3). Opposed characteristics had LAR_4 values. These values were lower than the environmental soil samples. Highest LAR_4 values in rhisospher soil samples were found in root transect located in the plaggen soil layer at 1.05 m depth. Such high values for C_{31}/C_{29} ratio were also detected in the other transect from PA at 0.75 m depth in the profile. Lowest values in rhizosphere soil of LAR_4 occurred in transects from cs horizon and rEP.

Phytane could be detected in most of the soil samples and the central root from root-transect in 1.80 m depth. Pristane was available in all rhizosphere soil samples.

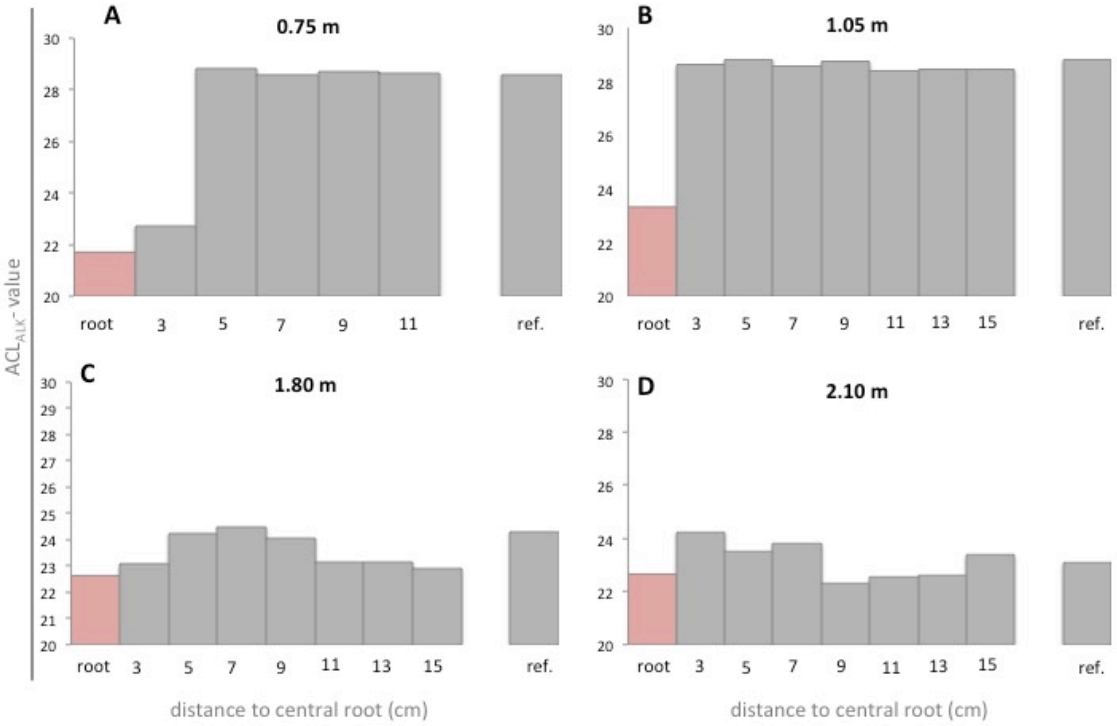

Figure 21: ACL_{ALK} values of root-transects. The root sample is colored in red. The rhizosphere samples showed only small changes in the ACL_{ALK} with increasing distance. The last bar stands for a reference sample that is not influenced by the central root.

Table 3: Different n-alkane parameters (ACL_{ALK}, CPI_{ALK}, LAR_{1-4}) and distribution patterns of n-alkanes in root-transects are shown.

	Part	Range	C_{max}	Pr	Phy	Pr/C17	C18/Phy	Distibution	ACL_{FA}	CPI_{FA}	LAR_1	LAR_2	LAR_3	LAR_4
Transect - 0.75m														
	root	C19 - C27	C20	x	x	-	-	unimodal	22.2	-	-	-	-	-
	2.0	C18 - C33	C31	x	✓		1.4	increasing ltr	28.8	5.7	0.4	0.5	0.8	1.26
	4.0	C16 - C33	C31	✓	✓	0.5	1.5	increasing ltr	28.6	5.8	0.4	0.5	0.8	1.26
	6.0	C16 - C33	C31	✓	✓	0.7	1.4	increasing ltr	28.7	5.7	0.4	0.5	0.8	1.28
	8.0	C16 - C33	C31	✓	✓	0.6	1.4	increasing ltr	28.6	5.5	0.4	0.5	0.8	1.32
	reference	C17 - C33	C31	✓	✓	2.70	3.80	increasing ltr	28.6	5.4	0.4	0.5	0.8	1.33
Transect - 1.05m														
	root	C17 - C31	C29	x	x			bimodal	23.3		0.3	0.7	1.2	0.87
	2.0	C16 - C33	C31	✓	✓	0.7	1.7	increasing ltr	28.6	5.6	0.4	0.6	0.8	1.31
	4.0	C16 - C33	C31	✓	✓	0.6	1.6	increasing ltr	28.8	5.6	0.4	0.5	0.7	1.36
	6.0	C16 - C33	C31	✓	✓	0.7	1.8	increasing ltr	28.6	5.5	0.4	0.6	0.8	1.29
	8.0	C16 - C33	C31	✓	✓	0.7	1.6	increasing ltr	28.7	5.5	0.4	0.5	0.8	1.33
	10.0	C16 - C33	C31	✓	✓	0.6	1.8	increasing ltr	28.4	5.3	0.4	0.6	0.8	1.26
	12.0	C16 - C33	C31	✓	✓	0.6	1.6	increasing ltr	28.5	5.4	0.4	0.6	0.8	1.27
	14.0	C16 - C33	C31	✓	✓	0.6	1.7	increasing ltr	28.4	5.5	0.4	0.6	0.8	1.29
	reference	C16 - C33	C31, C33	✓	✓	0.80	5.00	increasing ltr	28.8	4.1	0.5	0.5	0.7	1.45
Transect -1.80														
	root	C16 - C32	C21	x	✓	0.0	3.1	bimodal	22.6	0.7	1.0	0.0	0.0	-
	2.0	C16 - C33	C21	✓	✓	1.2	0.9	bimodal	23.1	2.8	0.3	0.9	1.1	0.94
	4.0	C16 - C33	C23	✓	✓	1.4	0.9	multimodal	24.2	1.9	0.3	0.9	1.1	0.94
	6.0	C16 - C33	C18	✓	✓	1.5	1.3	multimodal	24.5	1.9	0.3	1.0	0.9	1.13
	8.0	C16 - C33	C28	✓	✓	1.0	1.0	multimodal	24.1	1.0	0.3	1.5	1.3	0.79
	10.0	C16 - C33	C18	✓	✓	1.0	1.3	multimodal	23.2	1.4	0.4	0.6	1.0	0.96
	12.0	C16 - C33	C18	✓	✓	1.0	1.1	multimodal	23.2	-	0.4	0.6	0.9	1.13
	14.0	C16 - C33	C18	✓	✓	1.1	1.7	multimodal	22.9	-	0.4	0.7	0.7	1.45
	reference	C16 - C33	C31	✓	✓	1.50	1.30	multimodal	24.3	10.8	0.6	0.1	0.5	1.87
Transect - 2.1m														
	root	C17 - C32	C20; C22	x	x			multimodal	22.7	0.7	1.0	0.0	0.0	-
	2.0	C16 - C33	C21	✓	✓	1.1	1.0	multimodal	24.2	0.9	0.3	2.1	1.4	0.66
	4.0	C16 - C33	C21	✓	✓	0.9	0.9	multimodal	23.5	1.2	0.3	0.9	0.9	0.93
	6.0	C16 - C33	C22	✓	✓	1.0	0.9	multimodal	23.8	0.8	0.4	1.2	1.1	0.86
	8.0	C16 - C33	C18	✓	✓	1.1	1.3	decreasing ltr	22.3	1.6	0.6	0.0	1.0	-
	10.0	C16 - C33	C18	✓	✓	1.4	1.3	decreasing ltr	22.5	1.7	0.6	0.0	1.0	-
	12.0	C16 - C33	C18	✓	✓	0.9	1.4	decreasing ltr	22.6	1.7	0.6	0.0	0.9	-
	14.0	C16 - C33	C29	✓	✓	0.9	1.5	decreasing ltr	23.4	2.9	0.4	0.9	1.0	1.14
	reference	C16 - C33	C16; C24	✓	✓		0.40	multimodal	23.1	2.0	0.4	0.5	0.8	1.30

3.2.3 Carboxylic acids in root- transects

Root- transects showed different fatty acid parameters. The ACL_{FA} (C_{9-33}) and the CPI_{FA} (C_{20-32}) value are shown in *figure 23*. In transect in 0.75 m depth (*figure 22,A*), situated in the plaggen soil, ACL_{FA} values were higher compared to the value from the root. Also in transect in 1.05 m depth, the ACL_{FA} value for the root was much lower than the rhizosphere soil. Compared to the other root- transects, the ACL_{FA} -differences between the central root and the rhizosphere soil in direct root vicinity was much higher in the plaggen soil root- transects (*figure 22,A-D*). In root- transect in 0.75 m depth, the ACL_{FA} values increased with distance (0-8 cm). From 8 cm distance to the center, the ACL_{FA} decrease to the ACL_{FA} value of the reference sample from the plaggen soil. In root- transect from the rEP another distribution of ACL_{FA} values with increasing distance was found. After the low ACL_{FA} value for the central root the soil from direct root vicinity showed a maximum and decreased with increasing distance from the center root. Also the coversand root- transect showed this ACL_{FA} value distribution as described for rEP. The effect looked much stronger in the coversand compared to the rEP.

CPI_{FA} values showed other distribution patterns than the ACL_{FA} values. The CPI_{FA} value for the central roots were highly enriched in the plaggen soil root- transects. The rhizosphere samples were much lower in their CPI_{FA} value than their central root values. Transect in 0.75 m depth couldn`t show a clear trend. The root- transect from the same layer in 1.05 showed fluctuating values in their CPI_{FA} values and also no clear trend was shown. Root- transects from deeper soil parts had lower CPI_{FA} values compared to the root samples from transects in 0.75 m and 1.05 m depth. Both root- transects (from rEP in 1.80 m depth, *figure 22,C* and from cs in 2.10 m depth, *figure 22,D*) showed an increasing trend of CPI_{FA} values with increasing distance from the central root.

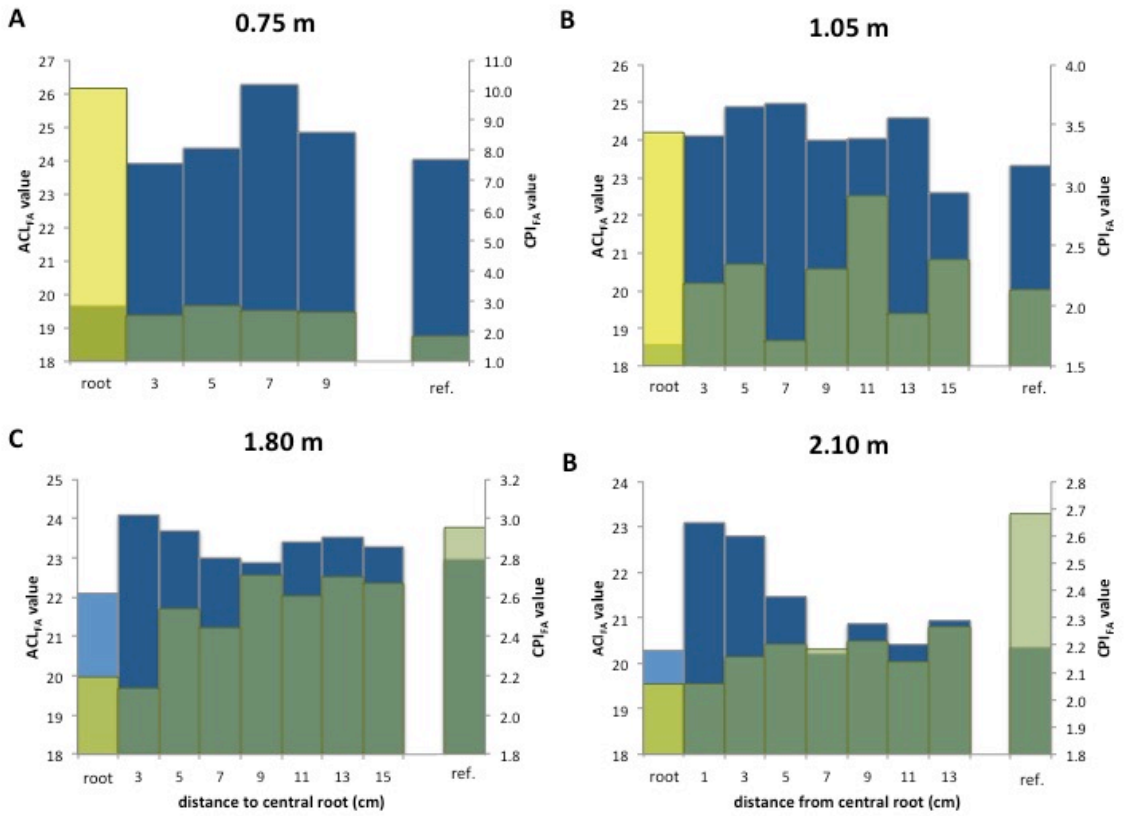

Figure 22: Average chain length for fatty acids (ACL_{FA}) and carbon preference index (CPI_{FA}) are shown in this figure. ACL_{FA} values are depicted in blue, while the root sample is in sky blue. The CPI_{FA} is depicted in green. In yellow depicted is the CPI_{FA} value for root.

In transects from 1.05 m and 2.10 m depth, unsaturated C_{16} and C_{18} were enriched compared to the other soil samples from the rhizosphere and the reference samples. In transect 1.80 m below surface the unsaturated fatty ($C_{16:1}$, $C_{18:1+2}$) acids decreased. ($C_{16:1}$)/C_{16} has its maximum in 6 cm distance to the central root. Unsaturated- to saturated- C_{18} fatty acid ratio has its highest level in 10 cm distance to the center. In transect from 0.75 m depth, values in 4 and 6 cm distance to the roots were not available because saturated C_{16} and C_{18} could not have been found in the GC-FID output. Therefore a calculation of the ratio of unsaturated to saturated C_{16} vs. C_{18} was not possible.

Mono-unsaturated fatty acids (MUFA) were calculated for root- transects. With increasing distance to the central root, the MUFA value showed an increasing amount with more distance to the central root. Four different classes were made. First class describes the root (R). Second class was called “root-soil” (RS). This class included three values from 0-6 cm distance to central root. The third class called “soil” (S) and was made by for values (6-14 cm distance from central root). Last class called “soil-reference” (SR).

The two root- transects from the Plaggic Anthrosol layer had higher values in their root samples in mono- unsaturated FAs then the other root samples from deeper root-transects. In transect at 0.75 m (*figure 23,A*) no clear trend was showed. The other root-transect from the plaggen soil (1.05 m depth, *figure 23,B*) showed an increase in the sum of mono- unsaturated FAs with increasing distance to the central root. Deeper soil layers could have shown this trend too. In the rEP (*figure 23,C*) the differences between the sum of MUFA from root and rhizosphere was much lower than in the plaggen soil. With increasing distance, the MUFA values were getting higher. The same trend was shown in the coversand (*figure 23,D*). MUFA are mainly microorganism derived but could also be plant derived(Harwood & Russell 1984). From Gocke et al. (2010) we use the term "rhizomicrobial-derived MUFA" and associate root source with microbial biomass source.

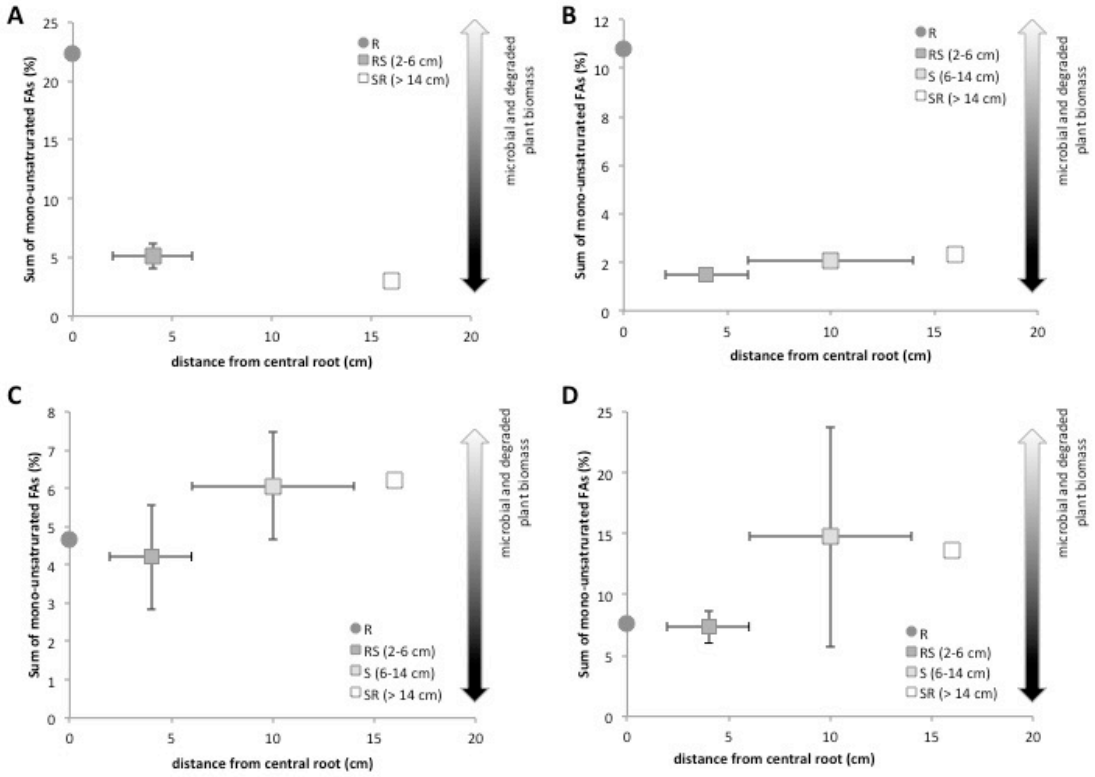

Figure 23: The Sum of mono- unsaturated FAs (normalized to total MUFA) were shown in a root-transect with increasing distance to the central root (depicted as a circle). Four classes showed the influence of the root to its environment. The soil in direct root vicinity (RS), the soil in the root environment with more distance to central root (6-14 cm) (S) and the reference soil (SR) that is not influenced by the root. Modified from Gocke et al. (2014).

Figure 24 shows the average chain length of n-alkanes related to the ACL from fatty acids even than the CPI_{ALK} to CPI_{FA} values in root- transects. Root samples from transect in 0.75 m (*figure 24,A/B*) and 1.05 m depth in profile (*figure 24,C/D*) were plotted within the dashed lines in the diagram that stood for highly microorganism- /root- derived OM in the ACL_{FA} and ACL_{ALK} diagram. Soil samples from rhizosphere could not have been related to higher microorganism or root derived OM along the $ACL_{ALK,FA}$ – values. The $CPI_{ALK,FA}$ values showed another distribution and plotted soil groups within the dashed lines. In the Plaggic Anthrosol, soil from the near root vicinity (RS), even then root with more distance to central root (S) and reference sample with no central root influence were plotted in the area, where it was expected to have microorganism or roots as source for OM. Only in root- transect from the coversand in 2.10 m depth, a differentiation between rhizosphere and soil with no influence to a root could have been showed.

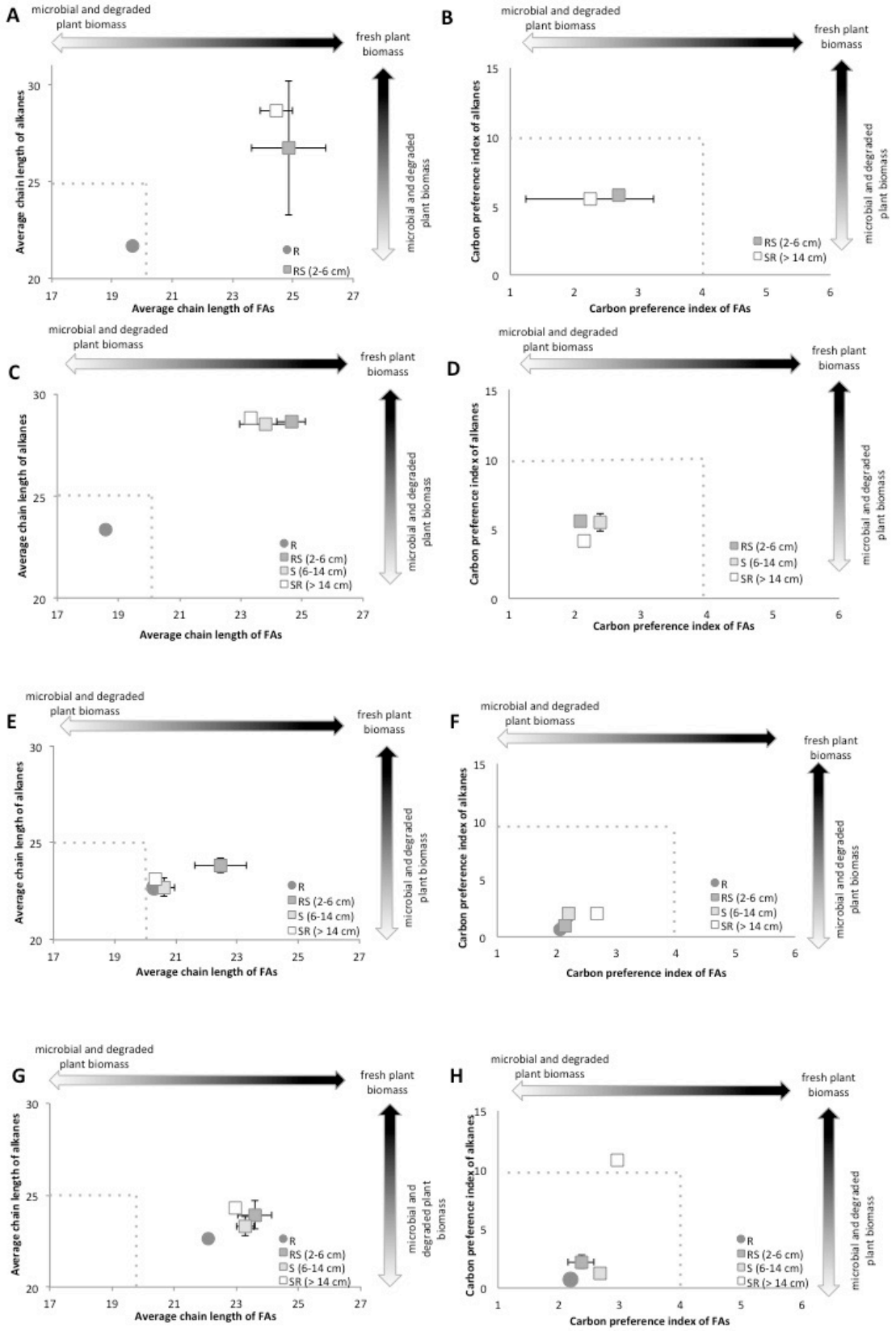

Figure 24: Comparison of ACL_{ALK} and ACL_{FA} (A,C,E,G) and CPI_{ALK} and CPI_{FA} (B,D,F,H) in rhizosphere is shown. Dashed lines indicate area of OM with large microbial contribution ($ACL_{ALK} < 25$, $ACL_{FA} < 20$); Kolattukudy et al.,1976; ore area of strongly degraded OM ($CPI_{ALK} < 10$, $CPI_{FA} < 4$); Cranwell, 1981; Cranwell et al., 1987; Xie et al., 2003. Modified from Gocke et al. (2010)

4 Discussion

4.1 Changes in the relative distribution of TLE , fatty acids and *n*-alkanes

4.1.1 Lipid content

Lipid contents (TLE) normalized to C_{org} revealed largest values for leaves and decreased in the order: leaves > bark > branches > roots > organic layer > soil. These results stand in a line with the results from Wiesenberg et al., (2012). In the profile the highest value was found in the Plaggic Anthrosol, followed by relict Entic Podzol > Epialbic Podzol > driftsand > coversand. In the root- transect samples roots showed the highest TLE followed by rhizosphere and soil. The total lipid content could well document the appearance of organic carbon. C_{org} and TLE showed a linear correlation (*figure 6*). The aboveground biomass was characterised by the high TLE values that represent the plant leaf waxes. All terrestrial plants produce leaf waxes which are relatively stable to degradation (Z. Zhang et al. 2006). In the fresh plant biomass the decomposition of the biomass didn`t start yet and therefore explain the huge amounts of TLE. In the organic layer the decomposition of incorporated plant biomass had begun and the TLE decreased immediately. Suggesting that during degradation of plant derived biomass, plant tissues were fed by destruents which relates to lower TLE. In Oi the value (25.07 mg/g) was comparable with samples from leaves or bark and decreased to 19.96 mg/g in Oe and 5.52 mg/g in Oa. Below the organic layer, the buried plaggen soil yielded the highest values in TLE (mean value of 1.07 mg/g). They correlated with the high values of soil organic carbon in PA and likely resulted from huge inputs of organic material during the plaggen cultivation in the Middle Ages (see 2.1) (van Mourik et al. 2016). The relict Podzol yielded a TLE mean value of 0.25 mg/g TOC. This value could be explained with high root abundance. Because oak trees from the recent vegetation penetrated the whole profile, they could also influenced the buried soil and sediment layers. In root-transects TLE values were decreasing with increasing distance to the central root. It is obvious that root alter the chemical composition in their direct vicinity (few mm) (D Sauer et al. 2006). How strong the impact of these alterations is, is still under debate. Along the total lipid contents it is not possible to answer the research question of this masterthesis. However, the lipid extracts in the root- transects seemed to show a clear trend, lipid amounts of the root vicinity might not necessarily indicate the presence of root derived

inputs of OM. The high TLE could also contribute to molecular remains of roots and microorganisms feeding on roots (Gocke et al. 2010). The analysis of extractable lipids could provide complementary information on vegetation history and soil processes (Angst, John, et al. 2016; Wiesenberg & Gocke 2016).

4.1.2 FA distribution patterns

FA pattern reflected the different and individual function of fatty acids in different plant parts. Leaves have a lot of protective epicuticular waxes with 16 and 18 carbons and particularly long chain FAs with more than 20 carbons (Harwood & Russell 1984). A dominance of long chain FAs could be detected in leave samples. Compared with those of leaves, roots have more short chain fatty acids. Stems have a lower surface to volume ratio than leaves and were characterized by very long chain acids (n-C_{28} and n-C_{30}) (Wiesenberg et al. 2012). The plant tissues from Bedaf Bergen stand in a line with the results from Wiesenberg et al., (2012).

The most abundant short chain saturated FA in the profile contained C_{16} and C_{18} carbons (*figure 15*). These fatty acids were non-specific and occurre in the cell membranes of microorganisms and plant cuticles or waxes (Kolattukudy, P.E., Croteau, R., Buckner 1976). Cranwell (1974) describes even carbon-numbered long-chain fatty acids with chain length more than C_{21} thought to originate predominantly from land plants. Therefore, long chain FAs are useful indicators of plant-derived organic matter (Dinel et al. 1990). In general, the FA distributions could be used as tool to analyse the composition of plant-derived OM (Xie et al. 2003).

Van Bergen et al., 1998; Wiesenberg et al., 2004 showed, that samples with low amounts of short chain acids and large amounts of long chain acids are typical for grassland soils. The plaggen soil and the rEP layer showed FA distribution that could relate to a grassland soil. In general the FA distribution in soil layers didn`t show clear trends. Only the coversand showed a shift in its FA distribution to more short chain acids.

4.1.3 *n*-alkane patterns

"*n*-Alkanes in soil and sediments can derive from multiple sources including microorganism, fungi, plant biomass, fossil fuel or other contamination as well as

degradation" (Gocke, Peth, et al. 2014). Bacterial n-alkanes are characterized by predominance of short-chain homologues (C_{16}–C_{24}) (Z. Zhang et al. 2006; Wiesenberg & Gocke 2016) in comparison to vascular plant *n*-alkanes which have a predominance of long-chain homologues (C_{27}-C_{33}) and high preference of odd over even carbon numbers (Eglinton & Hamilton 1967). Among the soil layers, the most prominent differences in *n*-alkanes were observed in the distribution of long and short chain alkanes. While the strongly rooted upper subsoil (0–0.25 m) had high relative content of plant- derived n-alkanes (C_{25}-C_{33}), the layer below contained lower relative amounts of long-chain alkanes (Gocke et al. 2016). The plaggen soil situated below the driftsand layer could be separated from the other layers based on remarkably high relative contents of long-chain *n*-alkanes. Below the PA *n*-alkane distribution described a shift to higher portions of short-chain *n*-alkanes. Based on the distribution of *n*-alkanes, potential sources of OM were assumed. The dominant *n*-alkanes in the topsoil (0-0.25 m) were C_{27} and C_{29} which relates to the recent woody vegetation (Cranwell 1973) growing at Bedafse Bergen. C_{31} was enriched in PA and in rEP. The coversand layer showed dominance of shorter-chain *n*-alkanes like C_{23}. The shorter-chain alkanes below the PA (in rEP and cs) possibly derived from the action of soil bacteria, algae and fungi (Z. Zhang et al. 2006). Alkane distribution patterns dominated by C_{31} n-alkane hint to grass vegetation as predominant OM source (Cranwell 1973).

4.1.4 Diagnostic ratios for determination of different sources

n-alkanes

The *n*-alkane CPI_{ALK} and ACL_{ALK} data from the different layers and plant samples provided additional information regarding the source apportionment of different layers. As discussed above (4.1.3) higher land plants contain generally *n*-alkanes C_{25} to C_{31} with a strong odd over even carbon number predominance (Kolattukudy, Croteau & Buckner 1976a; Eglinton et al. 1962). While degradation of plant biomass there is decrease of the odd predominance. CPI_{ALK} values ($<< 10$) stands for degraded OM or root-derived biomass, high CPI_{ALK} values (> 10) characterize leaf biomass (Cranwell 1981). The carbon preference index (CPI_{ALK}) represents this circumstance. The odd over even distribution for microorganisms has only little differences and is represented in low CPI_{ALK} values (Meyers & Ishiwatari 1993). Therefore the CPI_{ALK} values in the soil could

give some information about the source of organic matter (Duan 2000). The CPI_{ALK} could also work as a proxy for the degree of degradation of the different lipids (Angst, John, et al. 2016). The layer with the lowest chain length maximum situated in the coversand and had the lowest value for CPI_{ALK} and ACL_{ALK}. Therefore it possibly derived from the microbial OM or root derived OM (Cranwell 1981; Cranwell et al. 1987; Xie et al. 2003; Kolattukudy, Croteau & Buckner 1976b). The plaggen anthrosol with the maximum in C_{31} documented the highest ACL_{ALK} mean value. Long chain *n*-alkanes account predominantly for cuticle waxes of terrestrial plants (Collister et al. 1994) and indicates for plant-derived SOM (Dinel et al. 1990). The CPI_{ALK} mean value of the plaggen soil was lower than the mean value of the rEP. At the bottom of the relict Podzol layer there was an outliner with a huge value for CPI_{ALK} which is three times higher than the other CPI_{ALK} values for the rEP. This outliner strongly influences this high mean value. That huge value could not be explained by additional root derived inputs because of low root occurrence in this section. A trend of a decrease was shown in the CPI_{ALK} values from top till down the profile, except the outliner at the bottom of the relict Podzol layer. In general a slight decrease of CPI_{ALK} with depth indicated that inputs in deeper soil horizons could origin predominantly from roots or microorganisms (Buggle et al. 2010). Between the soil groups there was no significant difference. In *figure 14* is shown, that it was not possible to build up clusters to identify a value to its specific layer. In ACL_{ALK} values cluster building was possible and also the significant (one-way ANOVA) test showed significant differences between EP, ds, organic layer, rEP and cs. Similarly to previously shown C_{org} and TLE contents, high variation in ACL_{ALK} contents could relate to potentially various source plants for different layers. The significant difference between upper parts of the profile (EP, ds, PA) and deeper parts (rEP and cs) indicated differences in OM derived sources. Eglinton et al., (1962) described ACL_{ALK} values and their use to differentiate between higher plant derived organic matter (ACL_{ALK} values ≥ 25) and degraded- or microorganism- derived OM (ACL_{ALK} values < 25) (Bray & Evans 1961). This allowed us to have an accurate analysis of input sources. The ACL_{ALK} values in the profile were higher than 25 for all soil layers and plants except for layer rEP and cs. This leads to the presumption that these low ACL_{ALK} values relate to root and microorganism derived OM (Wiesenberg et al. 2010). Based on this fact and the actuality of enriched root frequency where lower ACL_{ALK} values are found, it seems to be a reasonable explanation. The ACL_{ALK} values of the ds and cs were similar. The Podzol layers were also similar and could differ from

the other layers. Plaggic Anthrosol documented the highest value in ACL_{ALK} and contribute of long chain plant derived components (Eglinton et al. 1962). By having a look to the single values, there was a low ACL_{ALK} value found in the upper part of the relict Podzol. Situated in the same depth was an enrichment of fine- (< 2 mm) and medium roots (2-5 mm). They decreased to a minimum at the bottom of the rEP layer. The ACL_{ALK} values increased along the rEP layer with depth. Therefore it was assumed, that recent roots strongly influenced the OM especially in 1.5 m depth, when rEP layer begins. Input sources of rEP could therefore differ from input sources of EP. The low ACL_{ALK} values in rEP could also relate to a higher degeneration of the plant material (Gocke, Gulyás, et al. 2014). While biodegradation, the *n*-chain length decrease (Rontani & Volkman 2003). In plaggen anthrosol the ACL_{ALK} values increased with depth and number of medium roots (2-5 mm). Therefore the OM in PA didn't seem to be microorganism derived. Roots could be an additional source for OM in the plaggen anthrosol.

Fatty acids

Fatty acids were common lipids in plants, microorganism and soils. Depending on chain length, a source differentiation of OM in soil was possible (shoot, roots ore microorganism derived) (Wiesenberg et al. 2012). The combination of the two biomarkers should confirm the results received from the *n*-alkane proxies.

High CPI_{FA} values indicate a stronger degradation and/or microbial remains dominating the source of the fatty acids (Gocke et al. 2010). Fresh plant biomass usually has CPI_{FA} values > 4, degradation after sedimentation and microbial reworking result in values close to 1 (Cranwell et al. 1987). Because of preferential decomposition of even homologues and contribution from odd homologues, e.g. of wax esters or other potential precursor compounds with long chain alkyl FAs, the value is situated close to 1 during degradation (Gocke et al. 2010). The even/odd predominance or the carbon preference index (CPI; *table 2*) for C_{20}–C_{30} FAs showed high values for plant tissues. Within plants, highest values were found for stems lower for leaves and lowest for roots (Wiesenberg et al. 2012). This stands in a line with the results from Bedafse Bergen. Instead of stem samples, branches were analysed. They had lower CPI values than leave tissues.

Mean values of CPI_{FA} from the profile showed slightly decreasing values from the organic layers to the relict Podzol. The coversand showed a higher mean value for CPI_{FA}

compared to the value of the driftsand. The microbial activity was high in the upper part of the profile where oxygen was available and enriched again in the coversand layer. Once more, the values suggested microbial activity in the cs layer.

Unsaturated fatty acids allowed a quantification of root derived compounds in rhizosphere and was performed by Gocke et al., (2010). The ratio of unsaturated vs. saturated C_{16} acids [$(C_{16:1})/C_{16}$] revealed high values for leaves and very low values for branches. In the profile the highest value was calculated for coversand, lowest in PA < rEP, ds < EP < organic layer. $C_{16:1}$ and $C_{18:1}$ unsaturated FAs are mainly microorganism-derive but also partly plant-derived (Harwood, J.L. & Russel 1984). Gocke et al., (2010) used in this term "rhizomicrobial-derived" – a term that include both: root and associated microbial biomass sources. The poly-unsaturated $C_{18:2+3}$ and long chain FAs ($\geq C_{20:0}$) are related to higher plant-derived organic matter (Kolattukudy, Croteau, Buckner, et al. 1976; Harwood, J.L. & Russel 1984). Sum of mono-unsaturated acids ($C_{16:1}$, $C_{18:1}$) were highest in driftsand and coversand. These values even surpassed the values from the organic layer. Lower sum reached from EP and rEP. The plaggen anthrosol had the lowest value. Along this mono- unsaturated amounts, the ds and cs layer seemed to have a different source than the other layers. The high root- or microbial- derived input in the coversand was multiply confirmed by different parameters. Once more, the plaggen soil seemed to have a low microbial activity and its OM related to the biomass input during plaggen cultivation.

4.1.5 Ratios for determination of plant source

The distribution of the individual hydrocarbons varies among the different types of plant type. Several Quatenary environmental reconstructions applied ratios of prominent n-alkanes C_{27}, C_{29}, C_{31} and C_{33} to differentiate between shrub- and tree- versus grass- and herb- dominated vegetation (Zech & Andreev 2010). While ACL_{ALK} and CPI_{ALK} could lead us to an assumption about the source of OM, ratios of different *n*-alkanes or ternary diagrams could give an information about the type of vegetation which influenced the soil layer. In the plaggen horizon, odd *n*-alkanes from C_{27} to C_{33} were dominant. In the EP C_{27} and C_{29} and in rEP C_{21} and C_{23} were enriched as discussed above. Aboveground plant biomass displayed *n*-alkane distributions dominated by C_{27} or C_{29}. This observation

stands in a line with results from other n-alkane studies (Cranwell 1973; Z. Zhang et al. 2006).

LAR_2 represent the ratio C_{27} to C_{31}. For all soil samples excepting PA, the LAR_2 value was 1. The value in PA was 0.5. This lets us assume that there is another source of OM than in other layers. In this case grass and heathland plant inputs because C_{31} was enriched (Cranwell 1973). The plaggen cultivation with heathland plants that could be comparable with grass reinforced this presumption. The ratio C_{29} to C_{31} (LAR_3) had its lowest value in the Plaggic Anthrosol (0.7 ± 0.2). The adjacent layers rEP and ds differed only slightly from the PA (rEP 0.1; ds 0.2). The uppermost (EP) and deepest layer (cs) in the profile had the highest values for LAR_2 compared to the other C_{27}/C_{31}-values from the soil layer. From the proportion of C_{31} to the other plant tissues it was shown, that the amount of C_{31} was very low in the organic layer, increased linear to a maximum in the PA and decreased linear down along the profile to cs. Therefore it could be assumed, that the plaggen soil, that derived by C_{31} enriched plants could also influenced its environment.

The lipidanalysis from the profile could therefore answer the research question about the origin of the soil and sedimentary organic matter sources in the individual layers. One could conclude, that the uppermost layer the EP contribute OM that is leave-, bark-branches- and root-affected zone. The followed layer the driftsand had low OM and was influenced by the overlaying EP layer. OM source from the plaggen soil layer differed from the other soil layers. Grass and heath plants have been found as a main source of the OM in this layer. The following rEP layer was comparable to the EP. But root- or microbial derived compounds haven been found to be an important source of the OM found in the relict Podzol. The coversand seemed to have OM that was from post-sedimentary inputs derived sources. Beause of low ACL_{ALK} and ACL_{FA} even than low CPI_{ALK} and CPI_{FA} values, it seemed to bee root- or microorganism derived.

Additional to the general analysis in each layer, several root-transect samples were analysed. This could focus more belowground sources threw root-derived compounds to be the source of the OM. In the PA layer, the root distribution of medium roots is enriched and even in the rEP. Root- transect samples could relate to a more specific look to root exudates and contribution on OM.

4.2 Root- and rhizomicrobial derived OM

4.2.1 Diagnostic ratios and distribution patterns

Beside distribution patterns from TLE, fatty acid- and *n*-alkane distributions, several diagnostic ratios were found to be useful in elucidating source of OM in rhizosphere.

Fatty acids and n-alkanes ratios

Root exudates and root-borne organic substances which released in the root environment during growth or root hairs are sources of organic carbon which also includes the FA (Kuzyakov and Domanski 2000). Distribution patterns of FAs in both roots (R) and root-surrounding (RS) soil showed high $C_{16:0}$, $C_{18:0}$ and long chain homologues (> $C_{20:0}$) as well as predominance of even/odd chain FAs and stands in a line with the results from Gocke et al. (2010). Because distribution patterns itself could not quantitatively estimate the contribution of root-derives OM, other parameters were used. From Gocke et al. (2010) it is assumed, that CPI_{FA} and ACL_{FA} have the highest value in root and slightly lower in the soil while rhizosphere having the lowes CPI_{FA} and ACL_{FA} values compare to all other (CPI_{FA}, ACL_{FA}) values. From the ACL_{FA} and CPI_{FA} values of the aboveground biomass it was known, that root tissues had very low ACL_{FA} and CPI_{FA} values compared to the other plant tissues. Root samples from the root- transects had much higher values than root samples from the aboveground biomass especially in roots from the PA- root transect. It is questioned, were these differences originate from. Fresh plant biomass was characterized by high ACL_{FA} and CPI_{FA} values (Peters et al. 2005) and microbial biomass or microbial reworking was expressed in low ACL_{FA} and CPI_{FA} values (Cranwell 1981). Low ACL_{FA} values in the rhizosphere and especially in the intermediate between soil and root (RS) corresponding therefore to large root and microorganism derived FAs. In *figure 19* it was shown that samples from the rhizosphere, the soil and mostly from the reference sample (distance more than 14 cm to the center) were area of strongly degraded OM ($CPI_{ALK} < 10$, $CPI_{FA} < 4$; (Cranwell 1981; Cranwell et al. 1987)). The root-transects showed lower CPI_{FA} and ACL_{FA} values in deeper soil layers. ACL_{FA} increased with increasing distance to the central root. The lower values in the rhizosphere attributed to a high abundance of root- or rhizomicrobial derived OM near the central root (Jones 1998). This distribution pattern doesn't showed the ACL_{FA} distribution in the PA horizon. The CPI_{FA} showed low values for the central root in PA and increasing CPI_{FA} values with distance to central root. In the rEP, the soil

in direct root vicinity showed very high CPI_{FA} values that decrease with increasing distance. Also the root- transect from the coversand layer showed this trend. One could assume, that roots do have an influence to its direct environment and that this effect decreases with increasing distance. The very low value in rEP and cs in transect parts with higher distance to the centre and unexpected low values in CPI_{FA} could relate to other roots that influence this soil part. The reason why ACL_{FA} and CPI_{FA} values were lower in the rhizosphere relates to microbial reworking. During lifetime of a plant its environment is full of microorganisms that are feed by root exudates and dead root biomass (Coleman 1994; Jones 1998). To estimate if a value of CPI_{FA} or ACL_{FA} in rhizosphere relates to root exudates or more on microbial biomass could not be answered by this parameters. Gocke et al., (2010) calculated quantities of mono- unsaturated FAs. The calculation with mono- unsaturated acids with the root-transect samples didn't show any trend patterns (*appendix*) and was not included to this masterthesis. From the given data ($ACL_{FA,ALK}$, $CPI_{FA,ALK}$) one could assume, that samples from the upper plaggen soil (0.75 m depth) seemed to have OM with large microbial activity along the whole transect ($ACL_{ALK} < 25$, $ACL_{FA} < 20$; (Kolattukudy, Croteau & Buckner 1976b). In deeper soil layers, the roots did strongly affect its environment. In coversand and in rEP layer the root influence was much higher and reached up to transect soil with 16 cm distance to the central root.

5 Conclusion

Lipid molecular proxies deriving from n-alkanes and fatty acids (FA) were used to assess source identification of soil and sedimentary organic matter (OM) in a multi- layered profile at Bedafse Bergen, Netherlands. Organic Carbon (C_{org}) measurement did not allow an identification of different OM sources in different soil layers. In contrast, *n*-alkane and FA proxies like average chain length and carbon preference index made the differentiation between fresh plant derived and root or microorganism derived OM possible. Long chain alkane composition (n-C_{25-33}) and ratios (n-C_{27}/n-C_{31}, n-C_{29}/n-C_{31}) could relate to grass vegetation of woody vegetation as origin of OM and confirm the assumption of different sources of OM in different layers of the multi-layered soil profile. FA proxies could confirm the assumptions of the n-alkane analysis and relates to more information about rhizomicrobial- and root derived OM. One could conclude, that the uppermost layer, the Epialbic Podzol (EP) contributed to OM that was derived from the fresh aboveground biomass (woody vegetation with lot of oak tree). The Plaggic Anthrosol *n*- alkane ratios indicated grass vegetation as origin of OM, while rhizomicrobial- or root derived OM were underpart compared to the OM derived from grass vegetation. The grass vegetation as main source of OM in plaggen soil confirmed the assumption of pre-sedimentary formation during plaggen cultivation. At Bedaf Bergen, Podzol (EP) in lower parts contained incorporation of fresh biomass- derived OM, whereas in depth with higher root abundance (relict Podzol, rEP) post sedimentary incorporated root- and rhizomicrobial- derive OM was obtained. By the help of lipid biomarkers, the assumption that EP and rEP have a similar OM source had to be denied. The coversand, which was the deepest soil layer in the profile showed the highest post sedimentary alteration of sedimentary OM.

For root- transects at Bedaf Bergen it was shown, that the remains of OM in direct root vicinity was influenced by the central root. Lipid analysis combining several FA and alkane proxies, including CPI and ACL could have shown post- sedimentary incorporation of OM in rhizosphere. Additional proxies like different chain-length alkanes or fatty acids even mono- unsaturated FA stands in a line with the assumption of root influence to its environment. ACL_{FA}, ACL_{ALK}, CPI_{FA} and CPI_{ALK} molecular proxies

showed that the influence of former roots led to a modification of the OM composition in the rhizosphere. The root- transects showed, that in direct root vicinity (0-2 cm distance from central root), the root- or rhizomicrobial- derived inputs were high. With distance, the influence decreased. The biomarker analysis showed, that in the plaggen soil, the root- or rhizomicrobial derived inputs could only an effect to its direct root vicinity and therefore have a small influence to the total OM in this layer. This stands in a line with the results from the profile layers, were plant biomass seemed to be the main source of OM. In Podzol situated deep (1.80 m) in the profile, the central root had an influence on root- or rhizomicrobial- derived inputs up to 8 cm distance to the central root. Furthermore, root- or microbial derived sources in the coversand had also a strong influence to its environment up to 11 cm. In deep soil layers, post- sedimentary incorporated root- or rhizomicrobial sources contributed to considerable inputs to the OM.

The approach to distinguish aboveground and belowground sources by lipid analysis, consequence most likely to an overprint of pre-sedimentary and post-sedimentary incorporations. Especially the influence of root- ore rhizomicrobial- derived inputs as affected by this overprint because of incorporated OM by younger biomass from other sources. A combination of source identification by lipid analysis with aided ^{14}C analysis might entail uncertainties in OM sources. Therefore, more research is required to elucidate the influence of root- and microbial- derived OM in deep soils. For a more certain differentiation of vegetation sources further proxies are required. For example n-alcohols or suberin and cutin molecular markers (Mendez-Millan et al. 2010).

6 Acknowledgments

I want to thank PD Dr. Guido Wiesenberg who gave me the chance to do my Master's thesis in his lab and allowed me to join his group. I really enjoyed working on the lipid analysis project. A huge "thank you" goes especially to Martina Gocke and Kavita Srivastava; they helped me a lot and always answered my questions with patience. I also want to thank Samuel Abiven, Michael Schmidt, Michael Hilf and Sandy Röthlisberger they also showed me a lot and helped me with my studies. The whole team deserves thanks for the great experience and support for my Master thesis.

I hereby declare that the submitted thesis is he result of my own, independent work. All external sources are explicitly acknowledged in this thesis.

Winterthur, 30.09.2016

Signature Rahel Widmer

7 Appendix

7.1 Raw data

7.1.1 Lipid content

	Sample	Depth (m)	Age (y AD)◆ OSL ages	Sand* (mass-%)	Silt* (mass-%)	Clay* (mass-%)	pH* ($CaCl_2$)	SOC* (mg g^{-1})	TLE (mg g^{-1})	TLE C_{org}^{-1} (%)
	Oi	1						453.1	25.1	5.5
	Oe	0.5						416.6	20.0	4.8
	Oa	0.2						98.8	5.5	5.6
96B14MG3	EP	0		97	2	1	3.1	9.4	1.0	10.9
96B14MG7		-0.1		98	1	1	3.2	4.7	0.2	3.2
96B14MG11		-0.1		98	1	1		4.7	0.2	5.0
96B14MG15		-0.2		99	1	0		1.5	0.1	4.5
96B14MG23	ds	-0.25	1,812 ± 9	98	2	0	3.5	1.9	0.1	4.1
96B14MG19	ds	-0.4	1,808 ± 8	99	1	0		1.1	0.1	6.8
96B14MG27	PA	-0.4		96	3	1	3.8	2.7	0.1	3.7
96B14MG31		-0.5		98	1	1		7.4	0.5	7.0
96B14MG35		-0.6	1,781 ± 9	93	4	3	4.0	8.3	0.4	5.0
96B14MG39		-0.75		92	5	3		9.9	0.7	7.4
96B14MG43		-0.9		91	7	2	4.0	8.8	0.5	5.8
96B14MG47		-1.05		90	6	4		12.8	0.6	4.7
96B14MG47_2		-1.2	1,593 ± 17	91	6	3	3.9	17.0	1.8	10.3
96B14MG48		-1.2		91	6	3		17.0	2.1	12.1
MW47 und 48		-1.2						15.1*	1.5	9.8
96B14MG51		-1.35	69 ± 89	92	6	2		17.4	0.5	3.0
96B14MG55	rEP	-1.5		95	4	1	4.1	12.6	0.4	3.5
96B14MG59		-1.65		96	3	1	4.5	9.9	0.1	1.5
96B14MG63		-1.8		97	3	0		2.1	0.0	1.5
96B14MG67	cs	-1.95		95	4	1		2.6	0.1	2.6
96B14MG71		-2.1		97	2	1		1.2	0.0	2.5
96B14MG72		-2.1					4.6	0.8*	0.0	3.1
96B14MG75		-2.25		98	2	0	4.7	0.7	0.0	3.6
96B14MG76		-2.25						0.6*	0.0	4.4

7.1.2 n-alkanes

Plant Samples

	SEQ1																SEQ2			
	Vol in Mikrovial	96B14MG80c	96B14MG219a	96B14MG219b	96B14MG201	96B14MG202	96B14MG203	96B14MG206	96B14MG207	96B14MG208	96B14MG210	96B14MG211	96B14MG212	96B14MG216	96B14MG217	96B14MG217a	96B14MG213	96B14MG80a	220
	200mikroliter	Soil around root	Fun	Fun	org Auflage Oi	org Auflage Oh	org Auflage Of	Fun	Stamm	Fun	Zweig	Fun	Wurzel	Wurzel	Zweig	Fun	Fun Fruchte	Wurzeln	Zweig
C15																			
C16		6.6																	
C17		31.9			7.0	6.1		8.9	9.1				6.2						5
Pr		3.1			5.2	2.9													
C18		8.8			5.6	5.1	3.1												
Ph		3.9			2.9														
C19		12.2			11.9	12.0	3.4			2.9									4.9
C20		13.5			7.6	9.7	3.6												2.7
C21		27.9			18.7	27.3	6.7	6.4		4.5	6.6								5
C22		20.0			11.4		5.1	4.0		3.2			2.4						6.8
C23		68.3	61.5	44.7	43.0	63.4	14.1	9.8	3.8	7.3	16.3	11.9	4.0	4.3	4.1			3.8	36.6
D50C24		84.5	147.5	91.4	116.3	134.0	113.3	217.9	218.2	184.9	92.5	73.5	222.0	239.4	114.8	110.6	234.6	239.2	90.4
C24		39.9	9.5	6.6	19.0	29.5	8.7	4.1					4.7	4.9	5.9			6.1	39.4
C25		422.2	153.2	109.5	230.8	384.2	72.6	17.1	3.8	10.6	19.7	49.5	17.9	15.2	20.4	4.2	7.3	9.5	443.9
C26		81.4	16.4	10.5	32.8	53.5	19.4					4.2	8.4	9.0		21.4		11.8	93.3
C27		1154.8	205.8	145.7	523.5	858.8	242.0	24.1	9.2	13.1	76.0	86.0	39.3	27.7	23.2	28.0	16.8	18.4	851.3
C28		138.1	20.0	12.2	68.5	121.2	46.9		4.1		17.7	31.6	12.1	11.4	180.9	16.6	3.1	20.6	45.3
C29		1610.4	203.5	139.5	537.8	856.8	522.3	24.0	77.2	7.3	876.6	959.8	43.0	36.6	582.3	83.1	26.5	35.9	463.1
C30		101.9	44.4	29.9	45.0	56.1	27.1				12.3	39.8	8.3	8.2	105.7	7.0		23.6	9.2
C31		585.1	55.3	36.4	145.6	253.2	149.3	11.6			36.3	151.1	15.5	17.1	351.1	52.9		24.1	14.0
C32		25.5																	
C33		108.4																	

Profile Samples

3	12.0	14.4	23.4	30.1	6.4	24.9	27.0	28.4	26.5	39.1	170.9	28.3	92.5	30.8	276.8	60.1	540.2	40.6	263.7	18.1	101.3
7	11.6		14.5	19.6	6.7	16.6	19.2	17.6	14.0	22.7	141.0	20.2	22.7	10.7	48.2	13.4	57.8	8.1	45.9		31.8
7_2	9.9		13.9	21.3	9.3	23.5	33.4	30.4	34.7	38.2	153.4	36.1	43.9	14.5	59.5	16.8	67.5	10.3	52.9		37.1
															53.8	15.1	62.6	9.2	49.4		
11	7.6		21.0	17.3	6.6	15.0	17.7	15.4	17.7	18.9	148.7	17.6	14.5	7.7	24.3	6.7	27.1	4.6	30.9		24.5
15	12.3		27.0	36.2	19.2	29.6	33.9	29.2	31.9	35.9	163.8	45.0	39.7	18.2	66.7	18.0	82.5	12.9	87.5	10.5	58.5
19			5.0	13.5	5.2	13.1	19.6	22.6	28.4	39.8	181.1	33.7	57.0	25.1	83.5	23.9	102.3	21.1	114.6	17.3	85.9
23	21.3		23.7	25.2	10.8	16.9	23.3	24.4	29.1	28.5	149.0	28.2	20.7	11.3	31.3	9.8	36.6	7.1	42.0		43.0
27	10.4		5.3	9.6	4.9	7.5	13.2	28.9	37.1	64.9	116.1	46.2	100.3	43.7	173.0	45.8	252.5	44.1	299.5	37.6	219.9
31	16.6	22.5	28.3	34.0	8.6	36.6	49.3	64.1	74.9	115.9	213.0	89.5	165.3	83.6	280.0	80.7	417.8	83.1	577.9	76.7	463.3
35		8.1	21.6	14.1	3.7	14.9	21.2	35.9	47.1	81.3	103.4	63.4	125.3	61.5	216.9	58.3	321.6	59.3	427.7	53.7	328.9
39		3.1	12.5			20.4	27.4	41.1	52.3	85.8	120.3	65.7	127.5	66.1	214.5	61.8	309.5	63.6	432.9	59.0	365.9
43	7.4	9.9	8.3	19.3	3.8	20.7	27.5	39.1	50.2	84.4	96.0	64.9		127.4	209.1	57.0	304.0	60.0	439.3	62.6	439.4
47		19.5	34.7	19.2	8.9	17.3	34.8	81.0	110.1	184.3	143.8	126.1	223.1	116.4	353.0	109.2	536.4	114.1	912.0	138.1	1068.1
47_2		19.0	14.7	19.2	8.3	17.2	34.0	77.6	108.5	182.1	102.2	129.8	220.6	117.8	380.0	107.1	540.0	119.7	949.6	147.9	1132.7
48		16.3	22.8	12.0	7.0	14.0	18.8	47.1	63.5	115.6	117.2	81.5	165.1	82.6	271.8	82.0	416.3	83.0	619.1	9.1	659.6
MW_47,48															318.3	99.5	497.6	105.6	826.9		
51		12.9	21.2	11.2	5.4	10.3	22.0	57.5	72.9	120.8	109.0	79.8	126.6	73.4	194.8	61.5	310.9	68.6	588.0	91.3	733.3
55	48.8	35.0	30.0	35.5	28.6	24.8	30.9	85.4	53.2	100.6	176.1	58.5	49.3	27.3	49.7	16.2	29.5		26.4		34.8
59	3.3	28.4	36.2	19.8	14.5	33.7	17.0	33.9	23.7	40.8	166.4	27.7	23.1	10.5	25.1	10.1	21.3		26.0		30.4
63	3.6	14.9	22.8	9.8	7.2	15.7	9.2	10.1	10.3	10.4	167.1	12.8	6.7	3.8	4.1		15.0		28.1		13.2
67	75.0	127.9		55.5	38.8	31.4	36.8	36.1	43.7	45.8	241.1	60.5	29.1	15.2	30.5	12.1	38.1	9.6	41.5	8.5	40.0
71	32.0		52.3	17.0	47.5	7.7	10.9		10.4	7.5	122.3	21.5	6.4	4.2	6.7	11.9	10.0		13.0		9.8
75	15.9	36.8		16.0	8.8	8.2	11.5	9.3	14.9	11.4	101.0	19.4	5.3	4.0	12.2	9.9	9.8		5.9		
76	8.2	10.5	8.5	14.2	6.1	10.5	11.6	8.4	10.3	7.0	93.9	10.5									

Transect Samples

	C16	C17	Pr	C18	Phy	C19	C20	C21	C22	C23	DSOC24	C24	C25	C26	C27	C28	C29	C30	C31	C32	C33
80c	6.6	31.9	3.1	8.8	3.9	12.2	13.5	27.9	20.0	68.3	84.5	39.9	422.2	81.4	1354.8	138.1	1610.4	101.9	585.1		
219a										61.5	147.5	9.5	153.2	16.4	205.8	20.0	203.5	44.4	55.3		
219b										44.7	91.4	6.6	109.5	10.5	145.7	12.2	139.5	29.9	36.4		
201		7.0	5.2	5.6	2.9	11.9	7.6	18.7	11.4	43.0	116.3	19.0	230.8	32.8	523.5	68.5	537.8	45.0	145.6		
202		6.1	2.9	5.1		12.0	9.7	27.3		63.4	134.0	29.5	384.2	53.5	858.8	121.2	856.8	56.1	253.2		
203				3.1		3.4	3.6	6.7	5.1	14.1	113.3	8.7	72.6	19.4	242.0	46.9	522.3	27.1	149.3		
206		8.9						6.4	4.0	9.8	217.9	4.1	17.1		24.1		24.0		11.6		
207		9.1								3.8	218.2		3.8		9.2	4.1	77.2				
208						2.9		4.5	3.2	7.3	184.9		10.6		13.1		7.3				
210								6.6		16.3	92.5		19.7		76.0	17.7	876.6	12.3	36.3		
211										11.9	73.5		49.5	4.2	86.0	31.6	959.8	39.8	151.1		
212		6.2	2.5						2.4	4.0	222.0	4.7	17.9	8.4	39.3	12.1	43.0	8.3	15.5		
216			2.3							4.3	239.4	4.9	15.2	9.0	27.7	11.4	36.6	8.2	17.1		
217				2.5						4.1	114.8	5.9	20.4	21.4	23.2	180.9	582.3	105.7	351.1		
217a											110.6		4.2		28.0	16.6	83.1	7.0	52.9		
80e	6.8	11.7	403.6							3.8	239.2	6.1	9.5	11.8	18.4	20.6	35.9	23.6	24.1		
213	681.4	33.6	12.7								234.6		7.3		16.8	3.1	26.5				
220		5.0				4.9	2.7	5.0	6.8	36.6	90.4	39.7	443.9	93.3	851.3	45.3	463.1	9.2	14.0		
226	16.2	17.8	11.4	20.2	11.8	15.7	33.0	78.4	105.1	196.8	92.2	129.7	298.5	131.0	450.1	106.0	690.3	111.9	773.8	104.4	686.2
227	15.2	16.7	10.6	19.4	12.0	16.2	34.4	85.1	115.8	220.8	100.7	146.5	341.2	148.0	512.5	127.4	681.6	127.4	863.8	117.6	767.7
228	13.2	22.3	14.3	25.2	13.9	19.3	41.9	99.2	134.3	252.3	122.4	166.5	384.3	168.2	568.1	149.9	753.9	160.1	947.2	128.1	833.6
229	13.9	17.7	12.7	22.0	13.7	16.5	36.3	88.3	121.7	235.7	99.6	158.6	377.1	168.7	584.1	157.2	810.3	153.8	1080.3	151.9	1026.0
230	20.6	22.2	15.2	23.2	12.8	17.1	35.8	83.2	118.0	223.6	96.0	150.9	354.6	155.7	546.4	132.3	728.3	136.7	940.2	131.4	878.0
231	15.6	18.0	10.5	19.3	11.8	13.4	30.1	70.2	99.3	194.0	179.2	132.5	315.8	141.9	498.0	134.3	700.2	133.7	949.1	135.4	928.8
232	7.0	8.5	5.6	11.2	6.6	7.4	16.5	35.4	47.9	89.5	101.6	58.9	136.4	59.4	210.2	50.6	286.2	54.0	376.3	53.6	364.6
233		2.5		2.0			1.6	1.1	1.4	1.4	204.2	1.3	1.4	0.0	1.5		2.3		2.0		
134a							0.9	0.0	0.7		164.8	0.6									
134b						0.6	1.9		1.5		194.6	1.5	1.2		0.9						
136				4.0	2.9		5.7	11.0	14.9	26.0	101.8	19.7	40.8	19.2	74.7	20.0	125.5	21.7	157.6	18.2	104.8
137	13.4	11.5	5.2	12.0	8.2	7.9	17.2	34.5	45.2	79.9	122.0	61.4	123.2	57.3	211.3	55.0	356.4	60.1	449.5	52.4	313.5
138	17.6	12.1	8.0	13.8	9.7	8.5	19.0	38.8	51.0	91.5	124.9	72.1	148.5	70.8	256.9	70.8	441.9	76.4	566.4	67.7	406.5
139	23.0	20.1	11.5	18.3	13.4	12.8	27.3	59.7	77.6	136.6	90.5	106.0	216.6	103.7	369.5	103.3	579.4	107.0	766.7	94.8	564.7
244	12.5	21.5	19.1	24.5	16.3	16.0	16.0	10.5	17.4	10.3	217.0	13.4	12.5	11.3	17.1	6.5	19.5	4.4	19.0		10.8
245	14.4	26.7	23.5	29.7	21.4	20.5	20.2	8.9	23.6	7.9	250.9	17.9	8.7	10.6		8.2	15.9	6.2	17.4		10.8
246	13.2	14.7	20.6	22.5	17.0	16.3	15.4	7.7	17.2	7.1	206.0	12.8	6.8	7.4		6.0	12.1	4.0	11.6		7.7
247	18.2	19.8	21.7	25.7	19.1	18.0	19.5	14.1	19.6	10.4	207.0	14.5	8.9	8.4		7.2	13.0	5.8	12.7		7.8
248	23.7	26.6	25.3	26.6	30.7	31.3	20.9	20.5	49.0	18.2	269.8	44.2	9.5	33.4	25.5	31.2	21.9	23.2	20.4	11.0	11.1
249	9.2	11.7	10.8	11.3	12.4	12.4	9.0	19.0	17.8	14.9	265.5	15.2	6.8	9.8	8.8	8.7	8.2	7.3	9.6	3.1	7.4
250	9.0	8.5	9.7	10.0	10.0	12.3	10.0	27.1	22.0	24.1	210.1	12.7	9.7	20.0	18.6	18.2	12.3	13.8	9.0	6.8	6.9
252		1.5		3.5			2.2	2.2	1.8	1.8	190.2	1.2						1.2	1.8	1.1	
234	10.6	12.9	14.7	20.8	12.4	6.2	13.3	11.4	9.7	10.7	111.2	7.0	8.4		10.4		10.5		15.3		8.3
235	16.1	12.9	13.5	17.9	16.4	4.4	11.1	12.7	9.3	12.7	144.4	7.0	10.5		10.2		14.7		16.5		10.4
236	11.8	13.9	14.3	17.9	13.7	5.3	9.9	12.1	8.6	11.9	90.0	6.3	7.8	5.3	7.7	11.7	12.7	9.5	12.2		
237	22.6	21.3	22.4	23.4	22.5	8.3	15.8	14.5	14.7	15.3	109.0	12.1	10.6	9.7	26.2	26.6	22.7	22.0	17.9	12.0	
238		21.5	33.2	31.3	24.3	10.2	22.1	29.9	18.2	27.6	146.7	16.1	18.1	12.0	26.2	17.0	22.4	14.4	25.3	8.0	18.8
239	5.9	5.3	7.6	7.1	7.8	2.3	6.2	11.0	6.0	11.7	100.5	4.6	7.4	2.7	6.8	6.1	7.8	5.0	7.4	2.4	5.5
240	12.2	9.6	12.0	11.3	12.6	5.8	12.0	40.7	18.1	37.9	123.7	15.8	17.5		8.6	7.7	10.5	6.0	9.9		6.6
242	1.7	2.6		5.3	1.7	1.8	4.6	7.2	1.5	6.0	208.2	3.6	3.6	2.3				2.3	2.3	2.4	
253		6.3	1.8	7.0	10.1	3.6	5.4	4.9	5.1	5.4	232.6	5.9	7.8		8.2	2.0	13.7	1.2	13.3	3.6	7.5
254a								1.4	1.6	2.7	206.0	3.9	5.5			6.8	6.8		4.1	2.7	1.9
254b	6.5	5.0		8.3	14.2	4.8	14.2	30.5	15.2	25.5	205.0	14.1	17.0		21.9	13.0	16.3		13.3		
255	1.5	3.7		4.8	6.8		3.6	4.2	4.3	5.9	240.2	7.2	11.3		1.9	1.4	17.8		15.7	6.2	9.0
256	1.3	3.2		4.0	6.1	2.2	4.2	6.1	4.2	5.7	216.2	3.9	1.8		4.4	1.3	7.0		8.1	1.6	4.8
257		2.2		3.4	4.6	1.9	3.5	6.6	5.3	9.6	231.5	11.4	1.0		21.5	24.4	26.1		19.5	11.1	10.9
258	2.3	2.0	1.2	4.0	7.1	4.3	8.8	32.9	15.0	25.1	207.7	12.5	1.1		8.1	1.6	3.2		3.3		2.1
259a																					
259b								1.5	1.2	1.9	174.3	2.1	2.6	3.2	3.6	2.6	2.7	2.2	1.7	0.9	0.9
157	16.6	31.0		11.0	6.1	15.9	36.7	171.9	85.6	168.8	94.4	64.3	68.0	35.0	59.7	22.2	58.3	10.6	102.9	13.9	127.4
158				0.5	0.5		0.8	2.0	1.5	2.4	73.6	1.7	1.8	1.7	2.1	1.4	1.8	0.9	1.3	0.8	1.2
105	11.6	51.9		17.3	11.4	8.7	14.2	19.0	15.1	29.4	210.0	25.8	35.5	15.9	58.5	13.7	79.4	11.7	79.6	9.6	59.3
106				2.3	0.9		0.9		0.6		193.1	0.6	0.8	0.7			1.1				
106_2				3.6	2.9		2.6	0.8	1.3	1.4	198.9	1.7	1.8	2.3	2.5	2.6	2.6	1.8	2.8	1.5	

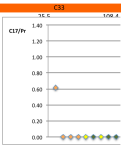

7.1.3 Fatty acids

Plant Samples

		219a	219b	211	96B14MG213	217a	96B14MG210	217	220	207	212	216	96B14MG80a	96B14MG205	96B14MG206	201	202	203
	C9:0			6.3														4.6
Nonanoic ac.	C10:0				17.6													5.6
Undecanoic ac.	C11:0				1.9													
Dodecanoic ac.	C12:0	54.1	46.0	33.3	11.5	89.7	17.1	81.1	20.4		32.7	56.2	19.7	8.2	2.6	17.7	12.6	14.8
Tridecanoic ac.	C13:00				4.2		4.7						1.2					
Tetradecanoic ac	C14:0	107.8	92.9	50.1	91.0	42.3	52.4	36.5	37.9	11.3	59.3	42.3	39.9	25.1	5.1	45.9	30.5	26.0
Pentadecanoic ac.	C15:0	14.1	11.1	18.2	31.8	7.0	57.6	14.3	31.2	3.3	77.3	33.6	15.6		1.5	17.0	8.5	10.8
	C16:1	17.9	14.0	6.1	34.4	45.1	70.3	0.0	13.3	8.1	88.5	30.5	34.4	12.2	3.5	74.7	19.8	35.0
Hexadecanoic ac.	C16:0	549.2	444.1	960.4	651.2	429.0	2213.9	1184.7	1341.8	4.9	2491.4	1416.7	319.0	173.5	51.1	392.8	210.3	241.9
Heptadecanoic ac.	C17:0	30.7	24.5	29.1	15.9	12.2	61.0	67.1	56.3	4.2	25.1	5.7	10.4	15.2	3.3	19.6	7.4	11.9
	C18:2	20.0	31.8	8.3	21.4	17.2	567.8	12.5	93.2	0.0	1168.9	347.3	21.0	175.3	12.0	214.8	62.8	25.8
	C18:1	53.8	75.6	4.1	65.0	68.6	871.2	11.9	85.4	147.1	1402.9	56.9	118.1	390.1	35.9	722.3	79.3	136.2
Octadecanoic ac	C18:0	177.9	135.7	334.8	85.7	218.8	550.9	633.2	212.0	66.5	471.3	709.1	351.6	147.0	40.3	186.0	157.1	159.1
Nonodecanoic ac.	C19:0	12.3		48.7	5.8	7.7	12.2	19.1	17.9		57.5	27.1	3.5	16.7	3.9	6.1	13.4	7.6
Eicosanoic acid	C20:0	256.2	226.8	118.7	36.5	51.9	415.5	58.2	112.5	15.2	388.8	98.8	16.5	135.5	32.2	210.3	278.9	255.2
Heneicosanoic ac	C21:0			14.1	6.2	9.5	4.6	17.1	42.7	34.7	389.9	20.9	3.4	44.1	13.3	55.2	52.6	263.3
	C22:1	0.0	0.0	0.0	0.0	0.0	51.8	8.8	0.0	0.0	142.4	0.0	10.2	18.5	0.0	7.0	0.0	47.4
Docosanoic ac	C22:0	117.1	98.5	70.9	30.9	29.2	927.6	42.8	174.2	117.6	280.8	69.4	17.7	430.8	149.2	339.3	583.3	529.3
Tricosanoic ac	C23:0	25.4	21.7	22.9	8.9	11.8	95.4	42.7	64.5	26.7	78.3	28.9	14.6	71.8	28.2	85.4	101.9	94.4
Tetracosanoic ac.	C24:0	102.2	89.4	156.8	176.0	33.9	2.2	42.8	177.6	341.1	113.7	39.6	18.5	1499.3	471.4	259.1	733.5	511.2
Pentacosanoic ac	C25:0	20.7	17.8	19.8	7.2	12.4	34.0	12.7	56.5	21.6	41.0	11.3	4.2	62.7	21.0	55.5	146.1	104.2
Hexacosanoic ac.	C26:0	299.7	269.2	87.3	95.6	75.8	95.2	49.1	454.6	124.0	3.2	37.2	12.2	691.6	172.6	286.2	1112.4	10.2
Heptacosanoic ac	C27:0	44.6	38.5	8.2	3.8	17.8	5.1	50.6	50.9		19.0	7.5	3.0	8.3	1.8	48.1	204.3	133.5
Octacosanoic ac.	C28:0	2.2	552.7	72.9	25.7	133.0	51.1	434.7	351.6	5.4	88.7	50.8	9.9	38.7	6.5	262.3	1285.5	3.9
	C29:0	54.2	43.5	13.8		25.9	11.8	85.7	23.9			4.9		2.1	5.6	33.9	180.0	5.8
Triacontanoic ac.	C30:0	322.5	257.1	118.7	7.2	169.7	87.3	598.6	94.1		80.9	33.5	8.0	51.3	4.9	130.0	759.8	390.6
	C31:0				67.5	94.3	6.0	157.4	43.3		261.8	131.7	2.3	92.6	26.1	41.5	36.1	31.8
	C32:0	45.3	34.8	25.9	2.7	93.4	16.1	300.3					18.7	105.8	3.8	28.2	152.4	80.7
	C33:0						36.6								18.6			
	C34:0												1.6	12.3				

Profile Samples

	96B14MG3	96B14MG7	96B14MG11	96B14MG15	96B14MG19	96B14MG23	96B14MG27	96B14MG31	96B14MG35	96B14MG39	96B14MG43	96B14MG47	96B14MG47	96B14MG48	MW47 und 48	96B14MG51	96B14MG55	96B14MG59	96B14MG63	96B14MG67	96B14MG71	96B14MG75
C9:0	6.3	6.2						9.5								12.7						
C10:0	6.9	36.9	22.4	41.9	16.0	70.1		3.7								4.4		24.0	22.8	2.2	59.1	66.1
C7:0 dioic ac																						
C11:0						15.8												4.4	4.8	14.4	10.6	10.9
C8:0		30.8	7.0	22.2	8.4	17.8										3.7		5.2		5.0	1.1	
C12:0	26.5	112.0	61.4	117.8	46.7	266.1	9.4	34.9	22.8	13.0	31.3		13.5	12.6	13.1	35.6	27.7	65.7	73.9	169.2	112.0	141.5
C9:0 dioic acid	44.8	78.2	18.3	54.2	20.1	44.5		16.1	13.3	8.0	12.3			22.2	22.2	30.1		20.6	2.4	22.5	4.2	
C13:00	4.9	11.8		9.3		18.0		3.3								3.8		5.9	8.2	15.8	14.9	18.3
C10:0		10.7		7.8		9.3												3.4	1.2	3.7		
C14:0	22.7	93.0	33.2	76.1	35.1	124.1	16.3	32.3	26.8	35.6	29.0	11.2	14.9	35.6	20.6	43.5	17.8	43.1	36.9	110.5	96.0	131.0
C11:0							6.6													3.8		
C15:0	10.9	50.0	13.0	29.9	15.2	48.2	11.3	21.5	15.5	27.3	16.3	10.5	12.5	19.9	14.3	26.5	16.8	32.3	15.8	54.5	48.5	52.3
C12 dioic ac	17.7	16.6			9.6	23.7	6.4	17.4	5.7	13.2	12.7	9.7	12.8	19.4	14.0	27.2	36.5	27.0	2.2	54.8		
C16:1		17.8			6.3	12.7										5.6		3.7	1.4	8.2	3.2	7.6
C16:1		73.5				36.6												16.2	14.9	59.0	82.3	111.5
C16:1		9.2	9.3	25.2	8.7	6.6												3.1	2.9		5.5	
C16:1	0.0	100.5	9.3	25.2	14.9	55.9	0.0	0.0	0.0	0.0	0.0	0.0	0.0	0.0	0.0	5.6	0.0	23.0	19.2	67.2	91.1	119.1
C16:0	153.8	489.2	207.9	481.9	195.0	613.9	144.0	193.1	171.3	279.6	170.4	95.2	122.3	252.8	156.8	249.2	110.3	267.6	232.6	724.4	562.8	665.1
J		10.1		10.3	6.7	15.0												9.5	5.4	22.4	10.9	
C17:0	9.8	22.4	7.4	17.0	9.3	23.8	9.2	18.5	13.3	24.4	19.4		9.2	23.2	16.2	22.4	8.5	13.0	6.8	24.8	19.7	16.0
C18:2	8.5	19.5		27.6		20.1	12.0	16.2	8.6	23.5	5.4			5.4	5.4		13.7	23.7	5.8	19.0	39.7	45.7
C18:1	88.2	291.4	92.2	299.3	57.4	354.0	100.6	127.1	78.8	240.0	62.2	21.6	30.1	54.7	35.5	65.2	71.0	191.1	124.7	432.1	289.6	336.0
C18:1 isomer	19.2	76.8	40.0	94.6	32.9	126.0	23.5	39.7	32.4	47.9	37.0	14.2	17.7	43.2	25.0	41.3	31.9	47.1	43.1	176.0	159.6	89.1
C18:1	107.5	368.1	132.1	393.9	90.4	480.0	124.2	166.8	111.3	287.9	99.3	35.8	47.9	97.9	60.5	106.5	102.9	238.2	167.7	608.1	449.2	425.2
C18:0	117.2	375.7	185.2	391.8	182.9	529.5	103.1	202.0	180.3	314.8	204.9	120.9	144.8	331.6	199.1	222.0	86.7	245.0	221.9	717.8	557.4	550.3
C19:0	9.5	49.6	9.8	20.4	16.4	42.2	12.8	30.3	38.1	59.3	41.9	32.0	32.7	56.4	40.3	51.2	30.1	50.2	8.0	29.5	9.1	
C16:0 dioic ac	123.9	112.2	18.7	75.8	15.0	43.8	12.1	28.5	37.1	36.2	20.8	24.7	25.8	34.4	28.3	45.3	12.6	32.1	2.1	20.4	2.0	81.2
C20D39	196.9	246.0	148.0	124.5	107.5	227.1	160.3	202.5	139.5	1011.3	183.2	231.0	213.8	1819.3	754.7	255.3	230.9	198.1	241.9	111.9	228.3	247.0
C20:1	205.9		16.1	35.8	12.2			293.4	401.0	585.5	467.2	429.4	464.5	703.4	532.4	508.1	163.1					
C20:0	290.3	266.5	99.2	228.3	186.9	476.1	224.6	295.6	5.6	391.6	263.9	322.1	296.6	6.8	208.5	366.5	315.3	253.6	45.0	111.4	46.9	31.9
C21:0	44.1	121.1	41.4	80.5	62.6	144.2	37.5	104.0	90.0	160.1	110.9	93.0	104.7	157.3	118.3	182.1	128.8	247.4	35.2		44.7	12.9
C18:0	34.7	42.0	10.1	32.2	16.5	27.7	7.5	18.1	27.6	31.9	19.0	24.2	25.5	36.8	28.8	35.1	14.4	31.4	2.5	16.6	1.7	
C22:1	16.5	118.8	69.7	158.8	55.7	278.7												133.5	213.1	834.7	407.1	498.4
C22:1?		47.4	14.5	40.6	13.7	31.0											34.5	91.8	62.6	123.9	221.3	538.7
C22:1		12.8																3.9			19.2	
C22:1	16.5	179.0	84.2	199.4	69.4	309.7	0.0	0.0	0.0	0.0	0.0	0.0	0.0	0.0	0.0	0.0	34.5	229.2	275.7	958.6	647.5	1037.1
C22:0	352.8	619.2	147.0	299.8	209.1	508.3	127.6	358.7	315.8	490.0	359.3	373.8	416.9	604.1	464.9	604.7	548.2	1179.5	195.3	582.5	175.4	54.4
C19:0 dioic acid	5.7	10.2				17.7	3.0	11.1	12.7	19.3	10.7	14.8	15.4	22.3	17.5	21.3	10.8	38.8	2.0	10.2	1.8	
C23:0	162.1	429.4	129.1	233.6	168.3	525.0	88.9	282.9	223.4	343.9	265.0	326.7	356.6	553.8	412.4	518.3	4.7	918.7	140.0	440.2	121.3	46.8
C20:0	45.5	68.1	19.2	50.4	25.4	68.5	14.7	44.5	55.2	69.3	42.4	71.3	75.0	129.1	91.8	86.7	52.1	186.6	15.7	41.9	7.0	
C24:0	524.5	1054.4	245.6	472.1	312.2	1083.0	165.4	541.5	473.7	634.1	556.7	835.3	880.2	1269.4	995.0	957.4	1164.3	2633.0	451.8	1284.6	315.3	108.6
C21:0 dioic acid	4.6	51.4	26.7	28.8	32.7	70.7	9.7	38.6	34.6	52.2	28.9	47.2	24.6	111.0	60.9	50.5	46.2	159.6	13.5	36.3		
C25:0	150.6	357.0	93.1	179.7	122.4	433.7	61.5	229.5	189.3	253.4	218.3	391.8	407.8	565.6	455.0	396.1	409.3	711.4	120.1	378.6	116.6	49.1
C22:0 dioic acid		355.7	65.2	164.0	82.5	463.3	32.2	161.2	180.9	172.4	138.6	368.0	376.7	502.8	415.8	280.8	281.0	1118.6	55.6	229.5	19.8	
C26:0	488.9	854.9	153.8	312.2	218.3	807.8	113.5	434.7	401.8	482.3	468.3	934.1	919.8	1371.4	1075.1	628.3	670.0	1412.8	282.0	723.7	224.3	104.7
C23:0 dioic ac	37.5	137.6	19.8	53.6	24.9	186.1	7.4	55.7	52.9	48.8	36.3	139.8	130.2	176.8	148.9	82.2	90.0	6.3	12.5	46.4	5.2	
C27:0	157.6	251.6	44.4	100.8	67.5	271.9	34.1	154.3	132.8	156.3	133.8	358.2	360.0	482.7	400.3	255.2	248.0	369.1	81.3		80.4	37.3
C24:0 dioic ac	194.6	592.6	59.4	176.5	65.7	772.6	21.6	165.1	167.6	118.2	103.1	536.0	473.9	682.0	564.0	220.1	317.5		51.6	199.6	17.5	
C28:0	614.9	775.2	85.1	214.2	130.7	676.8	78.6	8.5	7.2	4.4	5.2	29.2	33.2	39.4	33.9	44.0	25.9	771.0	206.4	511.4	177.2	101.1
C29:0			13.3	37.8	25.5	131.1											88.8	131.3	34.6	98.1		22.9
C30:0			24.1	78.5	42.4	333.6											89.7	210.2	71.9	194.5	75.7	51.1
C31:0						113.3											51.5	144.1	17.2	56.6	22.8	
C32:0						237.1											26.6	112.1	118.8	56.6		
C33:0																						

Transect-Samples

	259a	259b	258	257	256	255	254a	254b	253	96B14MG67	252	250	249	248	247	246	245	244	96B14MG71	242	240	239	238	237	236	235	234	96B14MG65	233	232	231	230	229	228	227	226	96B14MG41	134a	136	137	138	139	96B14MG35	105	106	157	158
C9:0	2.1	2.7		17.2	6.5	14.8	6.5	19.1	24.7	2.2	11.7	54.3	30.0	50.0	61.6	23.5	33.6	230.7		3.8										3.0						2.8	4.1	6.0	8.1		46.7							9.2		8.0
C10:0	2.8	2.5									15.0	4.1	3.6						59.1	13.8		41.9	77.3	92.4	51.2	38.0	27.9	22.8	11.1																35.7	24.8		26.1
C7:0 dioic ac																																													16.5	23.7		
C11:0		1.4		3.2	1.7	3.2	1.2	3.1	4.5	14.4	3.2	9.7	7.7	9.6	18.3	5.4	9.5	49.9	10.6	4.7		9.0	19.1	19.1	10.3	7.1	7.2	4.8	1.6								1.2							8.1	8.5		
C8:0		1.0								5.0									1.1	9.5		3.6	12.8	2.6	3.3				4.2									1.1	11.7						22.4	77.3		
C12:0	12.1	15.3	17.9	32.8	17.4	29.7	25.3	35.5	43.7	169.2	27.4	91.6	58.7	83.4	135.5	51.7	67.1	455.0	112.0	37.8	55.7	75.0	144.3	137.4	86.1	71.8	53.4	73.9	36.0	12.1				3.6	5.9	7.6	31.3	10.1	114.3	8.7	26.9	13.1	22.8	134.1	65.1		40.5
C9:0 dioic acid	7.7	2.3	1.3	2.7	0.0	2.4	5.4	4.1	2.3	22.5	31.9	16.8	9.7	3.7	4.3			26.7	4.2	32.3		20.9	37.8	12.2	17.0	11.0	4.0	2.4	33.8					1.1	1.8	3.3	12.3	8.4	27.7				13.3	62.0	291.7		48.0
C13:00			2.1	3.1	2.0	3.1		2.8	4.6	15.8	2.3	11.3	9.6	11.1	28.6	9.3	16.3	61.6	14.9	2.5	10.5	15.1	30.1	24.1	12.6	10.3	12.6	8.2	11.2						2.5	3.0		1.0	18.4					11.0	9.0		
C10:0			1.3	1.3		1.4	1.8	1.3	2.0	3.7	4.8	2.9	2.0		1.2			9.5		3.1		3.6		3.0	2.8	2.1	1.2	1.2	10.3						1.5	1.8								8.6	32.3		5.7
C14:0	27.5	34.0	23.9	46.9	24.0	43.7	44.4	37.6	45.5	110.5	48.6	97.2	63.4	108.0	138.3	53.8	59.8	521.3	96.0	57.3	61.0	85.4	149.4	130.4	85.4	81.8	50.5	36.9	69.7	31.5	29.8	6.7	7.0	7.5	9.8	13.4	29.0	11.2	146.0			26.3	26.8	142.0	155.1	19.2	66.7
C11:0		3.6	3.3							3.8			1.8																12.9								8.8		5.0									
C15:0	16.2	26.4	10.2	18.4	10.2	17.0	22.9	18.4	19.5	54.5	28.3	48.6	30.3	51.2	59.0	24.3	28.0	216.4	48.5	29.7	37.8	50.8	82.4	73.3	45.7	43.8	27.5	15.8	35.3	11.6	11.8	7.7	8.3	4.6	6.8	8.1	16.3	5.0	68.1			9.4	15.5	53.5	76.9	9.9	36.2
C12 dioic ac		7.3	4.4	7.1	4.3	7.4	16.3	15.9	8.5	54.8	4.0	36.6	11.8	22.2	24.3	6.3	10.8	103.8		9.3	53.0	40.9	67.1	55.8	45.9	40.7	18.9	2.2	3.1	10.9					4.5	8.2	10.2	12.7		15.0				5.7	24.9	29.3		
C16:1		4.2	3.1	4.6	2.4	4.6	13.8	6.5	4.6	8.2	28.6	6.4	4.3	4.6	4.7	2.0		22.0	3.2	29.7	7.4	5.2	10.5	5.0	5.0	4.8	3.0	1.4	4.2					3.9	2.9	4.3								35.0	37.7	12.6	11.9
C16:1			11.2	24.1	10.0	20.9	18.3		15.0	59.0	5.3	83.4	49.3	108.2	71.6	6.5	7.6		82.3			61.5	114.8	108.0	55.5	64.1	24.3	14.9	11.2						3.5	5.7	8.1			72.3					66.3	11.1		22.7
C16:1			2.4	2.6	7.7	13.6	14.2	17.7			14.9	7.5	4.9	5.9	7.3	27.2	30.1	348.5	5.5			6.9			7.7	7.9		2.9	23.1											14.0	47.7	118.1			24.3	13.4		12.4
C16:0	685.4	453.4	209.6	430.9	212.5	407.2	380.2	363.7	380.9	724.4	711.0	701.0	355.6	786.2	919.7	427.5	467.0	3845.8	562.8	469.2	358.7	671.6	945.8	1000.3	652.1	633.9	345.3	232.6	1747.3	121.2	123.2	71.9	75.1	46.8	71.5	78.2	170.4	105.7	744.0			102.9	171.3	716.1	12.0		825.1
i		5.8	1.3	1.8	1.4	1.9	1.2	2.7	2.2	22.4	2.2	10.4	6.2	6.0	7.7	3.4	3.4	40.1	10.9	2.9		8.1	11.4	9.2	6.1	5.3		5.4	1.5								1.2									75.6	22.9
C17:0	35.6	20.6	10.0	8.8	9.6	8.5	7.3	27.3	11.6	24.8	44.3	25.7	20.9	25.8	22.3	8.4	9.6	74.9	19.7	9.6	20.2	16.8	20.5	21.7	12.1	15.6	8.6	6.8	96.5		9.1			6.1	10.4	11.9	19.4	7.3	37.7				13.3	32.2	106.3		46.4
C18:2	56.0	152.5	18.2	29.8	13.5	28.7	101.3	30.2	27.6	19.0	311.3	42.1	21.6	59.6	16.3	5.6	9.2	77.5	39.7	166.1	24.2	34.9	42.1	70.4	27.8	23.1	8.7	5.8	615.8								5.4	29.5		27.6	38.3	10.0	8.6	47.3	234.7	7.0	532.9
C18:1	83.0	319.6	96.0	166.9	91.3	159.0	299.3	186.4	155.7	432.1	170.7	429.9	244.4	359.8	215.1	59.5	67.7	795.4	289.6	174.6	179.7	421.1	511.1	705.3	468.2	324.5	59.5	124.7	441.5	39.1	39.9	24.8	24.3	13.2	20.0	21.0	62.2	187.7	346.6		13.3	94.7	78.8	404.1	3395.2	59.2	984.1
C18:1 isomer	30.3	29.9	31.5	41.3	27.9	37.8	31.6	42.5	83.3	176.0	29.1	127.9	93.8	97.7	40.9	5.6	7.5	161.8	159.6	42.8	71.2	155.4	177.3	316.7	192.4	123.9	19.4	43.1	40.8	29.4	27.6	18.2	19.5	12.6	21.1	22.5	37.0	28.4	26.3			14.1	32.4	85.9	196.7	13.9	72.2
C18:0	269.8	359.1	211.6	491.6	212.8	466.4	347.9	271.2	343.3	717.8	311.7	531.9	249.8	547.0	491.9	239.3	247.2	2155.4	557.4	266.8	281.1	472.7	585.6	821.3	473.8	472.5	214.3	221.9	578.7	127.8	144.8	83.8	85.4	51.9	88.4	85.0	204.9	84.7	655.6			99.4	180.3	534.3	2128.4	67.3	259.6
C19:0	4.4	6.3	11.0	11.0	11.3	10.9	3.8	36.4	14.5	29.5	6.4	29.7	23.3	25.8	21.8	9.7	9.8	87.5	9.1		59.4			38.5	28.3	26.2	16.1	8.0	8.9	29.8	30.6	19.6	24.1	12.3	22.8	23.0	41.9				18.2	19.3	38.1	30.8	61.9	14.7	23.8
C16:0 dioic ac							8.7	4.2	2.5	20.4	24.9	25.5	13.5	6.3				15.6	2.0	65.0	26.4	25.6	44.0	14.3	19.8	8.0	4.6	2.1	9.8								20.8	11.3	56.4			12.4	9.1	37.1	79.3	250.4		44.3
C20:0:39	141.5	152.6	220.2	391.4	221.6	372.4	315.7	225.8	350.8	111.9	222.1	267.9	301.4	263.5	300.2	178.5	217.4	1617.3	228.3	239.1	170.6	345.9	234.3	254.5	214.5	56.0	220.3	241.9	238.7	152.8	311.6	172.8	156.3	133.3	180.3	245.4	183.2	177.5	242.4	211.9	137.9	151.2	139.5	317.1	1201.2	178.5	221.7
C20:1	21.0	104.9																												262.4	298.3	190.3	212.2	100.1	195.1	167.6	467.2	9.6					157.0	401.0	32.8	17.6		
C20:0	193.5	215.3	20.9	27.0	21.4	25.3	65.6	109.3	27.1	111.4	66.7	134.5	76.8	77.7	57.8	24.6	24.9	234.3	46.9	149.5	196.9	149.0	183.5	148.9	126.8	118.4	66.3	45.0	66.8	205.2	387.5	237.8	218.2	182.9		335.2	263.9	247.6	595.7	67.1	191.4	194.4	5.6	327.3	118.7	90.6	49.3
C21:0	12.7	25.0	25.6	20.9	25.8	20.0	22.4	191.7	25.2		46.7	217.0	111.8	99.9	66.8	27.5	26.7	233.3	44.7	106.5	333.2	189.8	213.1	145.0	134.2	122.3	77.6	35.2	39.1	83.0	87.5	54.6	60.6	32.8	56.6	53.1	110.9	6.5	191.9	17.5	53.8	55.5	90.0	177.5	63.5	71.6	51.4
C18:0		11.6					10.9	8.0		16.6	18.1	22.5	9.8	5.5	4.2			14.2	1.7	35.5	29.2	20.8	32.6	9.3	13.3	5.8	4.9	2.5	4.9	8.7	11.0			3.1			19.0	3.6	34.7			9.6	7.8	27.6	30.7	55.8		
C22:1			48.0	70.3				107.8	84.3	834.7	2.7	296.0	172.5	259.4	381.6	107.3	150.7	53.8	407.1									213.1	15.3	23.2	17.5	10.2	8.4	6.8	8.2	6.5			83.3	14.2	32.9	27.3		137.1	28.1		
C22:1					47.6	66.4													19.2		102.7	276.3	382.8	607.8	381.7	294.8	95.9																		174.3	10.9		
C22:0	48.5	225.6	83.4	67.8	83.5	64.5	155.6	766.2	83.5	582.5	223.4	979.8	502.3	446.2	284.1	114.6	103.2	996.7	175.4	580.5	1495.9	1048.6	1015.1	854.3	742.6	703.7	408.2	195.3	161.6	301.9	317.9	204.2	216.2	110.8	199.2	174.7	359.3	29.0	863.7	65.6	189.5	203.8	315.8	796.1	286.3	269.4	179.4
C19:0 dioic acid	9.2	1.9								10.2	23.7	23.8	41.2	3.5	3.9				1.8		37.7							2.0	17.5									10.7	5.1	22.2				12.7		11.6	7.2	13.5
C23:0	33.9	85.2	53.5	48.9	54.4	45.5	62.5	517.4		440.2	133.2	811.8	398.0	343.9	216.5	97.7	87.6	831.9	121.3	313.2	1206.0	850.0	787.2	660.7	585.2	549.1	299.4	140.0	112.6	254.0	262.5	171.1	169.7	86.4	159.0	129.0	265.0	13.3	704.9	45.7	129.4	160.8	223.4	644.0	125.1	213.6	116.9
C20:0		14.9	6.4	10.3	6.4	10.0	25.9	48.2	9.6	41.9	34.4	158.6	59.1	26.1	16.9	7.9	6.0	60.3	7.0	96.5	241.7	107.5	174.6	57.2	65.5	25.7	25.6	15.7	12.7	28.6	34.1	20.8	17.7	9.8	17.7	15.1	42.4	6.3	104.7		23.1	23.2	55.2	76.1	113.3	22.3	18.9
C24:0	50.8	142.4	108.2	94.8	109.3	86.6	114.6	1019.5	137.5	1284.6	210.3	1730.7	869.5	790.9	488.7	231.9	199.5	2010.4	315.3	613.2	2787.8	2402.2	2052.2	2039.8	1729.3	1702.3	878.2	451.8	243.1	640.6	652.2	11.1	386.5	186.3	361.1	275.0	556.7	28.3	1759.7	95.7	263.8	344.0	473.7	1423.9	274.3	416.3	172.5
C21:0 dioic acid	16.8	4.6	21.9	44.2	15.4	40.9	31.9	40.9	7.3	36.3	20.6	134.6	47.0	27.5	14.9				45.8	46.9	87.0	116.5	53.0	48.0	22.7	19.5	13.5			22.2	70.9	422.7	12.3	9.3	14.3	9.1	28.9	10.1	90.5		13.7	17.4	34.6	60.3	14.5	17.4	18.2
C25:0	12.7	42.6	36.4	34.7	37.5	33.0	35.8	414.3	52.1	378.6	62.1	713.8	317.4	269.8	168.2	89.6	77.7	769.6	116.6	220.2	1044.5	782.8	682.4	612.3	554.0	530.0	262.1	120.1	54.0	282.8	289.7	188.1	157.6	74.6	150.9	109.6	216.3	4.7	833.3	38.7	110.3	155.5	189.3	528.9	42.6	133.0	45.4
C22:0 dioic acid	5.0	35.6	3.1	1.9	3.1	1.8	67.4	256.3	3.5	229.5	113.6	1212.5	356.1	139.4	58.8	11.5	4.8	52.4	19.8	517.6	1996.1	692.0	984.7	374.1	413.4	129.0	104.7	55.6	15.9	167.1	182.4	108.4	82.8	35.0	72.9	48.2	138.6	6.2	640.6	26.3	76.0	106.8	180.9	457.4	132.1	111.7	40.3
C26:0	9.0	32.5	56.2	59.3	56.7	55.5	40.6	632.5	94.2	723.7	58.1	1032.1	458.1	392.9	250.4	144.7	132.3	1332.3	224.3	252.1	1607.7	1366.4	1179.4	1185.0	1037.5	1042.1	508.7	282.0	107.0	722.6	745.5	476.3	355.5	172.8	366.5	245.6	468.3	8.2	2042.6	79.8	225.3	330.6	401.8				
C23:0 dioic ac	16.8		1.1				8.0	45.4	1.6	46.4	38.6	256.5	72.3	32.0	15.1	3.7	2.7	22.6	5.2	106.4	460.9	135.9	170.3	92.6	87.0	37.5	20.7	12.5		58.9	66.2	38.2	25.2	11.0	23.8	13.6	36.3		251.5		21.9	37.5	52.9	1010.6	42.4	178.5	30.4
C27:0	3.1	9.5	18.6	21.0	19.2	19.8	16.1	255.8	35.4		53.0	407.0	164.8	128.5	83.1	53.1	47.9	473.1	80.4	113.7	651.9	439.7	402.6	342.7	321.8	312.1	151.5	81.3		227.9	234.9	147.2	100.6	50.2	113.0	71.4	133.8		768.8	26.3	77.4	121.1	132.8	164.5		36.0	7.8
C24:0 dioic ac	7.0	14.5	2.5	1.8	2.7	5.5		124.9		199.6	51.9	900.1	264.7	118.5	45.5	11.8	5.0	46.7	17.5	387.0	1745.4	571.9	678.9	393.9	391.5	148.9	63.9	51.6	14.6	230.8	264.6	149.0	84.0	35.2	88.2	44.0	103.1		1024.1	21.6	66.0	127.5	167.6	343.6		66.3	9.2
C28:0	60.6	43.5	36.4	44.9	36.7	41.5	24.1	454.8	72.1	511.4	144.6	706.2	305.0	232.8	148.7	100.3	99.0	999.1	177.2	182.2	1123.3	944.0	821.3	788.3	709.5	710.1	347.6	206.4	69.0	19.8	25.2	11.0	11.7	141.4		8.5	5.2	5.1		66.6	195.6	323.3	7.2	659.3	45.1	114.5	40.4
C29:0			7.4	10.0	7.2	9.5	5.0	47.1	19.7	98.1	7.6	89.1	41.6	45.3	33.6	25.8	31.1	220.4		26.4	137.6	132.8	136.3	133.1	117.4	116.7	59.2	34.6			152.4	91.3	51.6	26.8	65.8	37.4	73.7	2.7		14.9	46.5	80.6	83.0	916.2	20.7	102.9	19.3
C30:0			12.5	18.6	11.9	17.1	4.5	65.5	37.5	194.5	9.7	120.4	57.3	68.6	53.9	45.1	43.2	413.0	75.7	23.2	192.2	252.8	252.3	264.7	239.6	248.8	126.1	71.9	74.5	33.4	403.1	229.3	114.5	62.5	164.3		163.0	9.2	1518.8	33.7	103.2	196.5	198.7	187.6	22.1	17.9	26.5
C31:0		39.5		4.2	2.9		43.6	21.5		56.6	91.2	63.4	16.2	22.0	15.0		10.9	140.3	22.8	85.9	130.1	58.9	59.0	70.4	61.2	60.9	31.2	17.2		36.7	74.7	40.4	24.7	35.9	12.7	46.8	61.1	13.3	354.5		17.5	37.3	44.3	502.0		26.0	
C32:0				8.6	4.8			13.1	19.1	56.6		49.3	28.8	44.9	33.0	31.6	27.9	281.9			40.5	123.3	135.5	156.3	136.5	148.5	71.0	118.8		33.9	36.5	20.1	16.0	31.7	95.6		90.9				53.1	122.2	120.4	121.7	144.9	19.6	66.1
C33:0																											58.6	4.8	15.6													400.7	47.5	46.7	333.3			434.0
C34:0	6.4	28.5																										10.0	36.4																53.7			30.5

7.2 Additional figures

Dicarboxylic acids

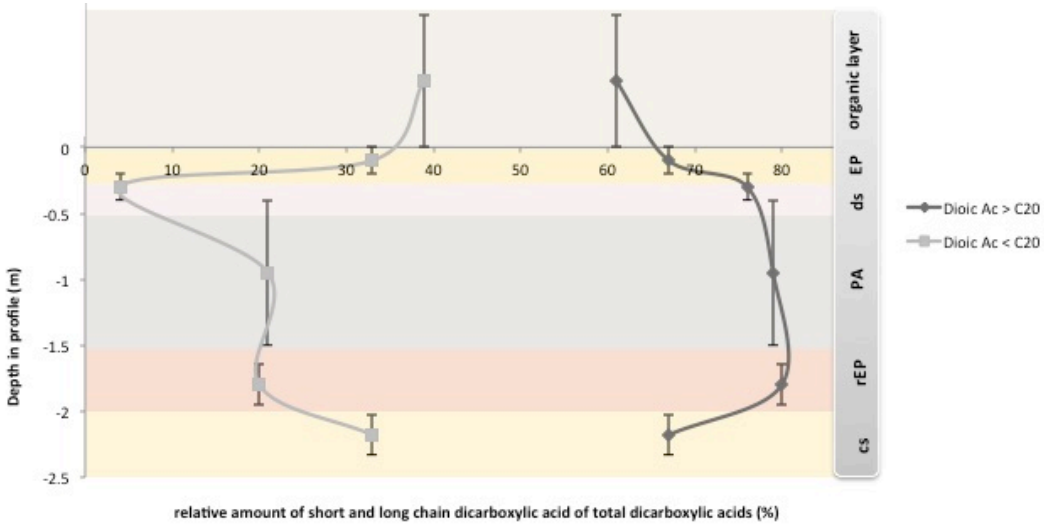

Figure 18: Long- chain dicarboxylic acids (>C_{20}) and short chain dicarboxylic acids (<C_{20}) along the profile. Y-axis showed the profile depth, the X-axis the relative portion of dicarboxylic acids. Short- and long- chain dicarboxylic acids were normalized to total dicarboxylic acids.

As shown in figure 19, Plaggic Anthrosol and Podzol layers had a higher relative amount of dicarboxylic acids than the other layers. The depth distribution of long chain dicarboxylic acids and of short chain dicarboxylic acids was contrary to each other. Where dicarboxylic acid > C_{20} were enriched in the EP horizon, there were lower values for Dicarboxylic acid < C_{20} in the same layer. Especially the driftsand layer showed big differences between long- and short chain dicarboxylic acids. Long chain compounds were enriched, short chain dicarboxylic acid was very low. In plaggen soil layer both are enriched, also in the rEP. In the coversand, where low total dicarboxylic acid amounts (shown in *figure 20*), short chain dicarboxylic acid. Increase relative to the rEP layer. The relative long chain dicarboxylic acid contents decreased down under the high value in the relict Epialbic Podzol. In all soil layers, long chain dicarboxylic acid was represented in higher amounts than short chain dicarboxylic acid.

Average chain length for long chain n- alkanes

The ACL_{lc} is different from ACLtot. Also the statistical test shows other significant differences ($F(9, 26)= 5.500$, $p= 0.006$). For example is the Plaggic Athrosol for ACL_{lc} significant different to the organic layer ($p= 0.000$), the EP ($p= 0.045$), rEP ($p= 0.041$) and cs ($p= 0.008$). Driftsand could not differ from other soil groups. The ACL_{lc} values are low for organic layer, decrease to a maximum in the PA and decrease again. The ACL_{lc} values in plaggen soil (29.9 ± 0.1) were higher than those of EP (29.0 ± 0.1) and rEP (29.0 ± 0.5). Driftsand (29.3 ±0.1) is slightly higher than those of coversand (28.7 ± 0.4) and organic layer (28.2 ± 0.2). The aboveground biomass values in leaves (28.2 ± 0.3) were lower than those of branches (28.5 ±0.5), but similar to those of roots (28.2 ± 0.2). Lowest values were found in bark (28.5 ± 0.5).

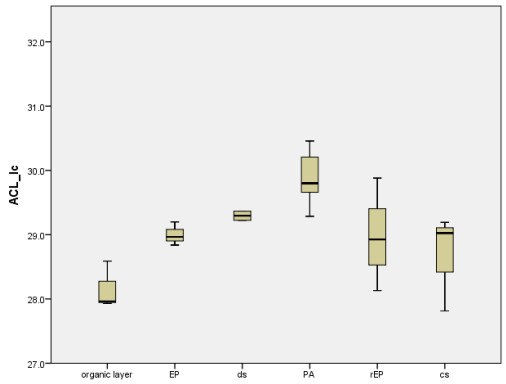

MUFA

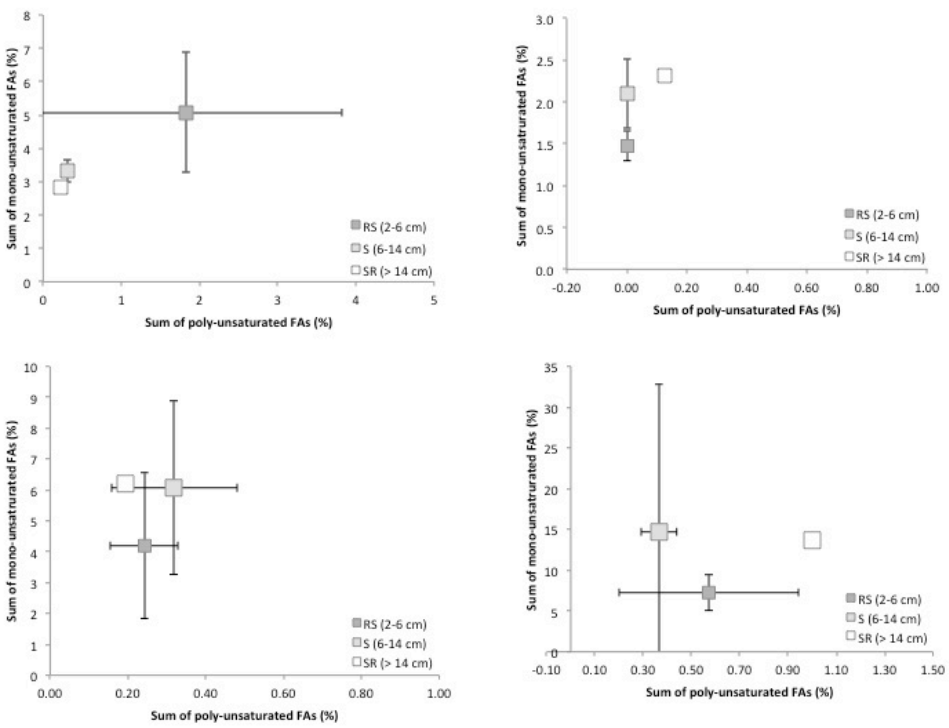

8 References

Amelung, W. et al., 2009. Combining Biomarker with Stable Isotope Analyses for Assessing the Transformation and Turnover of Soil Organic Matter. In *Advances in Agronomy*. Elsevier Inc., pp. 155–250.

Angst, G., Kögel-Knabner, I., et al., 2016. Spatial distribution and chemical composition of soil organic matter fractions in rhizosphere and non-rhizosphere soil under European beech (Fagus sylvatica L.). *Geoderma*, 264, pp.179–187.

Angst, G., John, S., et al., 2016. Tracing the sources and spatial distribution of organic carbon in subsoils using a multi-biomarker approach. *Scientific reports*, 6, p.29478.

Blume, H.P. & Leinweber, P., 2004. Plaggen soils: Landscape history, properties, and classification. *Journal of Plant Nutrition and Soil Science*, 167, pp.319–327.

Borges del Castillo, J., Brooks, C.J.W., Cambie, R.C., Eglinton, G., Hamilton, R.J., Pellitt, P., 1967. The taxonomic distribution of some hydrocarbons in gymnosperms. *Phytochemistry*, 6, pp.391–398.

Bray, E.. & Evans, E.., 1961. Distribution of n-paraffins as a clue to recognition of source beds. *Geochimica et Cosmochimica Acta*, 22, pp.2–15.

Buggle, B., Wiesenberg, G.L.B. & Glaser, B., 2010. Is there a possibility to correct fossil n-alkane data for postsedimentary alteration effects? *Applied Geochemistry*, 25, pp.947–957.

Cameron, P.M.* † ‡ et al., 2007. Determining the Extent of Biodegradation of Fuels Using the Diastereomers of Acyclic Isoprenoids. *Environmental Science Tehcnology*, 41, pp.2452–2458.

Chabbi, A., Kögel-Knabner, I. & Rumpel, C., 2009. Stabilised carbon in subsoil horizons is located in spatially distinct parts of the soil profile. *Soil Biology and Biochemistry*, 41, pp.256–261.

Coleman, D.C., 1994. The microbial loop concept as used in terrestrial soil ecology studies. *Microbial Ecology*, 28, pp.245–250.

Collister, J. et al., 1994. Compound-specific δ13C analyses of leaf lipids from plant with differing carbon dioxide metabolisms. *Org Geochem*, 21, pp.619 – 627.

Cranwell, P.A., 1973. Chain-length distribution of n-alkanes from lake sediments in

relation to post-glacial environmental change. *Freshwater Biology*, 3, pp.259–265.

Cranwell, P.A., 1981. Diagenesis of free and bound lipids in terrestrial detritus deposited in a lacustrine sediment. *Organic Geochemistry*, 3, pp.79–89.

Cranwell, P.A., Eglinton, G. & Robinson, N., 1987. Lipids of aquatic organisms as potential contributors to lacustrine sediments—II. *Organic Geochemistry*, 11, pp.513–527.

Crow, S.E. et al., 2009. Sources of plant-derived carbon and stability of organic matter in soil: Implications for global change. *Global Change Biology*, 15, pp.2003–2019.

Dinel, H., Schnitzer, M. & Mehuys, G.R., 1990. Soil lipids: origin, nature, content, decomposition, and effect on soil physical properties. In *Soil biochemistry*. Marcel Dekker New York, pp. 397–429.

Driessen, P.M. & Dudal, R., 1991. The major soils of the world. *Koninklijke Wohrmann BV, Zutphen, The Netherlands*.

Duan, Y., 2000. Organic geochemistry of recent marine sediment from Nansha Sea, China. *Org. Geochem*, 31, pp.159–167.

Duan, Y. & He, J., 2011. Distribution and isotopic composition of n-alkanes from grass, reed and tree leaves along a latitudinal gradient in China. *Geochemical Journal*, 45, pp.199–207.

Eglinton, G. et al., 1962. Hydrocarbon constituents of the wax coatings of plant leaves: A taxonomic survey. *Phytochemistry*, 1, pp.89–102.

Eglinton, G. & Hamilton, R.J., 1967. Leaf epicuticular waxes. *Science (New York, N.Y.)*, 156(3780), pp.1322–1335.

Freeman, K.H., Colarusso, L.A., 2001. Molecular and isotopic records of C4 grassland expansion in the late Miocene. *Geochim. Cosmochim. Acta*, 65, pp.1439–1454.

Giani, L., Makowsky, L. & Mueller, K., 2014. Plaggic Anthrosol: Soil of the Year 2013 in Germany: An overview on its formation, distribution, classification, soil function and threats. *Journal of Plant Nutrition and Soil Science*, 177, pp.320–329.

Gocke, M., Gulyás, S., et al., 2014. Biopores and root features as new tools for improving paleoecological understanding of terrestrial sediment-paleosol sequences. *Palaeogeography, Palaeoclimatology, Palaeoecology*, 394, pp.42–58.

Gocke, M.I. et al., 2016. Paleosols can promote root growth of the recent vegetation – a case study from the sandy soil-sediment sequence Rakt , the Netherlands. *SOIL*, 2, pp.1273–1308.

Gocke, M., Kuzyakov, Y. & Wiesenberg, G.L.B., 2010. Rhizoliths in loess - evidence for post-sedimentary incorporation of root-derived organic matter in terrestrial sediments as assessed from molecular proxies. *Organic Geochemistry*, 41, pp.1198–1206.

Gocke, M., Peth, S. & Wiesenberg, G.L.B., 2014. Lateral and depth variation of loess organic matter overprint related to rhizoliths - Revealed by lipid molecular proxies and X-ray tomography. *Catena*, 112, pp.72–85.

Gocke, M.I. et al., 2016. Paleosols can promote root growth of the recent vegetation – a case study from the sandy soil-sediment sequence Rakt , the Netherlands. *SOIL*, 2, pp.1273–1308.

Harwood, J.L. & Russel, N.J., 1984. *Lipids in Plants and Microbes*, London.

Harwood, J.L. & Russell, N.J., 1984. Lipids in Plant and Microbes George Allen & Unwin.

Jandl, R. et al., 2007. How strongly can forest management influence soil carbon sequestration? *Geoderma*, 137, pp.253–268.

Jobbágy, E.G. & Jackson, R.B., 2000. The vertical distribution of soil organic carbon and its relation to climate and vegetation. *Ecological applications*, 10, pp.423–436.

Jones, D., 1998. Organic acids in the rhizosphere–a critical review. *Plant and soil*.

Kalbitz, K. et al., 2000. Controls on the dynamics of dissolved organic matter in soils: a review. *Soil science*, 165, pp.277–304.

Kolattukudy, P.E., Croteau, R., Buckner, J.S., 1976. (Ed.), In P. E. Kolattukudy, ed. *Chemistry and Biochemistry of Natural Waxes*. Amsterdam: Elsevier.

Kolattukudy, P.E., Croteau, R., Buckner, J.S., et al., 1976. Biochemistry of plant waxes. In P. E. Kolattukudy, ed. *Chemistry and Biochemistry of Natural Waxes*. Amsterdam: Elsevier, pp. 290–347.

Kolattukudy, P.E., Croteau, R. & Buckner, J.S., 1976a. Biochemistry of plant waxes. In P. E. Kolattukudy, ed. *Chemistry and Biochemistry of Natural Waxes*. Amsterdam:

Elsevier, pp. 290–347.

Kolattukudy, P.E., Croteau, R. & Buckner, J.S., 1976b. Biochemistry of plant waxes. In *Chemistry and biochemistry of natural waxes*. Amsterdam: Elsevier, pp. 290–347.

Kuzyakov, Y. & Domanski, G., 2000. Carbon input by plants into the soil. Review. *Zeitschrift für Pflanzenernährung und Bodenkunde*, 163, pp.421–431.

Mendez-Millan, M. et al., 2010. Molecular dynamics of shoot vs. root biomarkers in an agricultural soil estimated by natural abundance 13C labelling. *Soil Biology and Biochemistry*, 42, pp.169–177.

Meyers, P.A. & Ishiwatari, R., 1993. Lacustrine organic geochemistryman overview of indicators of organic matter sources and diagenesis in lake sediments. *Org. Geochem*, 20, pp.867–900.

van Mourik, J. et al., 2016. The added value of biomarker analysis to the genesis of Plaggic Anthrosols; the identification of stable fillings used for the production of plaggic manure. *EGU General Assembly Conference*.

van Mourik, J.M. et al., 2012. Impact of human land use on soils and landforms in cultural landscapes on aeolian sandy substrates (Maashorst, SE-Netherlands). *Quaternary International*, 265, pp.74–89.

Van Mourik, J.M. et al., 2012. Impact of human land use on soils and landforms in cultural landscapes on aeolian sandy substrates (Maashorst, SE-Netherlands). *Quaternary International*, 265, pp.74–89.

Ohta, S., Suzuki, A. & Kumada, K., 1986. Experimental Studies on the Behavior of Fine Organic Particles and Water-Soluble Organic Matter in Mineral Soil Horizons. *Soil Science and Plant Nutrition*, 32, pp.15–26.

Peters, K.E., Walters, C.C. & Moldowan, J.M., 2005. *The biomarker guide*, Cambridge University Press.

Rasse, D.P., Rumpel, C. & Dignac, M.-F., 2005. Is soil carbon mostly root carbon? Mechanisms for a specific stabilisation. *Plant and Soil*, 269, pp.341–356.

Rontani, J.-F. & Volkman, J.K., 2003. Phytol degradation products as biogeochemical tracers in aquatic environments. *Organic Geochemistry*, 34, pp.1–35.

Rumpel, C. & Kögel-Knabner, I., 2011. Deep soil organic matter—a key but poorly

understood component of terrestrial C cycle. *Plant and Soil*.

Sauer, D., Kuzyakov, Y. & Stahr, K., 2006. Short Communication: Spatial distribution of root exudates of five plant species as assessed by 14C labeling. *J. Plant Nutr. Soil Sci*.

Sauer, D., Kuzyakov, Y. & Stahr, K., 2006. Spatial distribution of root exudates of five plant species as assessed by 14C labeling. *Journal of Plant Nutrition and Soil Science*, 169, pp.360–362.

Schöning, I., Totsche, K.U. & Kögel-Knabner, I., 2006. Small scale spatial variability of organic carbon stocks in litter and solum of a forested Luvisol. *Geoderma*, 136(3), pp.631–642.

Schwark, L., Zink, K. and Lechterbeck, J., 2002. Reconstruc- tion of Postglacialto Early Holocene vegetation history in terrestrial Mid-Europe viacuticular lipid biomarkers and pollen records from lake sediments. *Geology*, 30, pp.463–466.

Tegelaar, E.W., de Leeuw, J.W. & Saiz-Jimenez, C., 1989. Possible origin of aliphatic moieties in humic substances. *Science of The Total Environment*, 81, pp.1–17.

Wiesenberg, G.L. & Gocke, M., 2016. Analysis of Lipids and Polycyclic Aromatic Hydrocarbons as Indicators of Past and Present (Micro) Biological Activity. In *Hydrocarbon and lipid microbiology protocols: isolation and cultivation Springer Berlin, Germany.* pp. 1–31.

Wiesenberg, G.L.B. et al., 2004. Source and turnover of organic matter in agricultural soils derived from n-alkane/n-carboxylic acid compositions and C-isotope signatures. *Organic Geochemistry*, 35, pp.1371–1393.

Wiesenberg, G.L.B. et al., 2012. Use of molecular ratios to identify changes in fatty acid composition of Miscanthus Â giganteus (Greef et Deu.) plant tissue, rhizosphere and root-free soil during a laboratory experiment. *Organic Geochemistry*, 46, pp.1–11.

Wiesenberg, G.L.B., Gocke, M. & Kuzyakov, Y., 2010. Fast incorporation of root-derived lipids and fatty acids into soil - Evidence from a short term multiple 14CO2 pulse labelling experiment. *Organic Geochemistry*, 41(9, pp.1049–1055.

Wiesenberg, G.L.B., Schwark, L. & Schmidt, M.W.I., 2004. Improved automated extraction and separation procedure for soil lipid analyses. *European Journal of Soil*

Science, 55, pp.349–356.

Xie, S. et al., 2003. Lipid distributions in loess-paleosol sequences from northwest China. *Organic Geochemistry*, 34, pp.1071–1079.

Zech, M. & Andreev, A., 2010. Quaternary vegetation changes derived from a loess-like permafrost palaeosol sequence in north- east Siberia using alkane biomarker and pollen analyses. *Boreas*, 39, pp.540–550.

Zhang, H.C. et al., 2008. Molecular fossil and paleovegetation records of paleosol S4 and adjacent loess layers in the Luochuan loess section, NW China. *Science in China*, (Series D), pp.321–330.

Zhang, Z. et al., 2006. Leaf wax lipids as paleovegetational and paleoenvironmental proxies for the Chinese Loess Plateau over the last 170 kyr. *Quaternary Science Reviews*, 25, pp.575–594.

Zhang, Z. et al., 2006. Leaf wax lipids as paleovegetational and paleoenvironmental proxies for the Chinese Loess Plateau over the last 170 kyr. *Quaternary Science Reviews*, 25, pp.575–594.